

UNIVERSIDADE DE LISBOA
FACULDADE DE CIÊNCIAS
DEPARTAMENTO DE GEOLOGIA



**Modelling emplacement of magmatism on the Iberia
microplate during the Late Cretaceous**

Bruno Miguel Duarte de Araújo

Mestrado em Geologia
Especialização em Geologia Estrutural

Dissertação orientada por:
João D. C. Duarte e Ricardo N. Pereira

I. ACKNOWLEDGEMENTS

This work could only be possible with the tremendous amount of help from several people around me. Firstly, I want to express my gratitude to everyone involved in my path, without them, this work would not have seen the light of day.

The first persons that I would like to thank are my supervisors Prof. João Duarte and Prof. Ricardo Pereira. Without them and the several meetings had, some at a personal cost, it would not have been possible.

To Prof. Ricardo Pereira, the one who started with this idea, and without him, my work would have stalled in several of the problems encountered along the way. Helping with the software, and with the conceptualization of the many ideas thought out.

To Prof. João Duarte, with several ideas and concepts that he introduced to me, and his critical analysis throughout my work. Which led to my writing and personal development.

Then I would like to thank Prof. João Mata, my scientific advisor, for his help and insights provided with the mantelic, magmatic, and petrologic knowledge that could only be known after a lifetime working on these subjects.

I thank all my colleagues and friends for their support: Francisco Pereira, Guilherme Martins, Bruno Ferreira, Tiago Catita, Nuno Rodrigues, and Diogo Neves.

I am also very grateful for the tireless support, help, and love given by my girlfriend and best friend, Francisca Leal. Without you, I would not have been here to tell this story.

Finally, I thank all my family, particularly my sister Beatriz, my mother Ana, and my father Joaquim. Without your love and affection, I would not have followed the academic life, that fills me with joy.

II. ABSTRACT

For over a century, the investigation of Late Cretaceous alkaline magmatism in the Western Iberian Margin (WIM) has focused on individual massifs, notably the Monchique massif, revealing unique rock types like Foyaite and Monchiquites (Blum, 1861; Hunter & Rosenbusch, 1890; Rock, 1982). Despite these studies, integrating these occurrences into a comprehensive geodynamic and mantle source framework has remained challenging. Existing analyses often treated them as isolated entities, relying on age dating and geochemical profiles (Grange et al., 2008, 2010; Martins et al., 2010; Mata et al., 2015; Miranda et al., 2009; Neres et al., 2012, 2018).

To establish correlations among these discrete magmatic events, a paleogeographic reconstruction model was executed via GPlates software. This tool enabled the exploration of tectonic plate positions over time, coupled with underlying mantle dynamics, seeking explanations for the non-linear distribution and varied timing of magmatism in the WIM. Three primary hypotheses were evaluated: a static or mobile Hot Spot model (Courtillet et al., 2003; Elder, 1976; Koppers, 2011; Morgan, 1971, 1972), the Superplume magmatism hypothesis (Civiero et al., 2021; Courtillet et al., 2003; Long et al., 2020), and Edge-Driven Convection (King, 2007; King & Anderson, 1998; King & Ritsema, 2000; Matton & Jébrak, 2009; Missenard & Cadoux, 2012).

Results indicate that a persistent and robust Super Plume better explains the distinct magmatic instances in the Western Iberian Margin than the Hot Spot theory. Edge-Driven Convection is deemed improbable due to a lack of conditions for initiation. Motion paths were analysed to validate or refute these hypotheses, including alignments like Tore-Sintra-Sines-Monchique, Tore-Madeira, and Monchique-Gorringe-Madeira. However, these paths were adjusted to better reflect regional geodynamics.

Notably, specific motion paths, such as the Lisbon Volcanic Complex, hint at the potential interconnection of all WIM intrusions, with overlapping patterns suggesting the magmatic plumbing in locations and time frames matching the intrusion of these formations. Moreover, the study suggests a potential link between the Madeira Archipelago and other seamounts like Ampère, Seine, and Unicorn, such as seen in the Ampère motion path.

This research demonstrates the complex interplay of geological and geodynamic processes shaping the magmatic history of the Western Iberian Margin, shedding light on the intricate relationships between magmatic occurrences and tectonic processes.

Keywords: Late Cretaceous alkaline magmatism, West Iberian Margin, Plate Reconstructions, Plate Tectonics, GPlates

III. RESUMO

A problemática relacionada com o magmatismo tardi-cretácico tem sido objeto de estudo desde a segunda metade do século XIX, concentrando-se inicialmente no maciço de Monchique. Esses primeiros estudos eram predominantemente petrológicos (Blum, 1861; Hunter & Rosenbusch, 1890; Rock, 1982), destacando tipos de rochas distintos, como Foítes e Monchiquitos. Ao longo do tempo, estudos individuais foram conduzidos para todos os maciços da Margem Oeste Ibérica (MOI), incluindo Sintra, Sines e Monchique. A maioria desses estudos realizou análises detalhadas sobre a geoquímica e idades apresentadas por esses maciços. Somente em tempos mais recentes, começaram a surgir estudos (Grange et al., 2010; Martins, 1991; Martins et al., 2010; Mata et al., 2015; Merle et al., 2018; Miranda et al., 2009; Terrinha et al., 2018) que se dedicaram a explicar modelos de intrusão e contaminação crustal/sublitosférica, buscando compreender melhor os processos geológicos subjacentes ao magmatismo tardi-cretácico. A partir destes novos estudos, a ideia de uma possível correlação entre os três maciços da MOI foi retomada, trazendo à tona a discussão sobre esses corpos geológicos distintos. Além disso, a descoberta de um corpo submarino, a elevação de Tore, localizado ao largo da península de Lisboa, trouxe novas perspectivas para a pesquisa. A teoria que sustentava essa ideia de correlação entre os quatro maciços baseava-se na presença de uma falha sublitosférica que conectava esses maciços, orientando as suas intrusões de maneira periódica (Ribeiro et al., 1979). Esta falha sublitosférica considerada um elemento-chave para compreender a possível relação entre essas formações geológicas, nunca foi descoberta ou descrita (Ribeiro et al., 1979).

Após minuciosa análise das publicações científicas e das idades obtidas por diferentes métodos e autores, concluiu-se que as idades mais antigas são menos confiáveis, privilegiando-se as datações recentes e robustas. O magmatismo em Portugal abrange o Cretácico Médio ao Tardio, enquanto nas regiões offshore (Cordilheira Tore-Madeira e Arquipélago das Canárias) ocorre do Cretácico Inferior à Atualidade. A hipótese de um evento episódico gerador dos maciços é inviável devido às sobreposições de idades desfasadas espacialmente. Com a inclusão das novas datações, a área de pesquisa foi ampliada para a Cordilheira Submarina Tore-Madeira, envolvendo a Placa Africana, além da Microplaca Ibérica. O contexto geológico tornou-se mais complexo e interconectado, conduzindo a uma abordagem abrangente no estudo do magmatismo tardi-cretácico e suas correlações regionais.

Para justificar qualquer alinhamento ou correlação entre os três maciços principais, três hipóteses foram propostas. A primeira hipótese considera o magmatismo como sendo do tipo "Hot Spot", que pode ocorrer de duas formas: uma variação mais clássica, onde o Hot Spot permanece estático ao longo do tempo, ou uma versão em que o Hot Spot possui alguma mobilidade (Courtilot et al., 2003; Foulger & Anderson, 2005; Kono, 1980; Koppers, 2011; Lawver & Müller, 1994; Morgan, 1971; Tarduno et al., 2003). Esta proposta tem como base o que é observado nas cordilheiras submarinas do Havai e do Imperador, onde ocorre alguma movimentação, conhecida como "drift" da posição inicial do Hot Spot ao longo do tempo. A segunda hipótese considera o magmatismo do tipo Superpluma. Em vez de uma única pluma (como no caso do Hot Spot) que se origina no manto profundo e se estende até a superfície, a superpluma é uma megaestrutura mantélica estacionada na transição entre o Manto Superior e o Manto Inferior (Civiero et al., 2021; Cloetingh et al., 2022; Courtilot et al., 2003; Long et al., 2020). Nesta hipótese, ocorrem pequenas emissões episódicas ou pulsativas de magma, conhecidas como "plumas secundárias" ou, mais recentemente, como "plumelets". Devido à composição heterogênea do manto, esta hipótese consegue explicar algumas alterações nas assinaturas geoquímicas das rochas resultantes. Por exemplo, mesmo que todas as rochas sejam alcalinas, elas podem apresentar assinaturas geoquímicas diferentes entre si devido às características específicas das plumas secundárias geradas pela superpluma. A terceira hipótese é o magmatismo do tipo "Edge-Driven Convection", que ainda é objeto de discussão na literatura científica (Elder, 1976; King, 2007; King & Anderson, 1995, 1998; King &

Ritsema, 2000; Matton & Jébrak, 2009; Missenard & Cadoux, 2012). Nesta hipótese, o magmatismo é gerado devido a uma anomalia no manto superior, seja de natureza térmica ou estrutural.

À medida que o trabalho avançou, foram incluídas outras áreas que estão na bordadura do cratão africano. Este cratão gera uma anomalia térmica no manto, o que pode servir como o gatilho para desencadear o processo de Edge-Driven Convection. Esta hipótese propõe que as interações complexas entre a anomalia térmica no manto, a estrutura da margem pouco estirada e outras características geodinâmicas podem estar relacionadas com o magmatismo tardi-cretácico algo que não é observado nas regiões em estudo. No entanto, é importante sublinhar que esta é uma hipótese ainda em debate e requer mais investigação para compreender melhor a sua validade e relevância nos eventos geológicos em questão.

Para testar a viabilidade das hipóteses, foi utilizado o software GPlates, que é de livre utilização e pode ser considerado um Sistema de Informação Geográfica (SIG) (Müller et al., 2018, 2019). Esse software permitiu reconstruir a geometria e posição das placas bem com dos eventos geodinâmicos que ocorreram ao longo do tempo geológico, tanto em escala global como regional, utilizando dados fornecidos pelo utilizador ou disponíveis nas bibliotecas de dados do programa. Ele oferece uma ampla variedade de funcionalidades, sendo as mais utilizadas a criação de polígonos e a geração de percursos. Para visualizar as imagens e resultados obtidos no GPlates, os produtos extraídos foram processados no software ArcGis Pro.

Os resultados foram obtidos traçando as sucessivas localizações de cada corpo magmático em estudo, o que permitiu a criação de uma linha única para cada corpo, conhecida como Caminho de Movimento ou Motion Path. Essa linha representa as posições geográficas que cada corpo tomou desde a sua formação até a atualidade. A análise destes caminhos de movimento revelou que o movimento da placa impede a presença de um Hot Spot, pois não é compatível temporal nem espacialmente com as idades aceites. Ao se obter uma disparidade de locais originais de intrusão, mostra que esta hipótese se torna inviável, contudo estes resultados permitem reforçar a hipótese da Superpluma uma vez que permite explicar magmatismo síncrono com uma grande dispersão espacial. A hipótese do Edge-Driven Convection é posta de lado devido à dificuldade em realizar um estudo aprofundado com esse modelo, além de não se verificar a existência das condições necessárias, o que torna essa hipótese menos plausível para a Margem Oeste Ibérica.

Por exemplo, ao examinar o caso da cordilheira Tore-Madeira, a intrusão Tore (mais ao norte) culmina muito mais a leste da Madeira (ocorrência mais ao sul). Isto levou à rejeição da hipótese do Hot Spot e foram realizados testes de alinhamento, para comprovar se são geodinamicamente possíveis, os que foram propostos na literatura. Os resultados mostram que as intrusões Complexo Vulcânico de Lisboa (CVL)-Sintra-Sines-Monchique podem ser relacionadas geodinamicamente, além de já o terem sido geoquimicamente. Além disso, o alinhamento proposto na literatura entre Monchique e Madeira não se aproxima do offshore da Ibéria, mas sim direciona-se para a placa africana, culminando nas Canárias. Para justificar a presença da Madeira na sua posição atual, foi feito um teste de alinhamento que resultou na aceitação parcial do percurso proposto na literatura, apenas rejeitando a parte que conecta a Monchique. O percurso iniciando no monte submarino Ampère e culminando na Ilha da Madeira justifica perfeitamente a conexão entre estes montes submarinos. Estes resultados reforçam a compreensão das correlações geodinâmicas entre as diferentes áreas de estudo, fornecendo novas luzes sobre os processos responsáveis pelo magmatismo tardi-cretácico nestas regiões.

Com este trabalho conclui-se que a hipótese mais provável de justificar este tipo de magmatismo verificado nas áreas de estudo é a hipótese do magmatismo tipo Superpluma. Este tipo de magmatismo permite a formação de corpos magmáticos maiores, gerando uma grande variabilidade espacial, mas apresentando uma relativamente baixa variabilidade geoquímica nas rochas resultantes. Rejeitando-se a existência de um Hot Spot singular tanto na MOI, como na Cordilheira Tore-Madeira.

Além das conclusões mencionadas, é provável que os maciços portugueses estejam correlacionados geodinamicamente, sugerindo uma mesma origem e fonte magmática. A correlação da Madeira com montes submarinos, comprovada espacialmente e geoquimicamente, indica eventos magmáticos relacionados em diferentes locais ao longo do tempo. Também há possibilidade de correlação entre o magmatismo na MOI e Canárias, sugerindo interconexão entre essas regiões e processos magmáticos similares ou relacionados na formação dos maciços.

Palavras-Chave: Magmatismo Tardi-Cretácico, Margem Oeste Ibérica, Reconstruções Paleogeográficas, Tectónica de Placas, GPlates

TABLE OF CONTENTS

I. Acknowledgements	I
II. Abstract	II
III. Resumo.....	III
1. Introduction	1
2. Geological Background.....	3
2.1. The West Iberian Margin.....	3
2.2. Magmatic Cycles.....	4
2.2.1. First Cycle- Tholeiitic	4
2.2.2. Second Cycle – Transitional to Mildly Alkaline.....	5
2.2.3. Third Cycle – Alkaline.....	6
2.3. Evidence of the Third Cycle.....	8
Introductory note on geochronology	8
2.3.1. Magmatism on Southwest Iberia.....	9
Sintra	10
Sines.....	11
Monchique.....	12
Lisbon Volcanic Complex.....	13
Loulé Dykes and Other Occurrences in Algarve Basin.....	14
Estremadura Spur Intrusion and Fontanelas Volcano	14
2.3.2. Tore - Madeira Rise.....	15
2.3.3. Canary Island Seamount Province	17
3. Models for intraplate magmatism.....	18
3.1. Single Linear Hotspot.....	18
3.2. Multiple Plume Model.....	18
3.3. Edge-Driven Convection.....	20
4. Methods.....	22
GPLates	22
5. Results	26
6. Discussion	33
Motion Paths and their connection to the hypotheses	33
Multiple Mantle Plume Provinces.....	38
7. Concluding Remarks	41
8. Bibliography.....	42

LIST OF FIGURES

Figure 1.1 - Study area, with the regions of interest in this work, showing the locations of the magmatic occurrences investigated in this work. Locations based on Grange et al. (2010); Merle et al. (2018); Miranda et al. (2009); Van Den Bogaard (2013).....	2
Figure 2.1 - Geochemical signature of the three magmatic cycles on the WIM (Mata et al., 2015).	4
Figure 2.2 – Map of the CAMP (red) with the location of the Iberian occurrences marked (dark red), adapted from Marzoli et al. (2018).....	5
Figure 2.3 - Position of the Iberian Peninsula at 150 Ma showing the relative paleogeographic position of the first (yellow) and second magmatic cycles (red).....	6
Figure 2.4 - Position of the Iberian Peninsula at 80 Ma with the relative position of the first cycle, second cycle and third cycle marked by the red, yellow and green ellipses, respectively.	7
Figure 2.5. Map of the SWIM, with the detail of every magmatic body under study and their respective age as used on the models. The ages marked with an asterisk (*) were estimated using seismic stratigraphy.ESI – Estremadura Spur Intrusions.	9
Figure 2.6 - Map of the Tore-Madeira Rise, with the respective age of each body. It can be seen in the Eurasian-African Plate Boundary	15
Figure 2.7 - a) Map of the Northern Group (Eurasian), b) Map of the Southern Group (African) ..	16
Figure 2.8 - Map of the Canary Island Seamount Province (CISP), with the respective age for each body.....	17
Figure 3.1 - Simplification of the Hot Spot formation, with three stages: I- Formation of the plume, in the core-mantle boundary, II- The arrival of the plume head on the Lithosphere-Mantle Boundary, III- Spread of the plume head below this boundary with a path penetrating through the lithosphere generating magmatism.	18
Figure 3.2 – Schematic cross-section of the earth, where can be seen the superplume hypothesis, with the superplume rooted on the CMB and that later station on the MTZ, with the two types of plume head represented. It is seen in the “plumelets” as well, adapted from Courtillot et al. (2003).	19
Figure 3.3 – Diagram of the EDC mechanism formation environment, near a craton where the structural or thermal anomaly can be created. Adapted from Matton & Jébrak (2009).....	21

Figure 3.4 - Simplified sketch of the hypotheses considered, the Shallow Advective Mantle, here shown as the EDC, originated near a fragility. The superplume with secondary “plumelets”, is the hypothesis that could generate dispersed occurrences with different geochemical signatures. And the primary plume or the hotspot, is the hypothesis that generates consistent magmatism, generating consistent plume tracks (such as the Hawaii archipelago). Modified from Koppers (2011)..... 21

Figure 4.1 - Workflow of the conceptualization of this work 22

Figure 4.2 - World map produced with GPlates, showing the outline of tectonic plates and microplates (in orange)..... 23

Figure 5.1 – Motion path (green) for the Lisbon volcanic Complex as part of the Iberia microplate. The star indicates the paleo-location of the intrusion in relation to the present day. Note the sinuous path of the Iberia microplate to its current location. 26

Figure 5.2 - Motion path (dark orange) for the Monchique Massif. The star indicates the paleo-location of the intrusion in relation to the present day. 27

Figure 5.3 - Motion path (orange) for the Tore Seamount. The star indicates the paleo-location of the intrusion in relation to the present day. 28

Figure 5.4 - Motion path (purple) for the Ampère Seamount. The star indicates the paleo-location of the intrusion in the present day..... 29

Figure 5.5 - Map showing the paleo-location of the modelled magmatic features (dark red polygons) and their motion path (green arrows). Please note that the arrows on this map may appear inverted compared to other maps because the model software presents movement in reverse order, starting from the current day and going back in time. 30

Figure 5.6- Map of the motion paths in detail, with their relative magmatic body. These paths are focused on the WIM area and the Madeira origin problem..... 31

Figure 5.7 – Two groups of plumes, the Eurasian group in green, and the African group in orange. 32

Figure 6.1 - Map with the area of influence (75 km) along the LVC motion path, the major effect was on the earlier stages that led to the intrusion of the WIM bodies..... 33

Figure 6.2 – Map with the area of effect caused by the Monchique motion path, here it can be seen two clusters of occurrences. One on the Iberian Plate, the WIM occurrences, and the other in the CISP, where the volcanism can be significantly younger..... 34

Figure 6.3 - Map with the postulated area of effect caused by the Tore motion path, displaying no connection whether to the WIM or the Madeira Archipelago..... 35

Figure 6.4 - Map with the area of effect caused by the Ampère motion path, here it can be seen a continuous trail that led to the formation of several occurrences. All of them are correlated as proven by (Geldmacher et al., 2005). 36

Figure 6.5 - Map of the plume tracks proposed in Geldmacher et al. (2005) and Merle et al. (2018), modified from Geldmacher et al. (2005) and Merle et al. (2018). The complete proposed track consists of both the full arrow and the dashed arrow. However, due to the significant age difference between the occurrence indicated by the dashed arrow and the occurrences depicted by the full arrow, a connection seems unlikely. So, it is proposed in this work that only the full arrow should be considered as previously discussed and displayed from the Monchique and Ampère motion paths (Fig. 6.2 and 6.4)..... 37

Figure 6.6 – Map with two plume areas. These regions encompass the surface projection of the underlying magmatic plume. The demarcation of these areas is derived from the multiple intrusion points identified, represented by the blue polygons. 38

Figure 6.7 – The South Plume, commonly referred to as the Moroccan Plume unequivocally displays the oldest occurrences in the CISP area. These occurrences have been grouped based on their age and paleogeographic proximity. The blue area on the map represents the plume head that generated the magmatism responsible for creating these occurrences. 39

Figure 6.8 - The Northern Plume, also referred to as the West Iberian Plume, is delineated by the red line depicted in this figure. This demarcation is established following the initial intrusion sites of each occurrence. This plume provides a plausible explanation for the observed magmatism in these areas, aligning with the temporal sequence. 39

LIST OF TABLES

Table 1 - Table with the ages of the different rocks presented in Sintra's massif. 1- Macintyre & Berger, 1982; 2- Storetvedt et al., 1987; 3- Miranda et al., 2009; 4- Grange et al., 2010; 10

Table 2 - Table with the ages of the different rocks presented in Monchique massif. 1- Storetvedt et al., 1987; 2- Miranda et al., 2009 ; 3- Grange et al., 2010 11

Table 3 - Table with the ages of the different rocks of the Monchique massif. 1- Rock, 1976; 2- Macintyre & Berger, 1982; 3- Bernard-Griffiths et al., 1997; 4- Miranda et al., 2009; 5- Grange et al., 2010..... 12

Table 4 - Table with the ages of the different rocks presented in LVC (s. l.). 1 -Miranda et al., 2009; 2- Mahmoudi, 1991; 3-Mendes & Bernard-Griffiths, 1973; 4- Ferreira & Macedo, 1979; 5- Neres et al., 2012..... 13

Table 5 – Assigned ages for each occurrence. Instances marked with an asterisk ("*") are founded on relative dating. In cases where multiple datings were available, an average of these datings was calculated. Notably, the error margin of these ages has not been incorporated, as it is not a prerequisite for the software used in the model generation..... 25

1. INTRODUCTION

The Mesozoic evolution of the North Atlantic region is characterized by a vast and intricate series of geological processes and events, including stages of rifting, upwelling of the mantle, volcanic activity, and significant tectonic activity (Manatschal & Bernoulli, 1999; Martins et al., 2010; Reston, 2009; Schettino & Turco, 2009). The rifting process, initiated in the Late Triassic period, and reaches its culmination in the Late Cretaceous, accompanied by seafloor spreading (Gaina et al., 2017; Péron-Pinvidic & Manatschal, 2009; Tucholke et al., 2007), as indicated by the first magnetic anomaly known as the J Anomaly (Bronner et al., 2011; Neres & Ranero, 2023; Nirrengarten et al., 2017; Sibuet et al., 2004; Szameitat et al., 2020; Tucholke & Ludwig, 1982). Concurrently, the once-unified supercontinent Pangea undergoes fragmentation, resulting in the formation of smaller tectonic plates, such as NW Africa, North America, and the Iberian Microplate (Schettino & Turco, 2009). This study primarily focuses on the Western Iberian Margin, situated within the Iberian Microplate.

The Iberian Margin serves as the location for numerous igneous features, comprising large laccoliths, volcanic edifices, and sills and dyke complexes, formed throughout the various stages of rift to drift (Escada et al., 2019; Grange et al., 2010; Martins et al., 2010; Mata et al., 2015; Merle et al., 2009; Miranda et al., 2009; Neres et al., 2018; Pereira et al., 2021; Pereira & Alves, 2011; Terrinha et al., 2018). These features are attributed to three distinct magmatic cycles, each exhibiting unique characteristics (Martins et al., 2010; Mata et al., 2015):

- 1) The Lower Jurassic magmatism is associated with the Central Atlantic Magmatic Province (CAMP) and with a tholeiitic signature (Martins et al., 2010).
- 2) The Upper Jurassic - Lower Cretaceous magmatism, is associated with small intrusions with a transitional signature (Mata et al., 2015).
- 3) The Late Cretaceous magmatism, associated with several occurrences on the Central-Northeastern Atlantic with an alkaline signature (Merle et al., 2018; Miranda et al., 2009; Neres et al., 2023; Van Den Bogaard, 2013).

Among these cycles, the Alkaline cycle stands out prominently due to its higher abundance and diversity of exposed formations compared to the other two cycles (Martins et al., 2010; Mata et al., 2015). Notable examples of this cycle include the Lisbon Volcanic Complex (LVC), Sintra, Sines, Monchique massifs, and several offshore formations, such as the Tore-Madeira Rise, and the Canary Archipelago (Canary Island Seamount Province) (Fig 1.1). Despite extensive research, there is a lack of consensus regarding the sublithospheric source or cause of this magmatic activity. Through geological surveys and age dating techniques applied to various outcrops, Ribeiro et al. (1979) proposed a theory suggesting a potential tectonic alignment among the three major magmatic bodies (massifs) and included the Tore seamount, a submarine mountain. This alignment supports the concept of a sublithospheric fault that could facilitate the intrusion of magmatic material. This postulated fault is believed to have been responsible for generating the former Cretaceous massifs.

In the present work, the current emplacement hypotheses are tested using GPlates (Müller et al., 2018). It is not tried to prove the validity of the theory but the geodynamic/palaeogeographical feasibility of these theories. Starting with the earlier occurrences at 150 Ma and finishing at the Present.

The present study was motivated by the theory proposed by Ribeiro et al. (1979), which suggested a potential alignment among the major magmatic bodies in the Iberian Margin. Considering recent information regarding deep mantle processes that could potentially explain the observed phenomena, the study aimed to investigate the validity of these ideas. To achieve this, the research was based on

three primary hypotheses: a) the linear Hot-Spot hypothesis advocated by Ribeiro et al. (1979), b) the Superplume hypothesis recently substantiated by Civiero et al. (2021), and c) the Edge-Driven Convection hypothesis proposed by King & Anderson (1998), which remains a topic of significant controversy within the scientific community. These hypotheses are discussed in Chapter 5.

To assess the validity of these hypotheses, multiple palaeogeographical reconstructions were conducted. These reconstructions aimed to examine the correlation between the initial emplacement spot of magma and the relative movements of tectonic plates. By utilizing the GPlates software (Müller et al., 2018), the study investigated potential connections between magma emplacement locations, mantle upwelling sources, and documented magmatic events.

As the research progressed, it became evident that the inclusion of additional areas was necessary to enhance the comprehensiveness of the study. The Tore-Madeira Rise, in the Central Northeastern Atlantic, and the Northwestern Moroccan Margin (NWMM), represented by the Canary Island Seamount Province (CISP), required consideration. These regions have a significant geological history, which dates to the Early Cretaceous and continues up to the present time (Fig 1.1).

Mineral carbonation and CO₂ storage have become critically important in the present day. Assessments by Gamboa & Pereira (2023), Moita et al. (2020), and Pedro et al. (2020) indicate that Late Cretaceous magmatism holds significant promise in creating a stable environment for these endeavours. Although this study is not directly related to mineral carbonation and CO₂ storage, it contributes to a deeper understanding of the focal area. Consequently, it has the potential to enhance and optimize future research efforts in this field, making them more efficient and effective.

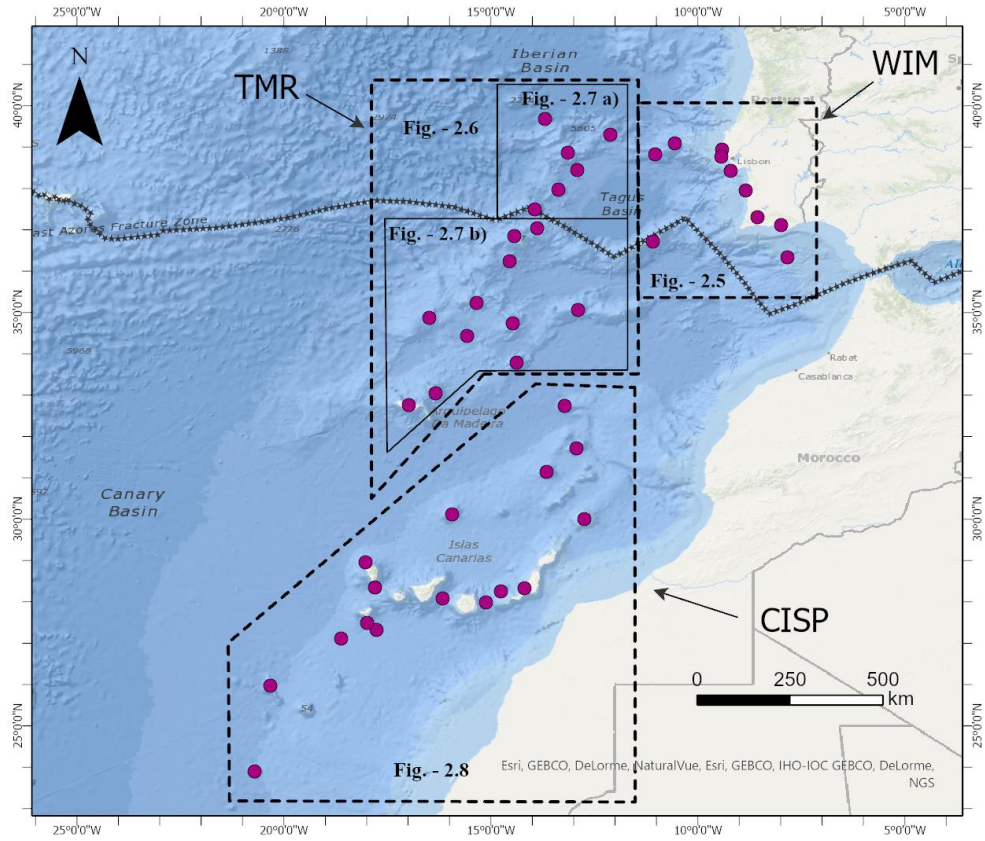


Figure 1.1 - Study area, with the regions of interest in this work, showing the locations of the magmatic occurrences investigated in this work. Locations based on Grange et al. (2010); Merle et al. (2018); Miranda et al. (2009); Van Den Bogaard (2013)

2. GEOLOGICAL BACKGROUND

2.1. THE WEST IBERIAN MARGIN

The classification of rifted continental margins, either as volcanic or non-volcanic (Boillot & Coulon, 1998; Mutter et al., 1988; White et al., 1992) was found to be inaccurate due to the presence of observable magmatism in supposedly non-volcanic margins (Desmurs et al., 2001; Whitmarsh, Manatschal, et al., 2001; Whitmarsh, Minshull, et al., 2001). To address this issue, a new classification system was proposed, which categorizes the margins along a spectrum from magma-poor (or magma-starved) to magma-rich (or magma-dominated) (Doré & Lundin, 2015; Reston, 2009; Reston & Manatschal, 2011; Sawyer et al., 2007). This revised categorization considers various morphological factors, which are used to calculate the magma budget of each margin (Doré & Lundin, 2015; Franke, 2013; Menzies et al., 2002; Reston, 2009; Tugend et al., 2020).

The West Iberian Margin (WIM) is a classic example of a hyper-extended magma-poor margin (Tucholke et al., 2007). However, the WIM records three discrete magmatic cycles (Martins et al., 2008; Mata et al., 2015; Miranda et al., 2009; Tugend et al., 2020).

The WIM was formed during multi-phase rifting, accompanying the Atlantic extension (Alves et al., 2009; Pereira & Alves, 2011), from the Late Triassic to the Early Cretaceous (Bronner et al., 2011; Pereira et al., 2021; Tucholke et al., 2007). During this period, rifting ultimately resulted in continental breakup. This process involved the upwelling of the mantle and the spreading of the seafloor, leading to the separation of the Iberian microplate, the NW Africa plate, and the North America plate (Boillot et al., 1989; Bronner et al., 2011; Féraud et al., 1988; Kneller et al., 2012; Nirrengarten et al., 2018; Sahabi et al., 2004; Sanchez et al., 2019; Schettino & Turco, 2009; Srivastava et al., 2000; Tucholke et al., 2007).

The magmatic activity on these kinds of margins (Figure 2.5) is preserved on the magma-rich margins, contrary to what is verified on the WIM, where the magmatic activity should be rare (Franke, 2013; Geoffroy, 2005). However, it is represented by three magmatic cycles, assigned to different mantle sources (Grange et al., 2010; Martins et al., 2008; Mata et al., 2015). The first two, respectively with tholeiitic and mildly alkaline signatures, are the consequence of the extensional episodes (Martins et al., 2008; Mata et al., 2015), whereas the latter, with an alkaline signature, is related to the post-rift evolution of the WIM (Grange et al., 2010; Merle et al., 2009; Miranda et al., 2009).

The Third cycle is of relevance to this study due to the ongoing discussion regarding the potential alignment of Late Cretaceous massifs found in the WIM, this debate served as the driving force behind this work. It is reported both onshore (Grange et al., 2010; Mahmoudi, 1991; Miranda et al., 2009; Neres et al., 2012, 2014, 2018; Rock, 1976, 1978; Terrinha et al., 2003) and on the offshore (Grange et al., 2010; Merle et al., 2019; Sanchez et al., 2019) (Fig. 1.1). This cycle is responsible for some of Portugal's most pertinent magmatic bodies, such as Sintra, Sines, and Monchique massifs', and the Lisbon Volcanic Complex (Miranda, 2010; Miranda et al., 2009; Palácios, 1985). Also, it's thought to create several seamounts in the Tore-Madeira Rise (TMR) and all the magmatism present in the Estremadura Spur (Escada, 2019; Escada et al., 2019; Pereira et al., 2021). More recently, new geophysical evidence of previously unreported magmatic features was investigated in the south of Portugal (the Portimão magnetic anomaly) and offshore the Lusitanian and Alentejo Basins (Neres et al., 2018, 2023)

2.2. MAGMATIC CYCLES

The WIM is the locus of several Mesozoic magmatic events, occurring in three cycles departing nearly 50 Ma from each other (Terrinha et al., 2018). The outcrops are distributed unevenly but, generally, occur southwards of the Nazaré Fault, whether onshore or on the offshore (Escada, 2019; Grange et al., 2008, 2010; Martins et al., 2008, 2010; Merle et al., 2009, 2018; Miranda et al., 2009; Neres et al., 2014, 2018, 2023; Pereira et al., 2021, 2022).

The first two cycles are well described whether their petrology or their magma genesis (Martins, 1991; Martins et al., 2008; Mata et al., 2015; Terrinha et al., 2018). However, the third cycle, which corresponds to the largest spatial extent and encompasses the longest period of activity, is still intriguing, and the magma emplacement mechanisms are still under discussion (Neres et al., 2018).

The first cycle occurs in the Early Jurassic, about 200 Ma ago, and has a basaltic tholeiitic signature (Martins et al., 2008). The second cycle with a mildly alkaline, sometimes referred to as a transitional cycle, is the result of the stretching of the lithosphere during the early stages of the Atlantic opening, during the Jurassic-Cretaceous transition (148 to 140 Ma ago) (Mata et al., 2015). The third and last cycle extends from 100 to 70 Ma, is characterized by a dominant alkaline signature, and is related to the drift phase of the Atlantic opening (e.g. Miranda et al. (2009); Neres et al., (2014)).

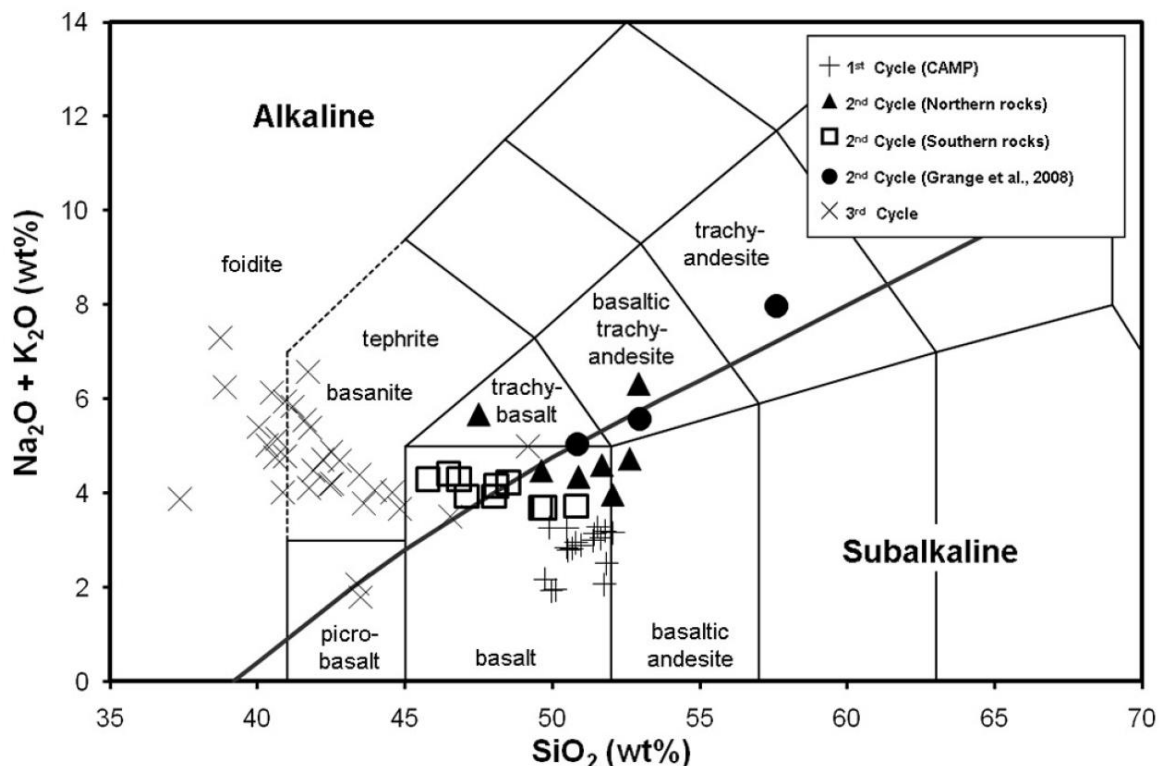


Figure 2.1 - Geochemical signature of the three magmatic cycles on the WIM (Mata et al., 2015)

2.2.1. FIRST CYCLE- THOLEIITIC

The first magmatic cycle is related to intracontinental rifting suffered by Pangea, this rifting led to the opening of the Central and North Atlantic (Martins et al., 2008). This episode generated a Large Igneous Province (LIP), this LIP is known as Central Atlantic Magmatic Province (CAMP) (Marzoli et al., 1999). The CAMP is dated from the Lower Jurassic (Verati et al., 2007), and it has occurrences in

the Iberian Peninsula, Newfoundland, and throughout the western coast of Africa and the East coast of the United States of America (Cebriá et al., 2003) (Fig. 2.2). The CAMP is characterized by basaltic rocks, assigned to continental flood basalts, these being titanium-depleted basalts (Martins et al., 2008).

In the WIM, the main occurrences outcrop on the Algarve Basin, but also Lusitanian and Alentejo Basins. The main outcrops consist of extrusive rocks such as subaerial lava flows, pyroclastic deposits, and peperites, these lithologies are mainly associated with swarms of dykes, with one of them being the Messejana-Plasencia Dyke (Cebriá et al., 2003; Martins, 1991; Schermerhorn et al., 1978; Schott et al., 1981).

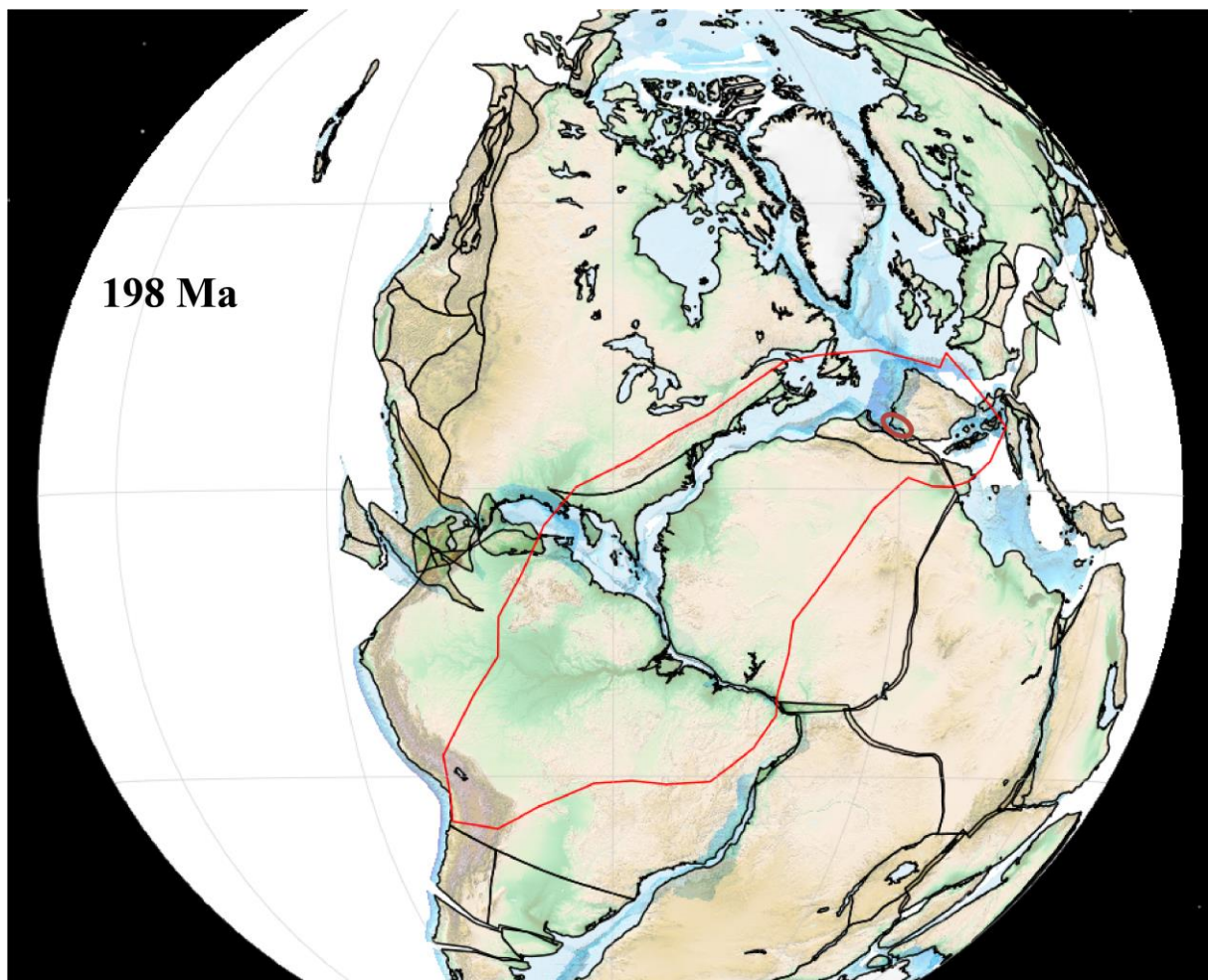


Figure 2.2 – Map of the CAMP (red) with the location of the Iberian occurrences marked (dark red), adapted from Marzoli et al. (2018).

2.2.2. SECOND CYCLE – TRANSITIONAL TO MILDLY ALKALINE

The second cycle is less widespread and less known of these three cycles (Fig. 2.3). Known occurrences are mainly in the northern and central parts of the Lusitanian Basin, distributed in two prevalent sub-meridional alignments (groups) (Grange et al., 2010; Martins et al., 2008; Mata et al., 2015).

One of the alignments occurs at the East of the basin from Rio Maior to Vermoil (Rio Maior – Porto de Mós – Alqueidão da Serra – Vermoil), and the other alignment outcrops on the West margin of the Lusitanian Basin from Nazaré to Soure (Nazaré – Monte Real – Monte Redondo – Soure) (Mata et al., 2015). These alignments are divided by the Nazaré fault, the first one in the South and the latter in the

North (Mata et al., 2015). Mainly constituted by swarms of dykes and sills, but with different lithologies in each group, showing that the southern rock display little to no alteration, dissimilarly the northern group shows a very intense hydrothermal alteration (Mata et al., 2015). The southern group comprises unaltered dolerites including porphyritic textures with phenocrysts of olivine on a cryptomicrocrystalline matrix (Mata et al., 2015). The northern group is constituted by very altered coarse-grained dolerites and gabbros with the most common texture being sub-ophitic displaying altered plagioclase and alkaline feldspar, with quartz, evidencing the sub-alkaline magma composition (Mata et al., 2015). Other magmatic bodies occur, although with limited expression, including, some small laccoliths (in the northern sector), and some sub-perpendicular dykes (in the central sector) (Mata et al., 2015). There's also a total lack of extrusive activity from this cycle, something not verified whether on the first or the third cycle (Mata et al., 2015).

As later shown according to the dating done by Mata et al. (2015) and Grange et al. (2008), both groups have a similar age, being considered contemporaneous. Also, several geochemical surveys showed that the northern rocks are more evolved, implying that there were different temperature profiles and that the northern magma chambers were more voluminous. More can be extracted from those surveys, that the southern rocks were the result of much less partial melting than the northern rocks generated by differentiation of magmas produced by higher partial melting (Mata et al., 2015).

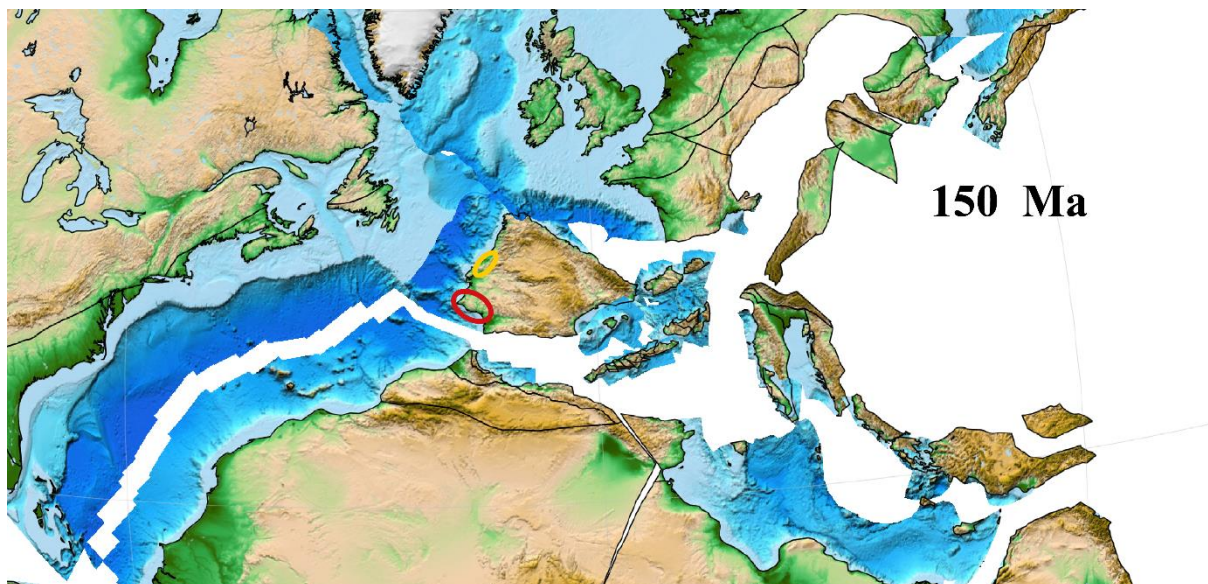


Figure 2.3 - Position of the Iberian Peninsula at 150 Ma showing the relative paleogeographic position of the first (yellow) and second magmatic cycles (red).

2.2.3. THIRD CYCLE – ALKALINE

Towards the end of the Mesozoic, the last magmatic cycle emerged within the Western Iberian Margin (WIM). Referred to as the Late Cretaceous Alkaline Cycle (LCAC), it is characterized by two distinct pulses of intrusive activity in the WIM (Miranda et al., 2009). The first pulse was initiated around 100 million years ago and persisted until 88 million years ago (Fig. 2.4). This initial pulse is notably more intense than the second, resulting in the formation of various intrusive features, including large magmatic bodies, as well as a range of sills and dykes (Miranda et al., 2009).

The second pulse of the Late Cretaceous Alkaline Cycle (LCAC) is characterized by a lower intensity compared to the first pulse (Miranda et al., 2009). However, it covers a larger geographical area due to the larger volume of extruded magma (Miranda et al., 2009). It is important to note that the accuracy of the age estimation for this pulse, particularly the ages ranging from 75 to 72 million years ago, may be questionable as these ages only consider the onshore occurrences (Mata et al., 2015).

The Sintra Massif is indeed associated with the first pulse. However, the accurate dating of the LVC that should be attributed to the second pulse is challenging. Despite the ages indicating its association with the second pulse, the precise dating of the LVC remains uncertain (see Chapter 2.3 Introductory Note on Geochronology and 2.3.1 LVC). Sines and Monchique Massifs are included in the second pulse (Miranda et al., 2009; Neres et al., 2018; Terrinha et al., 2018). The Estremadura Spur Intrusion (ESI) and the Fontanelas Volcano (FV), are also thought to be included in this cycle, being described based on seismic stratigraphy, with their age estimated at 87 and 81 Ma, respectively (Escada et al., 2022; Pereira et al., 2021, 2022).

Indeed, the magmatic occurrences associated with the Western Iberian Margin (WIM) are not limited solely to that region. Notably, similar magmatic events are documented in the Pyrenean and Catalan Coastal areas, as described by Solé et al. (2003) and Ubide et al. (2014). These authors have provided dating information for these occurrences, which aligns with the Cretaceous age assigned to the magmatism in the WIM. Thus, these additional occurrences further support the broader extent of Cretaceous magmatism in the studied region. This magmatism was not considered in this work, because of the large distance between the WIM and these occurrences.

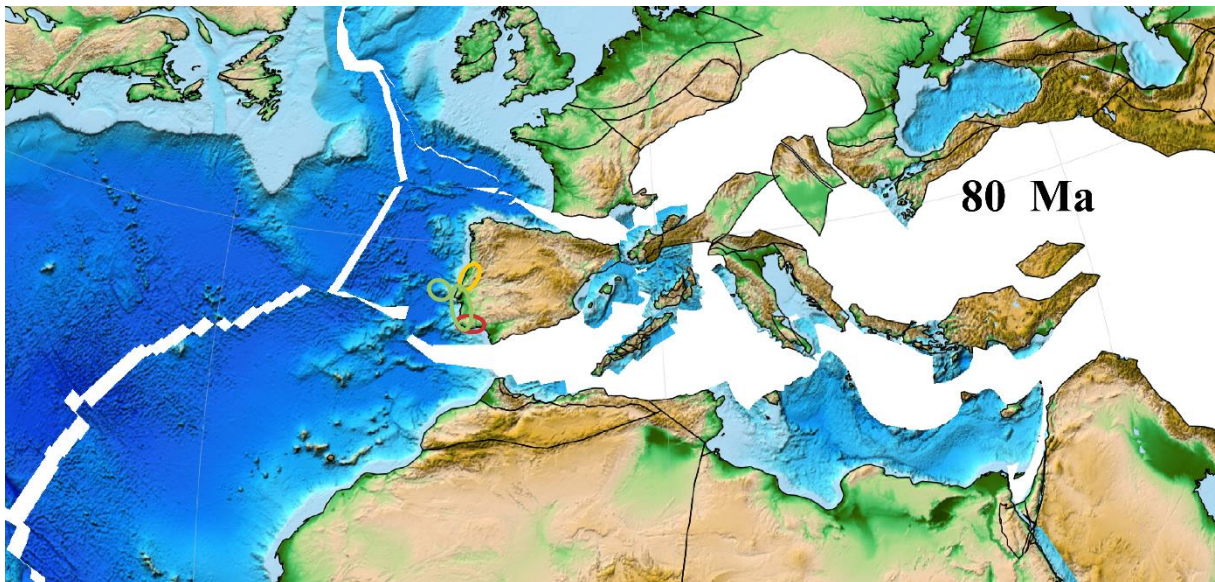


Figure 2.4 - Position of the Iberian Peninsula at 80 Ma with the relative position of the first cycle, second cycle and third cycle marked by the red, yellow and green ellipses, respectively.

2.3. EVIDENCE OF THE THIRD CYCLE

Introductory note on geochronology

To construct the models for this work, the main inputs needed were the spatial place of the intrusion and their age. The several presented intrusions have been studied since their discovery, which led to an abundance of ages. The model done did not necessarily need the exact age dating, but instead a fixed age, within the ages given and their associated error. To pick the ages given to each intrusion, it was needed to filter them. The main filter was based on geochemical elements, such as the robustness of the dating method (see next paragraph). This led to a shorter number of datings, and then based on these fewer ages, it was done the average between them and used as the given age of the magmatic body (see Table 1, 2, 3, and 4).

Datings were performed using the K/Ar, the Ar/Ar, the Rb/Sr, and the U/Pb methods. All these methods have pros and cons, starting with the less reliable one, the K/Ar method. This method is the least dependable, based on the variance this procedure presents. From the freshness of the rock to simple analytical techniques, this method incorporates a big error. This means that the degree of alteration interferes with the dating, to exemplify this, should be a rock with an increase or decrease in potassium, which would deviate the age from the rock's accurate age (Bradley, 2015). The Rb/Sr method incurs the same problem. These elements are LILE (Large Ion Lithophile Elements), so they are very mobile in fluids, so it is possible to remove these elements, which causes a variance in the age of the rock.

Both the U/Pb and Ar/Ar methods are the more reliable of the presented ones (Bradley, 2015). Either for the elements in use (Ar/Ar) or for the very high temperature on which the system closes (U/Pb). The U/Pb method is one of the most reliable methods, if not the most, derived from the very high temperature of system closure, nearly 900 °C (Bradley, 2015). This provides an accurate age of the first mineral crystallization, the age of emplacement. The Ar/Ar method is the replacement for the K/Ar method because uses the same procedures. This method only needs to measure the ^{39}Ar , instead of ^{40}K . This isotope of Ar is produced in a nuclear reactor to replace the K isotope (Bradley, 2015). Consequently, when needed to filter the ages given, the latter methods were chosen over the first ones.

2.3.1. MAGMATISM ON SOUTHWEST IBERIA

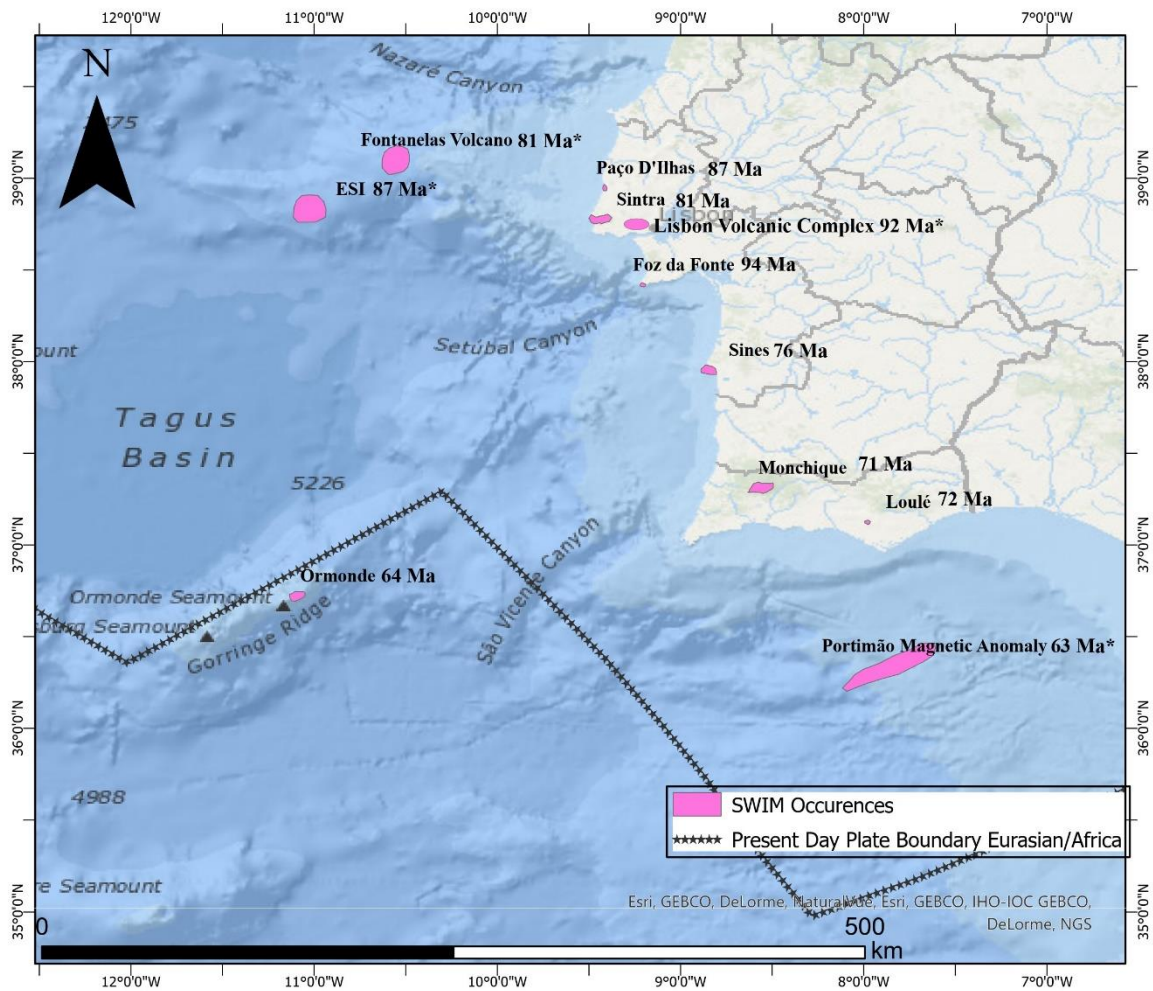


Figure 2.5. Map of the SWIM, with the detail of every magmatic body under study and their respective age as used on the models. The ages marked with an asterisk (*) were estimated using seismic stratigraphy. ESI – Estremadura Spur Intrusions.

SINTRA

Sintra Massif (50 Km²) (Fig. 2.5) is one of the most critical Cretaceous reliefs on Portugal's mainland. The massif reaches 579 meters above sea level between Cascais and Sintra. Presenting itself as an elliptical body elongated in the W-E direction, it has two segments, both approximately equal in size, one on the onshore and the other on the offshore (Terrinha et al., 2018).

The massif intrudes Jurassic and Cretaceous sedimentary rocks, ranging from limestones to sandstones. The Upper Jurassic rocks are mainly limestone but also include some marl and claystone. Only one of these units (São Pedro limestones, Late Jurassic) appears metamorphized. It also intrudes some Cretaceous units, starting and ending with calcareous-clastic lithologies, dated from the Cenomanian (Late Cretaceous). Sintra appears cutting the Cenozoic cover: from the Benfica formation, the first unit to appear since the Cenomanian, dated from the Oligocene to the Quaternary deposits (Ramalho et al., 1999).

This intrusive complex ranges in composition from gabbros to granites, which are not considered comagmatic (e.g., Leal, 1991). It consists of a granite laccolith resulting from the Variscan basement anatexis (Leal, 1991) associated with a gabbro-syenitic body, whose magma was produced in the mantle with minor to no crustal contamination (Leal, 1991; Palácios et al., 1995). Field data suggest that the granite laccolith is younger than the gabbroic body (Kullberg & Kullberg, 2020). It also displays a complex network of sills and dykes, with both mafic and felsic signatures, as well as multi-compositional breccias (Alves et al., 1964). The mafic dykes pre-date the gabbroic body and the felsic ones appear after the granite intrusion (Kullberg & Kullberg, 2000, 2020; Terrinha et al., 2018). This is verified by the age diversity and range from 84 to 75 Ma. (Table 1).

Table 1 - Table with the ages of the different rocks presented in Sintra's massif. 1- Macintyre & Berger, 1982; 2- Storetvedt et al., 1987; 3- Miranda et al., 2009; 4- Grange et al., 2010;

Reference	Lithologies	Age (Ma)	Error (Ma)	Mineral	Method
1	Granite	81.9	0.4	Biotite	K-Ar
2	Granite	84.0	1.1	K Feldspar	K-Ar
2	Syenite	76.4	1.4	Whole Rock	K-Ar
2	Syenite	76.1	1.1	Whole Rock	K-Ar
2	Syenite	78.3	1.9	Whole Rock	K-Ar
2	Gabbro	74.9	1.0	Whole Rock	K-Ar
3	Granite	79.2	0.8	Zircon	U-Pb
4	Micro-Granite	82.0	0.7	Zircon	U-Pb
4	Gabbro	83.4	0.7	Zircon	U-Pb
4	Micro-Syenite	80.1	1.0	Zircon	U-Pb
4	Granite	81.7	0.4	Zircon	U-Pb

Based on the provided data, it is possible to establish an intrusion sequence, as it is observed that the gabbros are the eldest occurrences. Followed by the granites, micro-granites and ending with the emplacement of the syenites.

SINES

The Sines Massif (Fig. 2.5) is a subvolcanic ring-shaped massif, with an elongated WNW-ESE direction, intruding through the pre-existent Variscan fractures of the basement (Inverno et al., 1986; Teixeira, 1962). Only a small portion of the original mass is outcropping, the largest being located offshore (Silva et al., 2000). In a recent study by Neres et al. (2023), a magnetic anomaly was documented along the extension of this massif. The authors propose that the Sines magnetic anomaly could potentially represent the offshore continuation of the same massif. This massif intrudes in limestone sequences, dated from the Lower Jurassic (Sinemurian) to the Upper Jurassic (Kimmeridgian) (Inverno et al., 1986; 1993). On outcrops, the Sines massif is overlain by Miocene and Holocene deposits (Inverno et al., 1986; 1993).

Its emerged portion displays several types of rocks: syenites, gabbro-diorites, dolerites/basalts dykes and mafic eruptive breccias (Canilho, 1972; Grange et al., 2010; Rock, 1978). The gabbro-dioritic unit is described as a mixed unit, with no sharp limit between the two lithotypes. However, the contact between the gabbroic unit and the syenites sometimes shows the presence of breccia with a syenitic cement and some gabbro fragments, showing that the syenites are younger than the gabbros (Canilho, 1972, 1989). The sills and dykes are very diverse consisting mainly of basalts, dolerites and micro-gabbros (Inverno et al., 1986) (Table 2).

According to Inverno et al. (1986), the emplacement of the massif was done in four phases: i) the emplacement of the gabbro-dioritic body, then ii) the emplacement of the syenites and micro-syenites, iii) the creation of the eruptive breccia, and ending with iv) the emplacement of the dyke swarm, both basic and acid rocks. However, the fact that breccias occur in the contact between gabbro and syenitic rocks and its matrix is syenitic suggests that they are synchronous of the syenite intrusion.

A geophysical study (Ribeiro et al., 2013) was carried out in this massif, which involved calculating the palaeopole positions. The palaeopositions of the massif align with other late Cretaceous occurrences in the Western Iberian Margin (WIM), such as Sintra, Sines, and LVC (Ribeiro et al., 2013). These findings have led to the dismissal of the previously proposed two-rotation model (Storetvedt et al., 1987) that occurred in Iberia and instead suggest a model without significant rotation in the region (Voo, 1993).

Table 2 - Table with the ages of the different rocks presented in Monchique massif. 1- Storetvedt et al., 1987; 2- Miranda et al., 2009; 3- Grange et al., 2010.

Reference	Lithology	Age (Ma)	Error (Ma)	Mineral	Method
1	Syenite	63.8	0.8	K Feldspar	K-Ar
1	Syenite	75.2	0.8	K Feldspar	K-Ar
1	Diorite	79.1	1.5	Whole Rock	K-Ar
1	Diabase	75.5	1.1	Whole Rock	K-Ar
1	Diabase	74.6	1.9	Whole Rock	K-Ar
1	Diabase	78.2	1.7	Whole Rock	K-Ar
1	Diabase	62.0	1.3	Whole Rock	K-Ar
2	Syenite	75.4	0.6	Zircon	U-Pb
3	Gabbro	77.2	0.6	Zircon	U-Pb
3	Gabbro	77.2	0.4	Zircon	U-Pb
3	Micro-Syenite	75.4	1.2	Zircon	U-Pb
3	Micro-Syenite	74	2.4	Titanite	U-Pb

Considering only the U-Pb datings, the massif would have been crystallized between ≈ 74 and ≈ 77 Ma, with gabbros being some 2 Ma more precocious than syenites. As mentioned, the earlier installation of gabbros is endorsed by the field information of geometry and cross-cut relations.

MONCHIQUE

Monchique Massif (Fig. 2.5) is the largest of three Cretaceous onshore massifs, with the recurrent elliptical shape elongated in the W-E direction (Grange et al., 2010). It was described by Rock (1978), as a subvolcanic laccolith intruding in late Carboniferous marine sediments. It is mainly composed of nephelinitic syenite, but also diorites and alkali gabbro (Grange et al., 2010; Rock, 1978), with some brecciated lithologies (basalt, syenite, phonolite, and some pelitic fragments) (Rock, 1978). There is also a dyke swarm, mainly formed of lamprophyres.

According to Rock (1978) and González-Clavijo & Valadares (2003), there is a specific order of intrusion, starting with i) the intrusion of the basic magma, ii) the intrusion of several nephelinitic syenite bodies (heterogeneous) and finally iii) the intrusion of the big homogeneous nephelinitic syenite body.

This massif is considered the youngest Cretaceous massif in Portugal based on determinations using the classic systems (Rb/Sr and K/Ar) (Bernard-Griffiths et al., 1997; Macintyre & Berger, 1982; Rock, 1976, 1978), and more recently with the U/Pb and Ar/Ar systems (Grange et al., 2010; Miranda et al., 2009) (Table 2.3).

Table 3 - Table with the ages of the different rocks of the Monchique massif. 1- Rock, 1976; 2- Macintyre & Berger, 1982; 3- Bernard-Griffiths et al., 1997; 4- Miranda et al., 2009; 5- Grange et al., 2010.

Reference	Lithology	Age (Ma)	Error (Ma)	Mineral	Method
1	Various	72.0	2	Whole Rock	Rb-Sr
2	Syenite	74.9	1.5	Nepheline	K-Ar
2	Syenite	74.8	1.5	Nepheline	K-Ar
2	Syenite	73.0	1.5	Nepheline	K-Ar
2	Syenite	69.0	1.4	Feldspar	K-Ar
2	Syenite	68.1	1.4	Feldspar	K-Ar
2	Syenite	66.8	1.4	Feldspar	K-Ar
2	Syenite	69.3	1.4	Nepheline	K-Ar
2	Syenite	69.3	1.5	Nepheline	K-Ar
2	Syenite	68.3	1.4	Nepheline	K-Ar
2	Syenite	72.0	1.5	biotite	K-Ar
2	Syenite	70.9	1.5	biotite	K-Ar
2	Syenite	72.0	1.6	biotite	K-Ar
2	Syenite	67.2	1.5	Feldspar	K-Ar
2	Syenite	67.8	1.4	Feldspar	K-Ar
2	Syenite	65.0	1.3	Feldspar	K-Ar
3	Various	72.0	1.5	Whole Rock	Rb-Sr
4	Lamprophyre	72.7	2.7	Amphibole	Ar-Ar
4	Nepheline Syenite	71.5	3.6	Whole Rock	Rb-Sr
5	Nepheline Syenite	68.8	1.0	Titanite	U-Pb
5	Gabbro	70.0	2.9	Titanite	U-Pb

Using only the ages obtained by the U-Pb method, the most reliable one, the nepheline syenites and gabbros crystallized at around 70 Ma. The obtained age by Ar-Ar is similar within the limits of the error.

LISBON VOLCANIC COMPLEX

The Lisbon Volcanic Complex (LVC) (Fig. 2.5) covers a total area of about 200 km² ranging between the Nazaré and Arrábida faults (Miranda, 2010). It is essentially formed by extrusive rocks, it also comprises some intrusive occurrences, including volcanic necks, lava flows, pyroclasts, plugs, dykes, sills, and breccias have been described (e.g.: Miranda, 2010). According to Palácios (1985), the main composition is dominantly basaltic (s. l.), but also includes, on a much smaller scale, intermediate and even acid terms (rhyolites).

The LVC overlies Late Cretaceous limestones, dated from the Cenomanian, and the Fanhões Conglomerates also with a Cenomanian age (Marques et al., 1998), a conglomeratic unit, displaying a dark limestone. This could fill the gap between the last preserved unit to the LVC and the Cenomanian rocks directly underneath (Manuppella et al., 2011; Marques et al., 1998; Pais et al., 2006). The LVC is overlain by the Benfica Formation of Oligocene age, and quaternary deposits (Manuppella et al., 2008; Pais et al., 2005) (Table 4).

From a geochronological viewpoint, there are only two published datings, both giving ages around 72 Ma, 72.6 ± 3.1 Ma (Ferreira & Macedo, 1979) and 72 ± 2 Ma (Mendes & Bernard-Griffiths, 1973).

This dating has been disputed considering, paleomagnetic pole data (Neres et al., 2012). Based on the magnetic pole of the LVC, its age should be comprised between 100 to 88 Ma, instead of circa 72 Ma. More concordant with the age inferred from the paleomagnetic pole, are two more recent age determinations, one using K-Ar (Mahmoudi, 1991) (Paço D'Ilhas, PDI) and the other using Ar/Ar (Foz da Fonte, FdF) (Miranda et al., 2009), both giving a much older age, around 90 Ma. The PDI has a mean age of 87 ± 2.7 Ma, and the FdF has an age of 93.8 ± 3.8 Ma. The age of FdF seems to be supported by several pieces of evidence that point to the beginning of the volcanism circa 100 Ma (R. Miranda personal communication in Neres et al., 2012). With this chronological information and the relative spatial closeness, these occurrences will be included in the LVC (s.l.).

Considering the above-mentioned constraints, we will consider that wider LVC was formed at about 88-90 Ma. However, given the scarcity of data, more isotope ages are needed to better constrain the time lapse during which volcanism was active in the region.

Table 4 - Table with the ages of the different rocks presented in LVC (s. l.). 1 -Miranda et al., 2009; 2- Mahmoudi, 1991; 3-Mendes & Bernard-Griffiths, 1973; 4- Ferreira & Macedo, 1979; 5- Neres et al., 2012

Reference	Lithology	Age (Ma)	Error (Ma)	Mineral	Method	Location
1	Tephrite	93.8	3.9	Amphibole	Ar-Ar	Foz da Fonte
2	Monzogabroic, Monzonitic, Syenitic beds	88.0	2.7	Biotite	K-Ar	Paço de Ilhas
2	Monzogabroic, Monzonitic, Syenitic beds	86.8	2.5	K Feldspar	K-Ar	Paço de Ilhas
3	Basalt	72	2	Whole Rock	K-Ar	LVC
4	Basalt	72.6	3.1	Whole Rock	K-Ar	LVC
5	-	100 - 88	-	-	Geophysical Pole Determination	LVC

1	Lamprophyre	71.8	1.9	Biotite	K-Ar	Loulé
---	-------------	------	-----	---------	------	-------

LOULÉ DYKES AND OTHER OCCURRENCES IN ALGARVE BASIN

According to Martins (1991), these late Cretaceous occurrences consist of dykes, sills, plugs, and necks ranging from basanitic to lamprophyric natures. They are thought to be correlated with the Monchique massif, as proposed by Martins (1991), based on the geochemical affinities suggesting that these have the same source, the sublithospheric mantle. This is also reinforced based on the closeness of ages for either the Monchique massif or the Loulé dykes (Table 3, 4).

ESTREMADURA SPUR INTRUSION AND FONTANELAS VOLCANO

The SWIM offshore occurrences were discovered through geophysical surveys conducted by Escada, (2019), Escada et al. (2019), Neres et al. (2014), and Silva et al. (2000). These bodies exhibit distinct geophysical signatures, prompting further investigation (Escada, 2019; Escada et al., 2019; Pereira et al., 2021, 2022). Based on seismic stratigraphy and geophysical field data, these authors described the bodies.

More recently, Escada et al. (2022) characterized the lithology of these bodies by comparing their physical properties with onshore occurrences. This analysis confirmed that Estremadura Spur Intrusion (ESI) is a granite body, likely a laccolith, while Fontanelas Volcano (FV) is a buried volcano with a basaltic nature. These bodies hold significant importance due to their proximity to the surface, offering insights into the shallow magmatic plumbing below.

Both occurrences have given ages from the Late Cretaceous, from Turonian to Lower-Campanian to Fontanelas Volcano, and Lower- to Mid-Campanian to Estremadura Spur Intrusion.

2.3.2. TORE - MADEIRA RISE

The Tore-Madeira Rise (TMR) is a seamount chain in the Central-Northeastern Atlantic (Fig. 2.6), alongside the Portugal and Morocco coast. Formed during the drifting and rotation of the Iberian Peninsula during the Cretaceous (Boillot et al., 1988), the TMR, includes nearly 12 seamounts, with an extension of nearly 1000 Km along with the Portuguese coast (Merle et al., 2018). Surrounded by several scattered seamounts, the main alignment trends are from NNE-SSW (Merle et al., 2009).

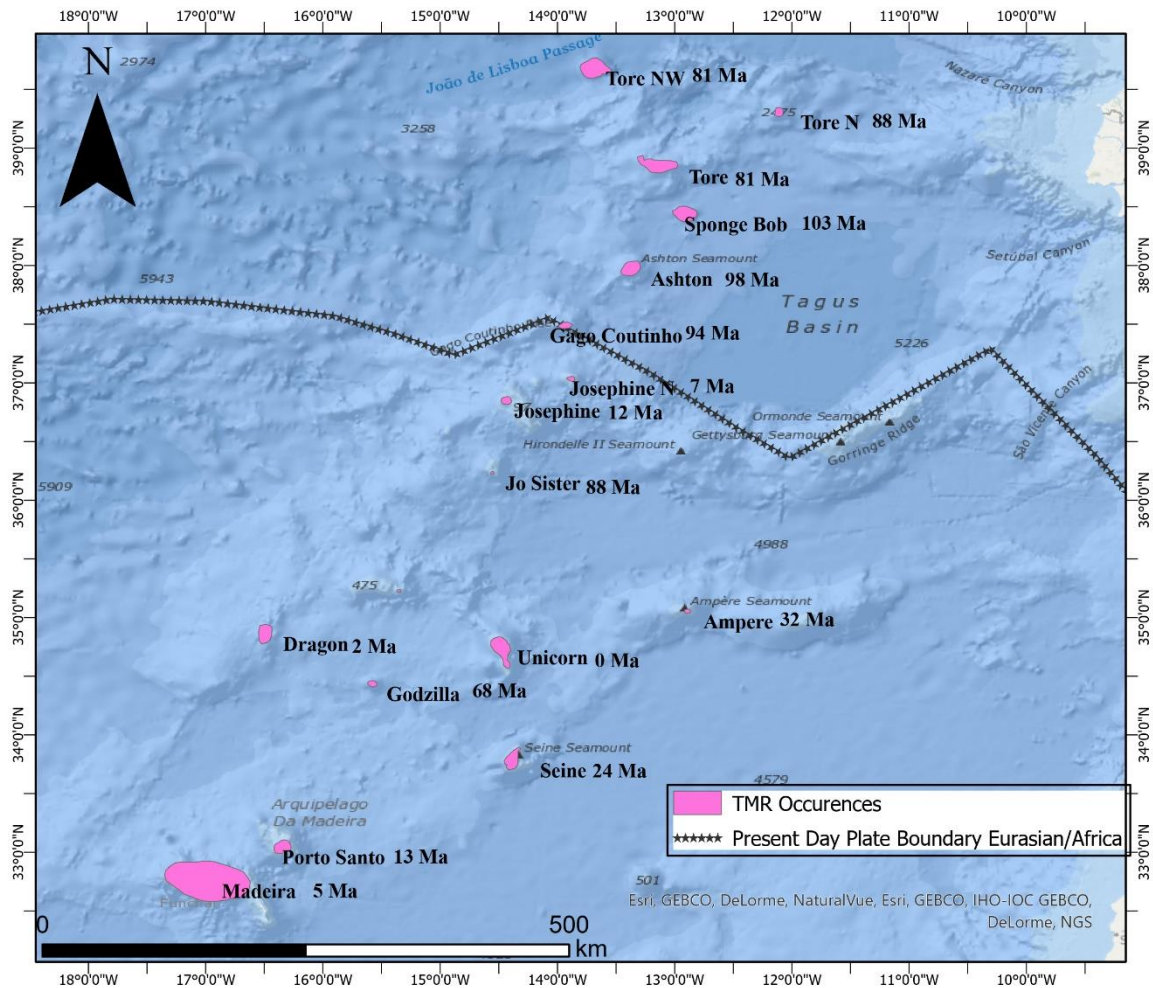


Figure 2.6 - Map of the Tore-Madeira Rise, with the respective age of each body. It can be seen in the Eurasian-African Plate Boundary

The TMR extends across the Azores Gibraltar Fault Zone (the boundary between Eurasian and African plates) (Merle et al., 2018). Displaying a range of ages from 103 Ma to the Present, it is postulated to be related to the third magmatic cycle, this being coeval with the ages provided by Geldmacher et al. (2005, 2006), Grange et al. (2010), Merle (2006), Merle et al. (2009), Miranda et al. (2009). The TMR can be divided into two smaller groups according to the tectonic plate that they are inserted. The Northern group consists of Tore (subdivided into NW, N and E), Sponge Bob, and Gago Coutinho, and are generally older than the Southern occurrences (Fig. 2.7a). According to Ribeiro et al., (1979), these occurrences can be correlated to the SWIM. The Southern group provides the youngest occurrences, that suggest a mantellic source beneath the African plate. This group includes the Madeira

Archipelago. However, the geographical spreading in this group is larger but broadly trends north to south with a decrease in age (Fig. 2.7b).

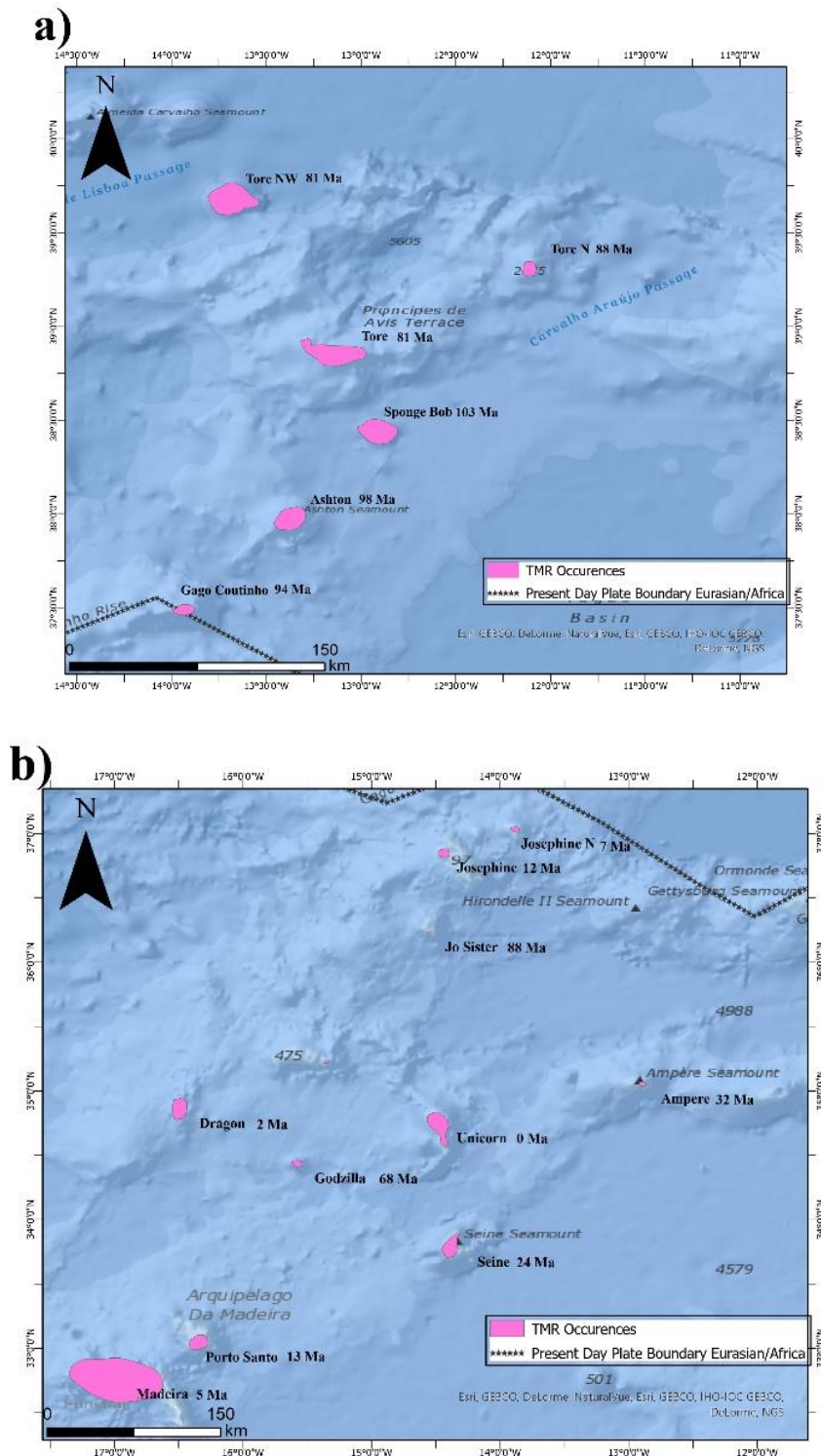


Figure 2.7 - a) Map of the Northern Group (Eurasian), b) Map of the Southern Group (African)

2.3.3. CANARY ISLAND SEAMOUNT PROVINCE

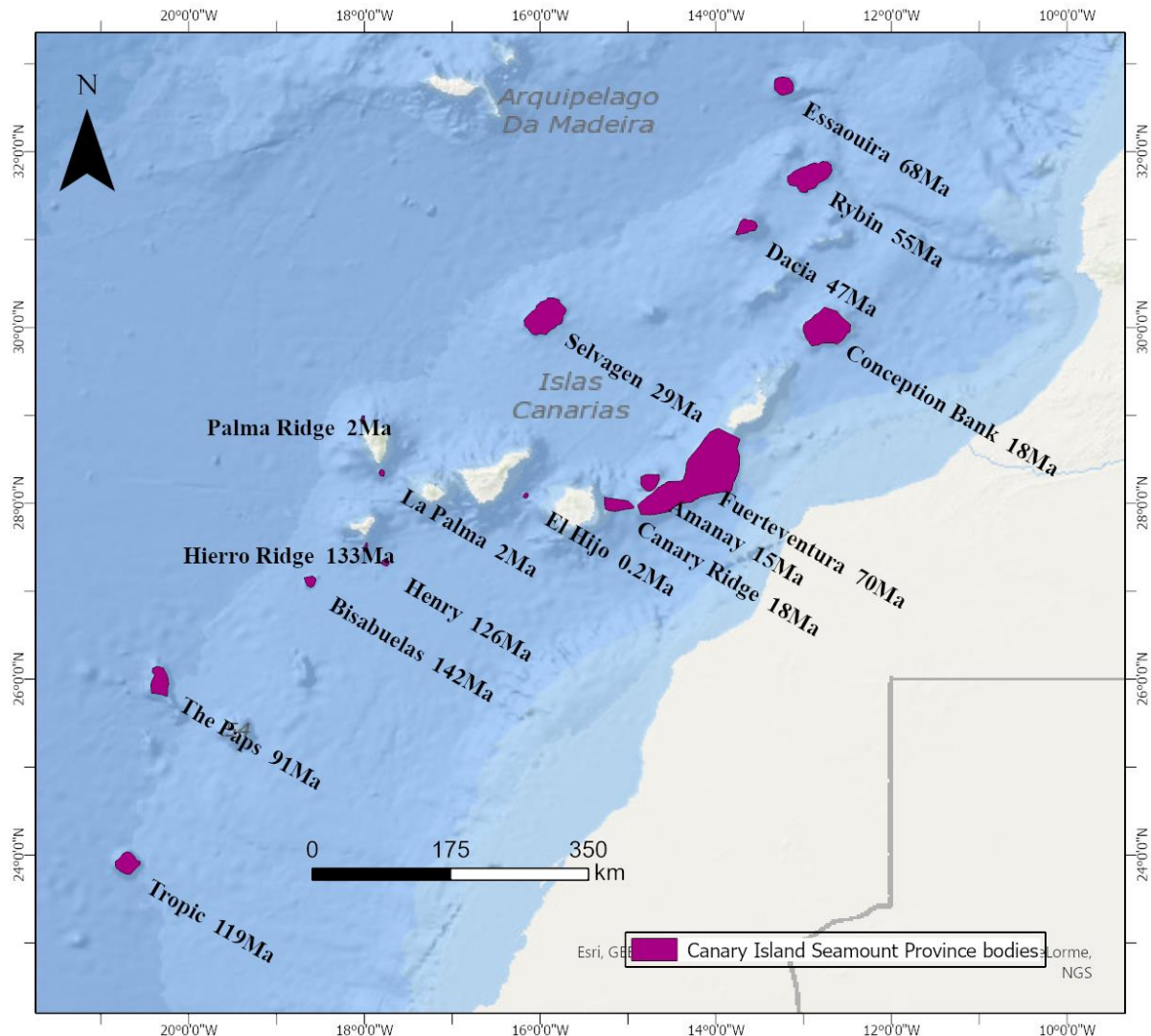


Figure 2.8 - Map of the Canary Island Seamount Province (CISP), with the respective age for each body.

The Canaries archipelago is located within the Canary Island Seamount Province (CISP) spanning for approximately 1300 km (Fig. 2.8). The CISP is positioned above the Jurassic oceanic lithosphere, which was formed during the early stages of the Central Atlantic opening. Age data reveal a trend, where seamounts within the CISP grow at a faster rate compared to the islands (Van Den Bogaard, 2013). However, the different islands and seamounts within the region are in various stages of the ocean island cycle (Negredo et al., 2022).

These islands exhibit a lithospheric sequence that is commonly attributed to the influence of a hotspot (Carracedo, 1999; Carracedo et al., 1998; Geldmacher et al., 2005). Nevertheless, Negredo et al. (2022) explored various models to determine the likely conditions that led to the formation of the CISP, considering possibilities such as Hot Spot magmatism (Morgan, 1972), Edge-Driven Convection, or a combination of both. Their research aimed to shed light on the underlying mechanisms responsible for the development of the Canary Island Seamount Province.

3. MODELS FOR INTRAPLATE MAGMATISM

3.1. SINGLE LINEAR HOTSPOT

This model is the model of a stationary hotspot. A hot spot refers to a localized area with an anomalously high heat flow from the Earth's interior, resulting in volcanic activity and the formation of volcanic features such as islands, seamounts, and continental flood basalts. Hot spots are often associated with mantle plumes, which are narrow upwellings of exceptionally hot rock from deep within the Earth's mantle. These plumes can lead to the melting of overlying rock, generating magma that eventually reaches the surface and forms volcanic structures (Foulger & Anderson, 2005; Lawver & Müller, 1994; Morgan, 1971).

However, not all seamounts share the same geodynamic context, prompting their categorization into three types (Courtilot et al., 2003). The first type, also called primary plumes or the Morgan-Style group, represents a long-lasting mantle plume originating near the core-mantle boundary (CMB) (Koppers, 2011) (Fig. 3.1, 3.4). This model will be based on this first group, the primary plumes. Yet, inherent gaps exist in this model due to the static nature attributed to this type of hotspot. This contradicts the fact that the mantle experiences convective flow, even if at a sluggish rate. This is exemplified by the Hawaiian hotspot, suggested to move southward (Kono, 1980; Tarduno et al., 2003).

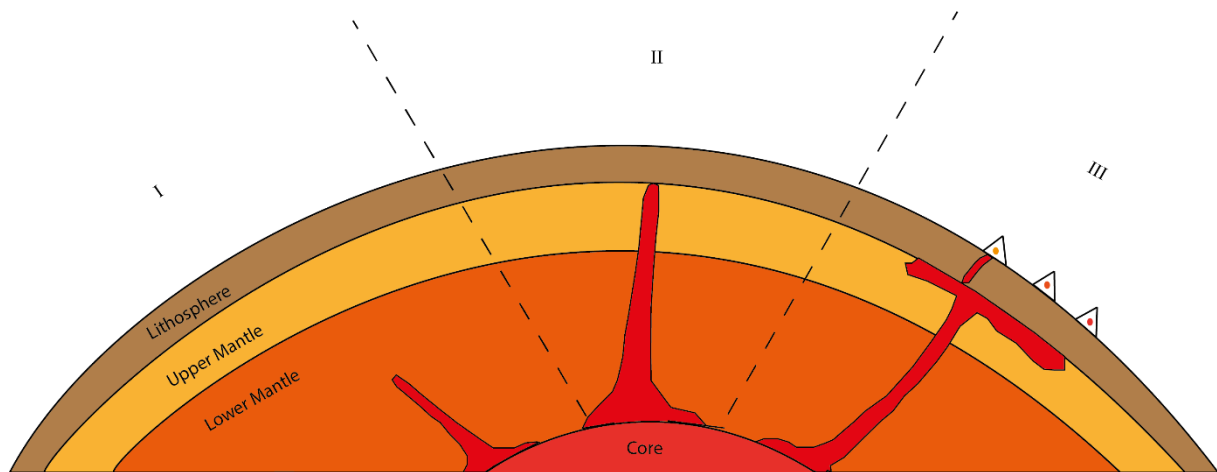


Figure 3.1 - Simplification of the Hot Spot formation, with three stages: I- Formation of the plume, in the core-mantle boundary, II- The arrival of the plume head on the Lithosphere-Mantle Boundary, III- Spread of the plume head below this boundary with a path penetrating through the lithosphere generating magmatism.

3.2. MULTIPLE PLUME MODEL

This model was discussed and introduced by Courtilot et al. (2003), and it's currently applied to the Canary Archipelago (Civiero et al., 2021; Long et al., 2020). In the literature, this hypothesis is generally preferred due to the improbability of other hypotheses in adequately explaining this type of magmatism (Civiero et al., 2021). The main hypotheses being considered are the Morganian plume (discussed in Chapter 3.1 - Single Linear Hotspot); the Shallow Advective Mantle processes (SAM), which encompass the Andersonian plumes (Courtilot et al., 2003), characterized by feedback mechanisms to accommodate tensile stresses in the lithosphere. Additionally, the SAM includes secondary plumes that root on the Lithosphere-Mantle transition (Courtilot et al., 2003), which are also being considered (Fig. 3.4).

The superplume hypothesis is considered the most suitable explanation for the Late Cretaceous Magmatism (Civiero et al., 2021; Long et al., 2020). It involves a giant thermochemical plume that originates at the Core-Mantle Boundary (CMB) (or the D" layer), at 2700-2400 Km deep, and halts and remains stationary below the Mantle Transition Zone (MTZ), at 410-660 Km deep (Courtilot et al., 2003). The plume remains stationary at this location due to buoyancy effects (Dannberg & Sobolev, 2015). Superplumes are described to exhibit two distinct geometries: a dome-shaped head, known as the African type (Civiero et al., 2021; Courtilot et al., 2003), or a spread head on the MTZ, known as the Pacific type (Courtilot et al., 2003) (Fig. 3.2). A superplume is considered as a union of two types of plumes: a primary mantle plume, and secondary mantle plumes or “plumelets” (Cloetingh et al., 2022). The primary plume is stagnant at the MTZ, and the “plumelets” root at this primary plume head (Courtilot et al., 2003). These “plumelets” can be emplaced in a large spectrum of geodynamic environments, from the foreland (WIM case) to the hinterland (China case) and even associated with subduction zones (Cloetingh et al., 2022).

This work explores the African case (dome-shaped plume head). This plume generates a thermal boundary layer, this is a layer that allows the permeability of the MTZ, conceding the buoyancy problem to be overcome. It is in this layer, that the secondary plumes (Courtilot et al., 2003), or “plumelets” (Civiero et al., 2021; Cloetingh et al., 2022; Long et al., 2020) root generating the observable magmatism.

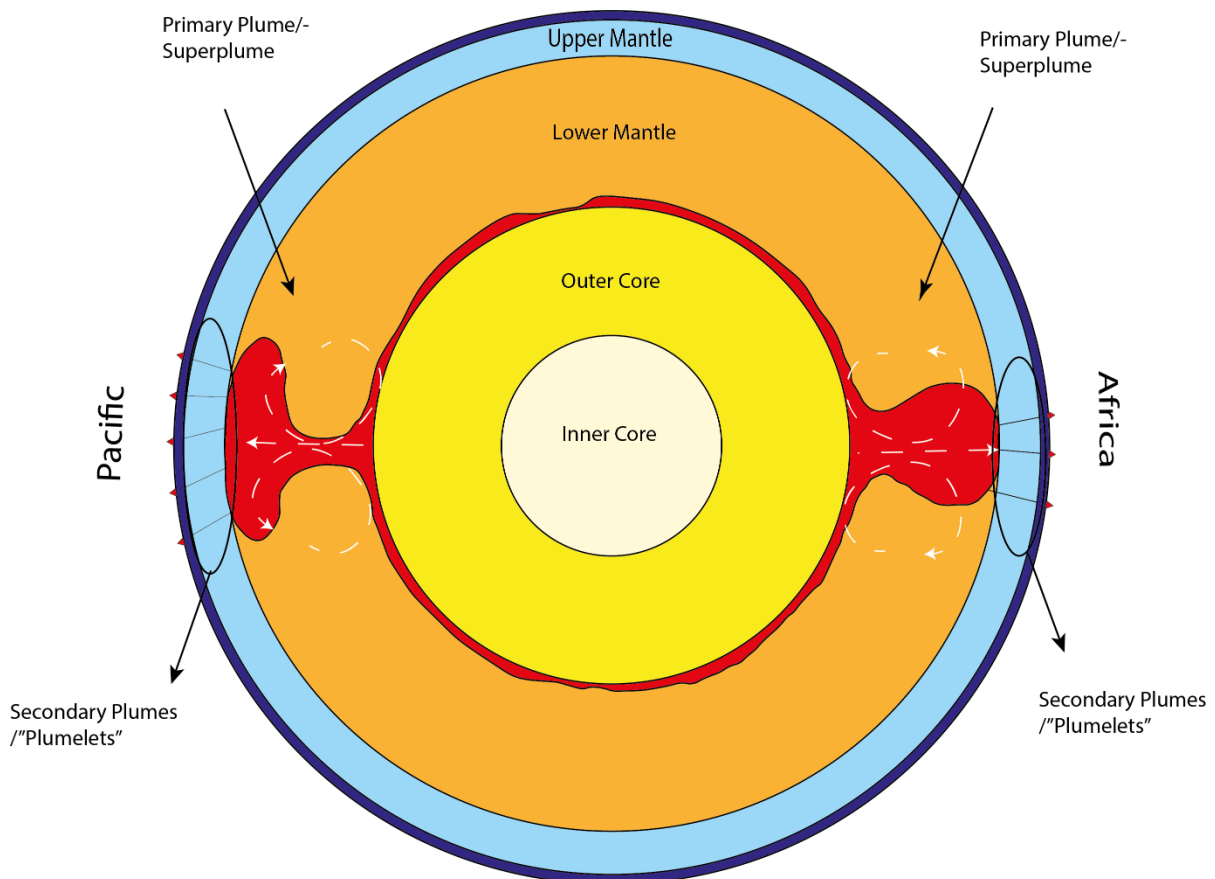


Figure 3.2 – Schematic cross-section of the earth, where can be seen the superplume hypothesis, with the superplume rooted on the CMB and that later station on the MTZ, with the two types of plume head represented. It is seen in the “plumelets” as well, adapted from Courtilot et al. (2003).

3.3. EDGE-DRIVEN CONVECTION

Edge Driven Convection (EDC) (Fig. 3.4) is a geodynamic process introduced by King & Anderson (1995), to explain the genesis of continental flood basalts. This initial model was later modified to be able to explain the formation of seamounts and LIPs on the rim of a lithospheric anomaly, this model is the EDC as known today (King & Anderson, 1998).

The existence of Edge-Driven Convection (EDC) relies on specific conditions without which, it cannot occur. These conditions are rooted in physical attributes, encompassing properties and structures that yield anomalies (King, 2007; Missenard & Cadoux, 2012). Physical property anomalies stem from temperature disturbances (thermal anomalies) and subsequent buoyancy anomalies, while structural anomalies arise from tectonic events driven by a brittle regime (King, 2007; King & Ritsema, 2000; Missenard & Cadoux, 2012). The convergence of these two anomalies initiates EDC, resulting in convective flow (King, 2007).

This flow can originate from a hot upwelling or a cold downwelling movement, both leading to similar thermal anomalies (King & Ritsema, 2000). Cratons are identified as environments conducive to generating EDC due to their favourable factors (King & Anderson, 1995, 1998; King & Ritsema, 2000). However, Missenard & Cadoux (2012) argue that continental margins with minimal extension also facilitate EDC creation, which isn't applicable in the hyperextended WIM.

Opposing the concept of the plume, which leads to a somewhat high magmatic activity accompanied by a hot mantle beneath (King & Anderson, 1998), the Edge-Driven convection, is unsteady and pulsating, this being proposed in some new LIPs (Elder, 1976). Elder (1976) also states that this type of magmatism is transient in newly opened oceans.

This hypothesis has been postulated for the alkaline magmatism on the Atlantic (Matton & Jébrak, 2009). These authors describe this mechanism as the one responsible for most of the Peri-Atlantic Alkaline Pulse (PAAP), in which the WIM magmatism is included. The same authors suggest that the mechanism that generated the PAAP was linked to the asthenosphere, and not a deeply rooted structure (Super Plume) (Matton & Jébrak, 2009). This objection is based on the absence of significant hot spots, and the unlikelihood of magmatic ascendance from the D'' layer (Matton & Jébrak, 2009).

The proximity to old continental passive margins led the authors to propose the EDC as an ideal model for these occurrences (Fig. 3.3).

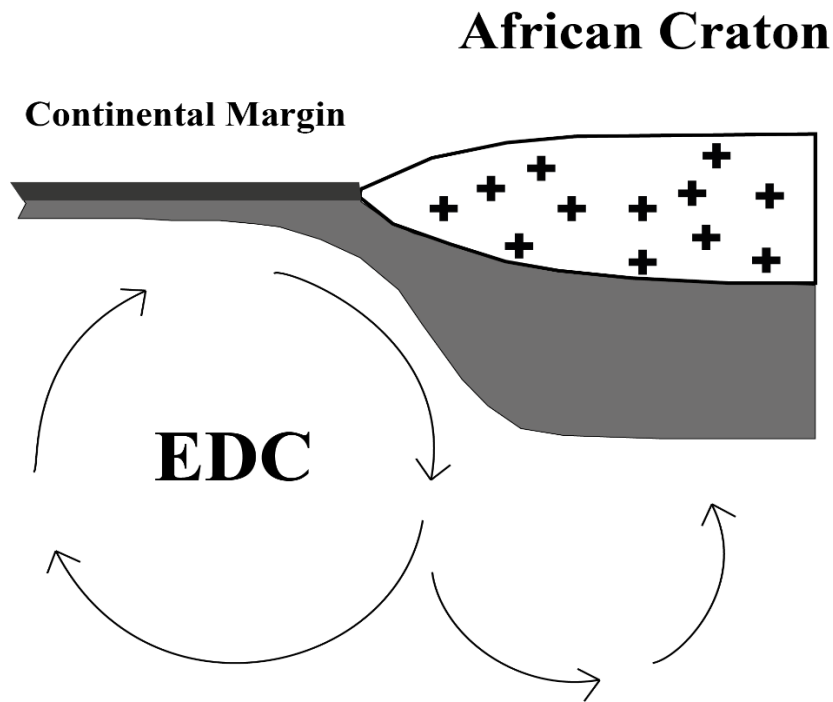


Figure 3.3 – Diagram of the EDC mechanism formation environment, near a craton where the structural or thermal anomaly can be created. Adapted from Matton & Jébrak (2009).

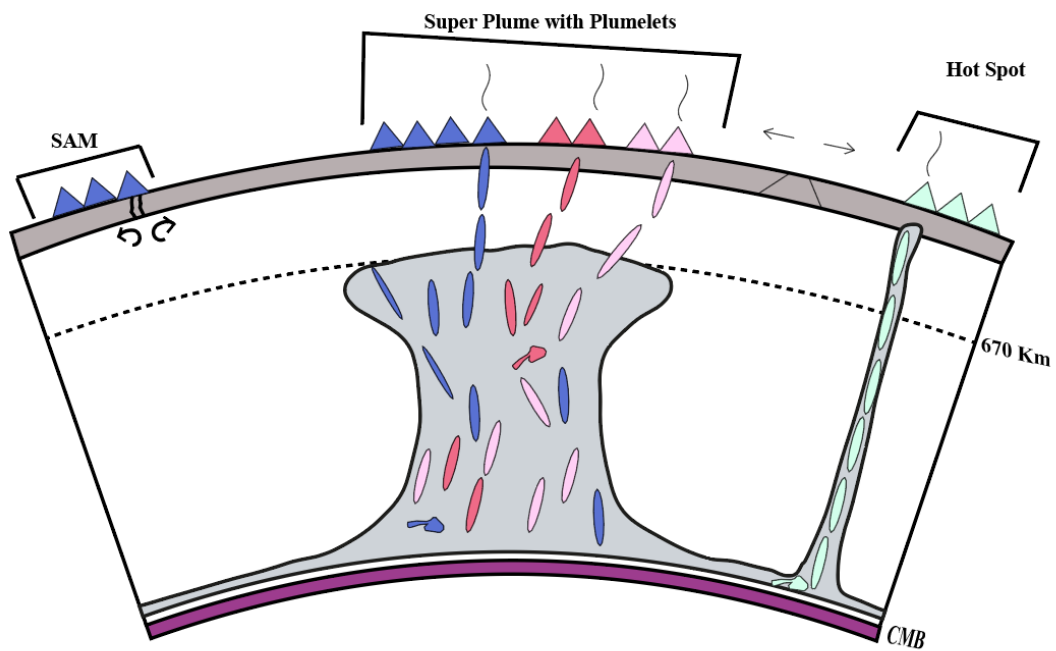


Figure 3.4 - Simplified sketch of the hypotheses considered, the Shallow Adveective Mantle, here shown as the EDC, originated near a fragility. The superplume with secondary “plumelets”, is the hypothesis that could generate dispersed occurrences with different geochemical signatures. And the primary plume or the hotspot, is the hypothesis that generates consistent magmatism, generating consistent plume tracks (such as the Hawaii archipelago). Modified from Koppers (2011)

4. METHODS

GPLATES

The primary objective of this study is to investigate the potential correlation between the late Cretaceous magmatism found in the WIM (West Iberian Margin) and the mantelic processes that could generate this magmatism. To achieve this, a model was developed to visualize the paleo-positions of the magmatic events, allowing for the examination of their possible origins (Figs. 4.1). By determining the relative positions of these magmatic bodies, it becomes possible to assess if they were closely located, testing the different hypothesis for mantle sourcing of magma on the WIM. The validity and suitability of these hypotheses can be evaluated based on this analysis. Accordingly, a model was created using individual polygons to outline the current shape, including a larger rim to account for the original size and the buried portion of each magmatic body. For this model it was also needed to input the ages for each occurrence, the inputted ages were done based on the more reliable methods (see Chapter 2.3 - Introductory note on geochronology) (Tab. 5).

To test the hypotheses and gain insights into the geological processes involved, palaeogeographical reconstruction software called GPLATES was used. This software aided in simulating and visualizing the changes in the palaeogeography of the region over time (Fig. 4.2).

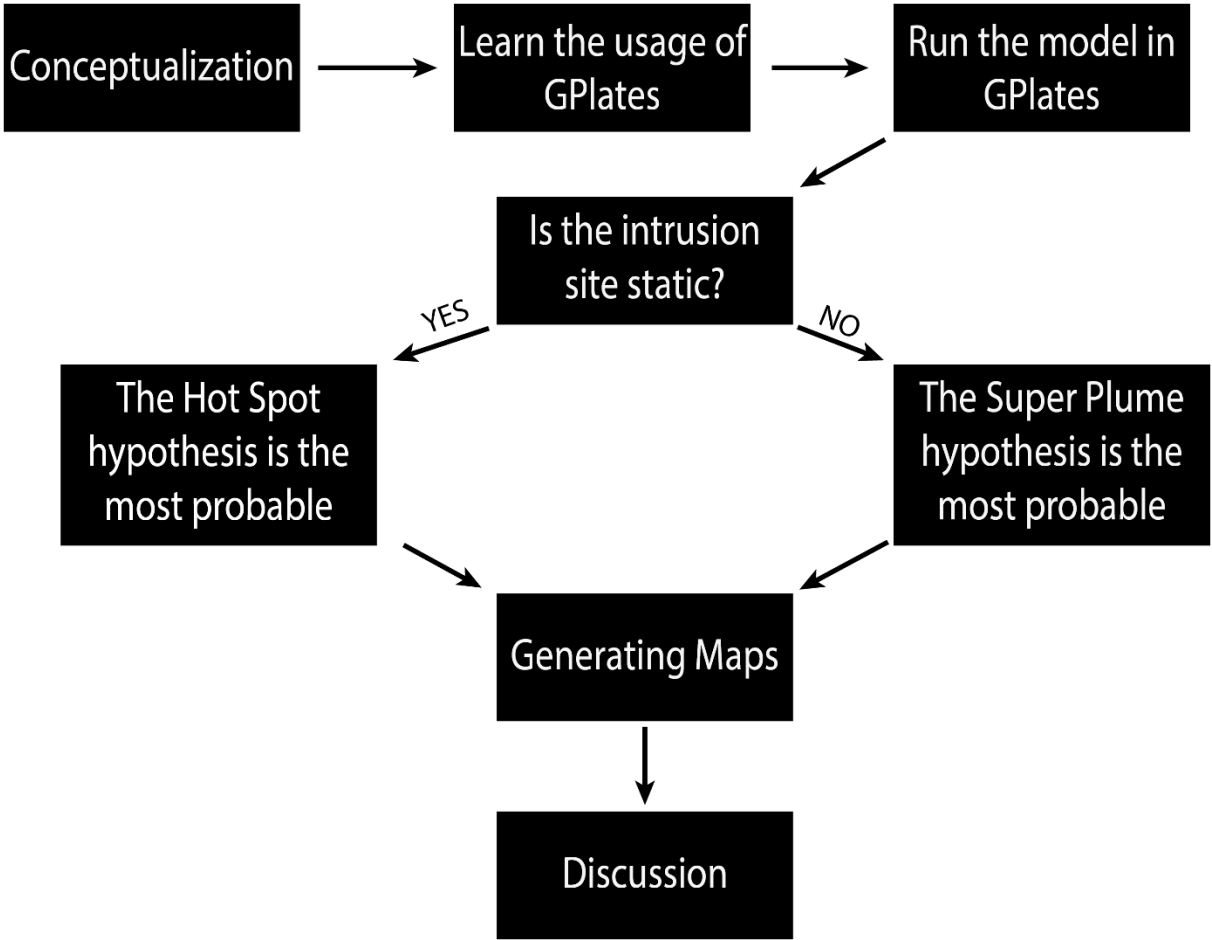


Figure 4.1 - Workflow of the conceptualization of this work

GPlates is an open-source software, a cross-platform plate-tectonic geographic information system, that allows the user to reconstruct the expression of geodynamic events throughout time. GPlates allow the user to manipulate plate motion models, whether on a regional or a global scale, it also allows data import from other users (Müller et al., 2018). The software library includes several types of geodata, from palaeomagnetic data (geophysics) to palaeotopography data (geology) (Müller et al., 2018). The users can also use more than one set of data at a time, meaning the user will be allowed to, for example, see the motion of Iberia evolving from its formation to the present time.

Rasters, whether numerical or colour, can be imported, georeferenced, assigned to the tectonic plates, and reconstructed through time. GPlates also allows exporting sequenced images in several file types (e.g. .jpg), and permits the stacking of several layers of imagery, from the topography to the mantle tomography (Müller et al., 2018).

One of the most remarkable features of this software is its ability to link tectonic models with geodynamic models (Gaina et al., 2015; Lacombe et al., 2020). This aspect represents a significant innovation, as it opens new possibilities for addressing geodynamic issues within GIS-type software. In essence, it enables the visualization of geodynamic processes over time, effectively rendering it a nearly 4-dimensional software. The decision to utilize this software for the present study was driven by the fact that it is well-suited for addressing such complex geodynamic problems, aligning adequately with the purpose of this research.

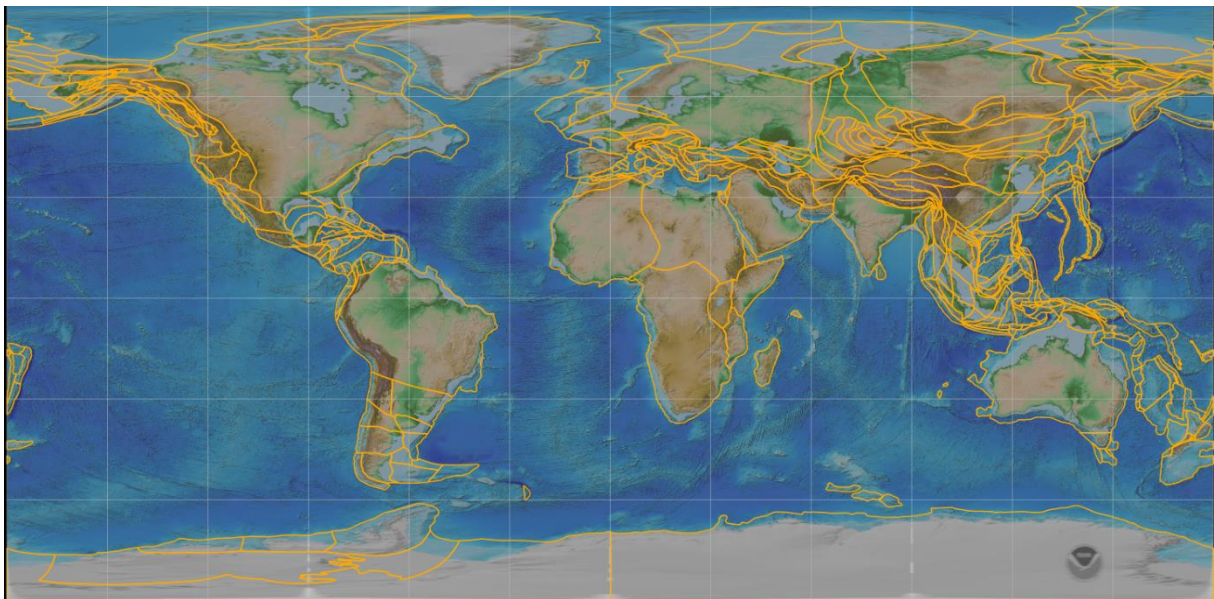


Figure 4.2 - World map produced with GPlates, showing the outline of tectonic plates and microplates (in orange).

However, there are several files available for the user to work on. The base model that was worked from, had already a base rotation file, a file that has tectonic movements installed (Cao et al., 2022; Müller et al., 2019; Young et al., 2019). Also, several other files provided the coastlines, the tectonic plates (and several other micro-plates), and the topography of the earth based on the National Geophysical Data Center (NGDC) data. It is possible to conclude that, even globally the plate boundaries template fits well, although locally, the available polygons and inputs can show some errors, so in the software, this template was not used.

To generate a single model for this study, individual polygons for meaningful magmatic occurrences were created using ArcGIS Pro. To make the polygons, the current shape and size were considered, applying a larger rim, to accommodate the error margin within the imagery and to accommodate the possible buried and former size (to exclude the erosion). These polygons were later imported into GPlates to generate the model and investigate any relations with deep-seating mantle plumes. The model

was run for 150 Ma, a timeframe determined by the age of the earliest intrusion in the study area. The simulation comprised 150 steps, each representing a 1 Ma interval. However, the visual outputs, in the form of maps, were generated at a larger interval. This intentional choice, ranging from 5 to 10 Ma, was made to ensure that the changes are easily distinguishable. In some instances, a difference of just 1 Ma might not be readily noticeable. By adopting this approach, the evolving geodynamic processes and their discernible impacts are more effectively portrayed and understood.

This model allowed to generate a paleogeographic reconstruction, based on this reconstruction it was possible to analyse the overall locations of the intrusions. To try to correlate the several intrusions, motion paths were created for the most relevant ones. The motion paths are lines that track the paleo-positions of the magmatic occurrences, from their potential point of origin to their current positions, migration patterns, and their relationship with their current geographic position and geological setting.

By analysing these motion paths, it can be assessed if there are any instances of overlapping, or if the paths followed by the magmatic events are not linear due to the non-linear movement of tectonic plates. This nonlinearity is a result of the dynamic nature of plate tectonics, where plates interact and move in complex patterns (although abrupt changes are not expected). The overlapping of the magmatic bodies with the motion path provides valuable information about the spatial and temporal associations between the two. If multiple magmatic bodies overlay a particular motion path, it suggests a potential connection or shared origin between them.

By examining these overlays and considering the spatial relationships and movement trajectories of these intrusions, researchers could hypothesize the most plausible model that aligns with the observed magmatic activity and evaluate the validity of their hypotheses. This analysis contributes to a better understanding of the processes and dynamics that influenced the magmatism observed in the study area.

Table 5 – Assigned ages for each occurrence. Instances marked with an asterisk ("*") are founded on relative dating. In cases where multiple datings were available, an average of these datings was calculated. Notably, the error margin of these ages has not been incorporated, as it is not a prerequisite for the software used in the model generation.

Province	Group	Body	Age (Ma)
SWIM		Estremadura Spur intrusion	87*
		Fontanelas Volcano	81*
		Paço D'Ilhas	87
		Sintra	81
		Lisbon Volcanic Complex	92*
		Foz da Fonte	94
		Sines	76
		Monchique	71
		Loulé	72
	Portimão Magnetic Anomaly	63*	
TMR	N	Tore NW	81
	N	Tore N	88
	N	Tore	81
	N	Sponge Bob	103
	N	Ashton	98
	N	Gago Coutinho	94
	N	Ormonde	64
	S	Josephine N	7
	S	Josephine N	12
	S	Jo Sister	88
	S	Ampère	32
	S	Dragon	2
	S	Unicorn	0
	S	Godzilla	68
	S	Seine	24
	S	Porto Santo	13
S	Madeira	5	
CISP		Essaouira	68
		Rybin	55
		Dacia	47
		Conception Bank	18
		Selvagen	29
		Fuerteventura	70
		Amanay	15
		Canary Ridge	18
		El Hijo	0.2
		Palma Ridge	2
		La Palma	2
		Henry	126
		Hierro Ridge	133
		Bisabuela	142
	The Paps	91	
	Tropic	119	

5. RESULTS

After running the model, multiple iterations were conducted in GPlates, extracting various motion paths, to test the mantle plume emplacement hypotheses and their possible correlation with the WIM occurrences about the mobile plates and the locus of each magmatic feature.

When scrutinising the motion path of the LVC, it becomes evident that it intersects with the trajectory of other occurrences on the WIM, although at a different temporal point than initially anticipated (Fig. 5.1). Illustrated by the green motion path, the trajectory of the LVC becomes apparent. Initially, it extends in the NNE direction towards present-day Morocco, subsequently veering northward, traversing the Cádiz Gulf, and concluding in its current location. This path presents an arch-like course, indicative of non-linear movement, this is a non-consistent movement through time, accompanying the plate movement. Notably, there is an overlap among all the WIM onshore occurrences during the Late Cretaceous period.

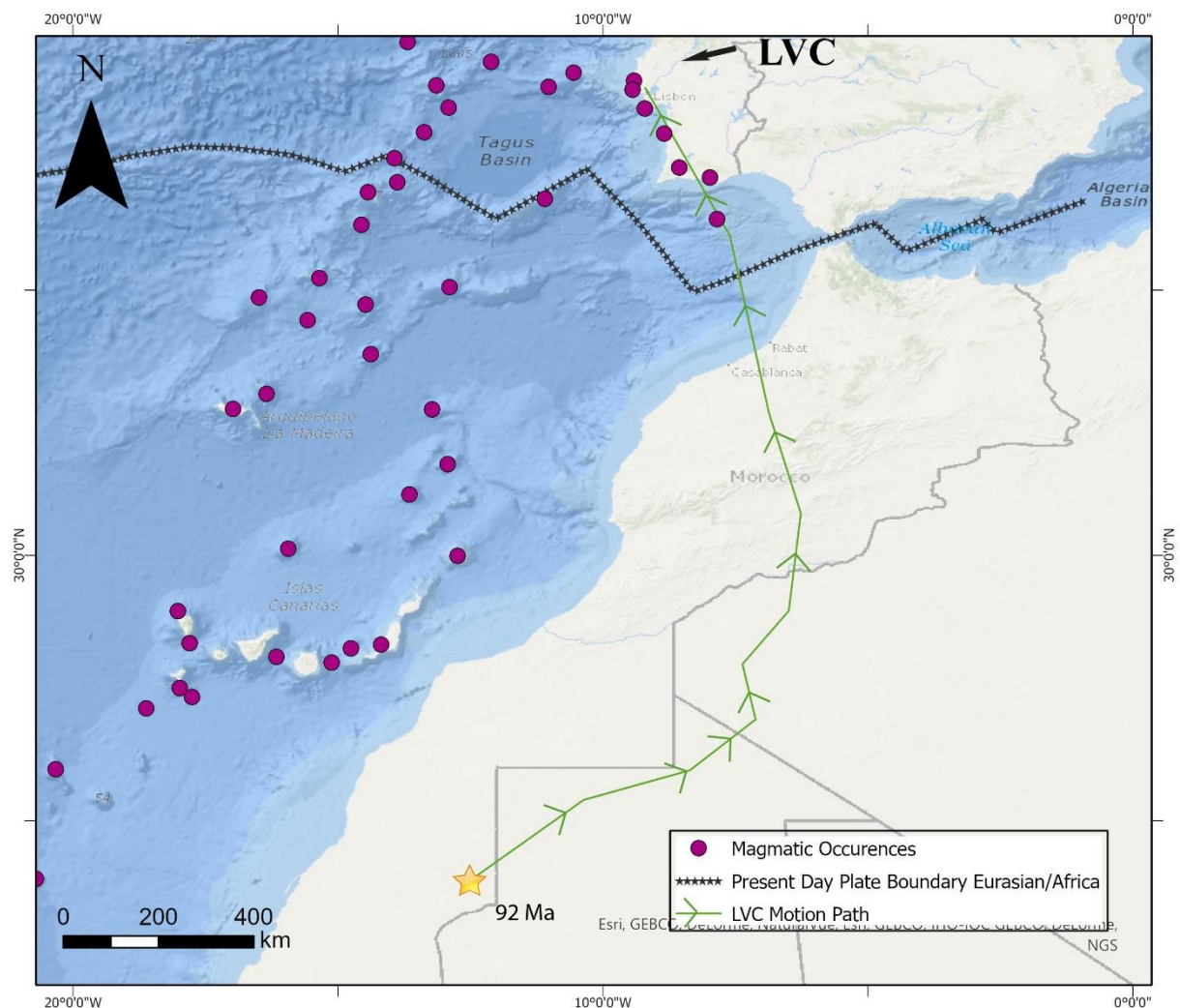


Figure 5.1 – Motion path (green) for the Lisbon volcanic Complex as part of the Iberia microplate. The star indicates the paleo-location of the intrusion in relation to the present day. Note the sinuous path of the Iberia microplate to its current location.

Additional motion paths were generated, specifically for the Monchique and the Tore magmatic features (Figs. 5.2, 5.3). The motion path of Monchique follows a similar curved trajectory to that of the LVC, with its initial intrusion site positioned currently beneath Fuerteventura Island (Fig. 5.2).

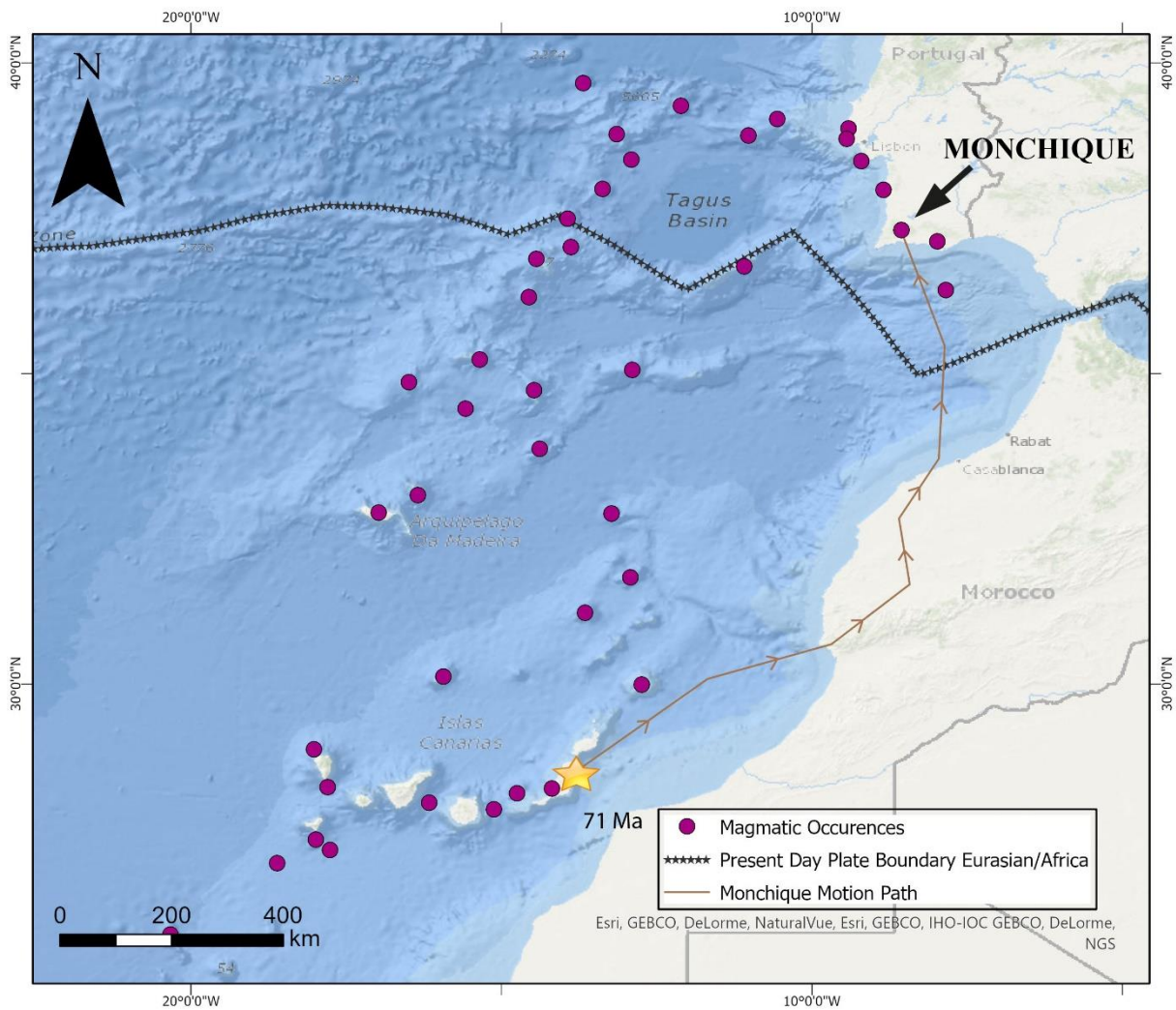


Figure 5.2 - Motion path (dark orange) for the Monchique Massif. The star indicates the paleo-location of the intrusion in relation to the present day.

A noteworthy seamount in this study is the Tore seamount, particularly due to its potential connection with the WIM intrusion, as theorized by Ribeiro et al. (1979). To explore the potential geodynamic correlation between the seamount and the onshore intrusions, a motion path analysis of the Tore seamount was conducted (Fig. 5.3). This analysis aimed to validate the suggested connection by Geldmacher et al., (2006) and Merle et al. (2009, 2018).

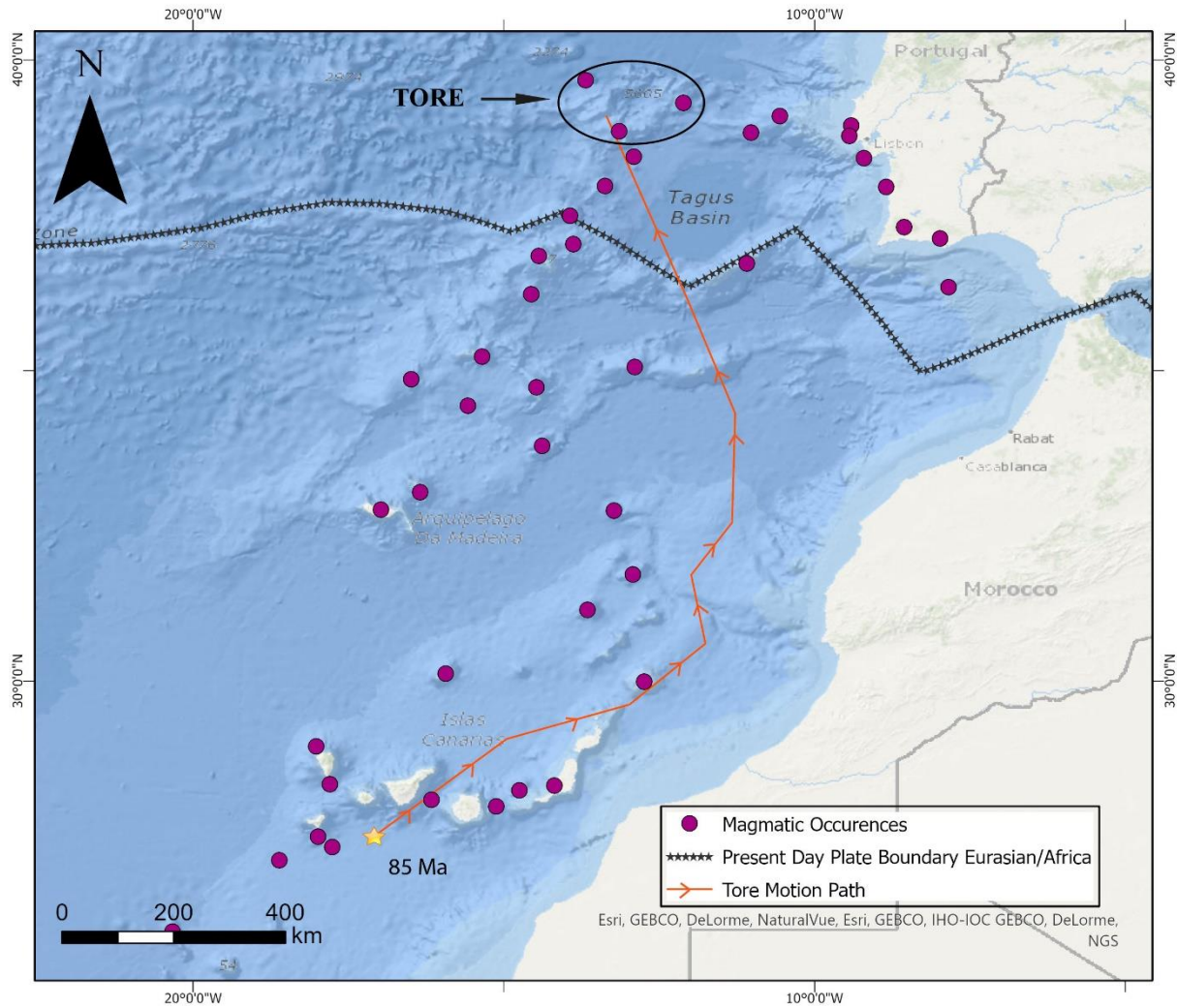


Figure 5.3 - Motion path (orange) for the Tore Seamount. The star indicates the paleo-location of the intrusion in relation to the present day.

The Tore motion path follows a northeastward direction initially, then transitions to a more general northwestward trajectory. Upon acknowledging that this path doesn't intersect the Madeira Archipelago, the Ampère motion path was subsequently investigated (see Fig 5.4), which is characterized by a consistent and continuous northeastward movement.

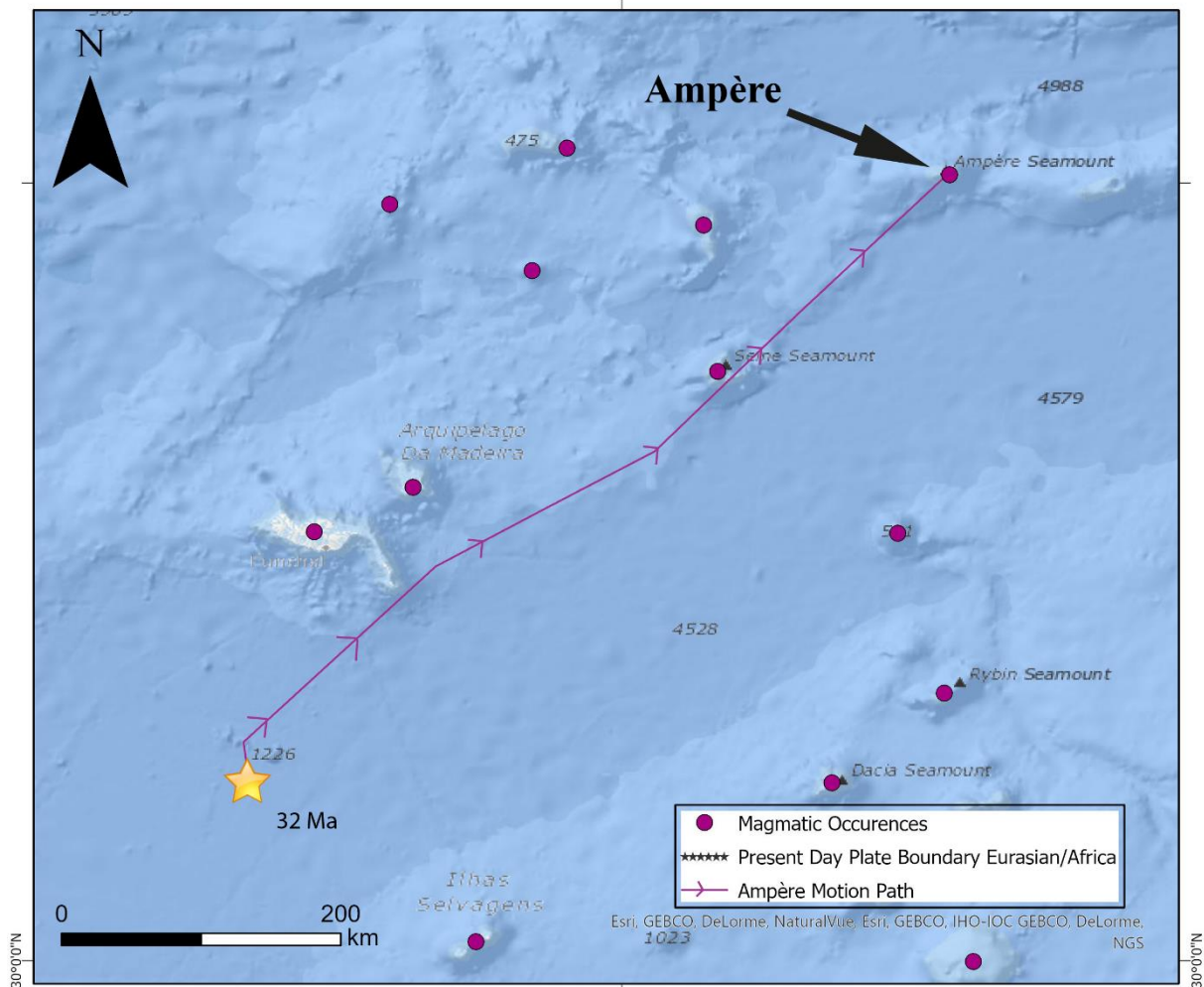


Figure 5.4 - Motion path (purple) for the Ampère Seamount. The star indicates the paleo-location of the intrusion in the present day.

These motion paths were of paramount significance for this study. Additionally, several other paths were generated to address various issues that arose during the model runs (Figs. 5.5, 5.6). Figure 5.5 presents the unprocessed model output, displaying its various iterations, with the 8 motion paths done (LVC, Sintra, Sines, Monchique, Tore, Ampère, Essaouira, and Ormonde). This offers a glimpse of the intricate nature of intrusion geodynamics and their interconnectedness. The polygons (in dark red) are stationary on the original place of emplacement, and as stated previously it is possible to check the overlapping of the several polygons with the present topography (Fig. 5.5).

In the raw output of the motion paths (Fig. 5.5), a software error is evident as the starting point corresponds to the current position of the magmatic body, rather than the original intrusion spot which should be the ending point. This error is presented by the arrow directions, that point southwards, not accurate with the plate movement. However, this error is rectified in the processed imagery (Figs. 5.1, 5.2, 5.3, 5.4, 5.6), where all movement arrows are now accurately directed northwards, towards the correct location.

In Figure 5.6, the refined outcomes of the raw outputs are depicted, featuring the, previously mentioned, 8 motion paths (LVC, Sintra, Sines, Monchique, Tore, Ampère, Essaouira, and Ormonde). Each sector of the study area is represented by at least one motion path, thereby providing a comprehensive perspective on the geodynamic interactions within the region.

Initially, the locations appeared to be relatively close, suggesting a common source. However, as the timeframe was expanded, it became apparent that it was not always possible to connect all the occurrences to a single source location. Instead, they were clustered within a larger area, indicating a broader region of magmatic activity rather than a singular source point. This observation highlights the complex and spatially variable nature of magmatic processes over time (Figs. 5.5, 5.6).

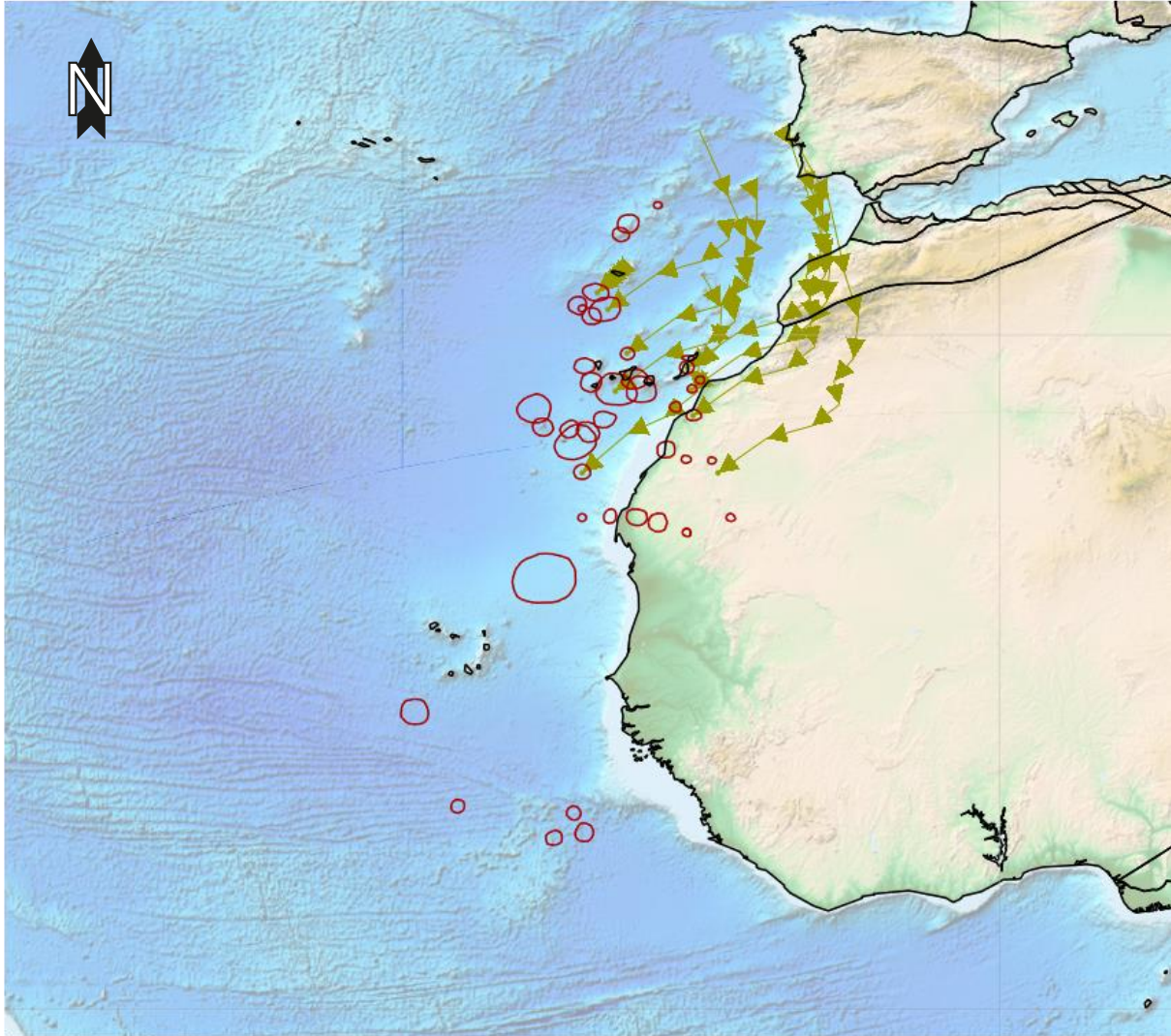


Figure 5.5 - Map showing the paleo-location of the modelled magmatic features (dark red polygons) and their motion path (green arrows). Please note that the arrows on this map may appear inverted compared to other maps because the model software presents movement in reverse order, starting from the current day and going back in time.

One observation from the model output is the presence of multiple overlapped polygons (Fig. 5.5). This particular outcome served as a key finding, which sparked discussions and further exploration of the hypotheses. An interesting observation emerged: the motion paths within the Eurasian plate exhibited consistent movement patterns, while those within the African plate displayed distinct orientations when compared to the former. This disparity prompted the need to differentiate between these two categories of intrusions and their associated motion paths.

The occurrences were categorized into two major groups: the Eurasian group and the African group. This classification is based on the respective tectonic plates within which they are situated (Fig. 5.7).

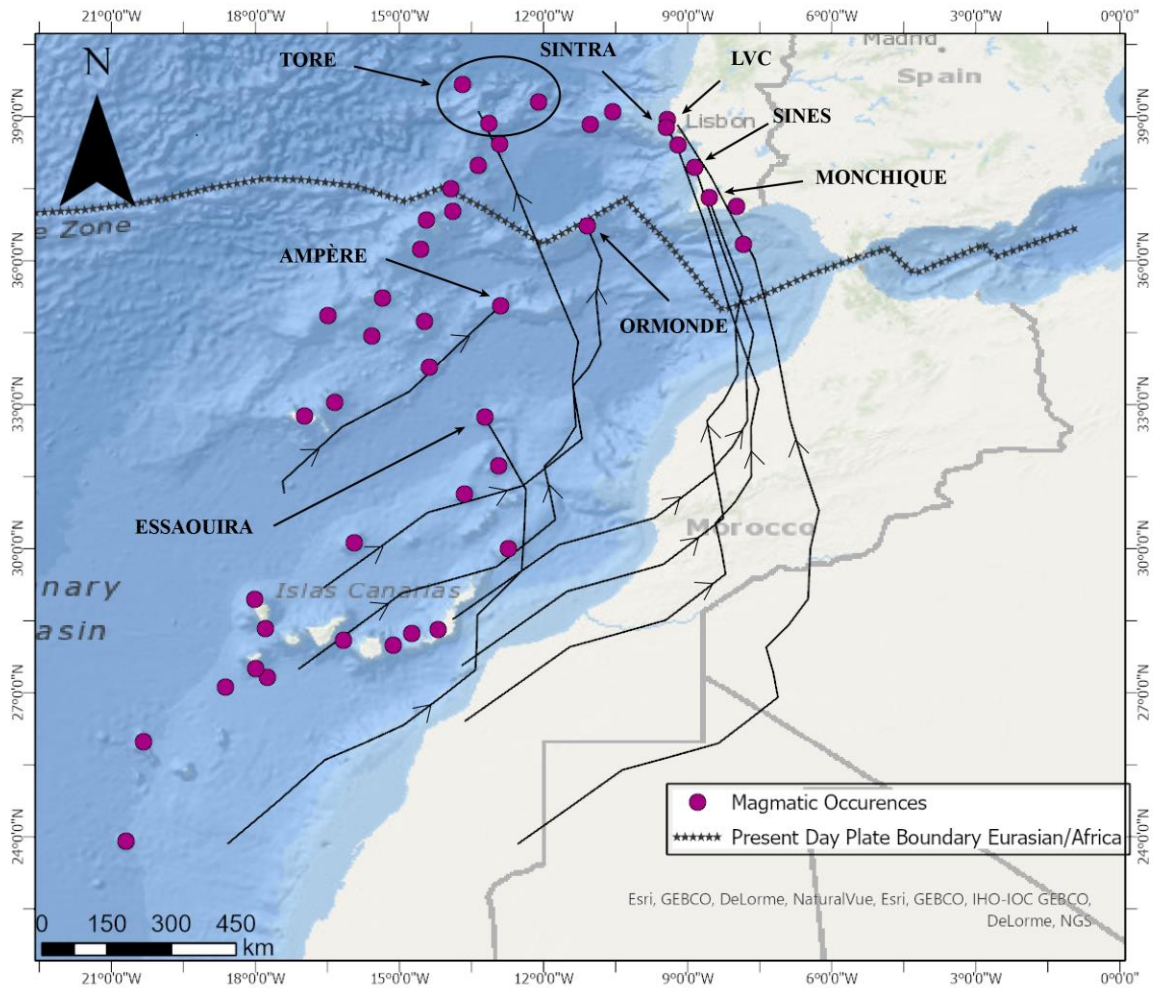


Figure 5.6- Map of the motion paths in detail, with their relative magmatic body. These paths are focused on the WIM area and the Madeira origin problem.

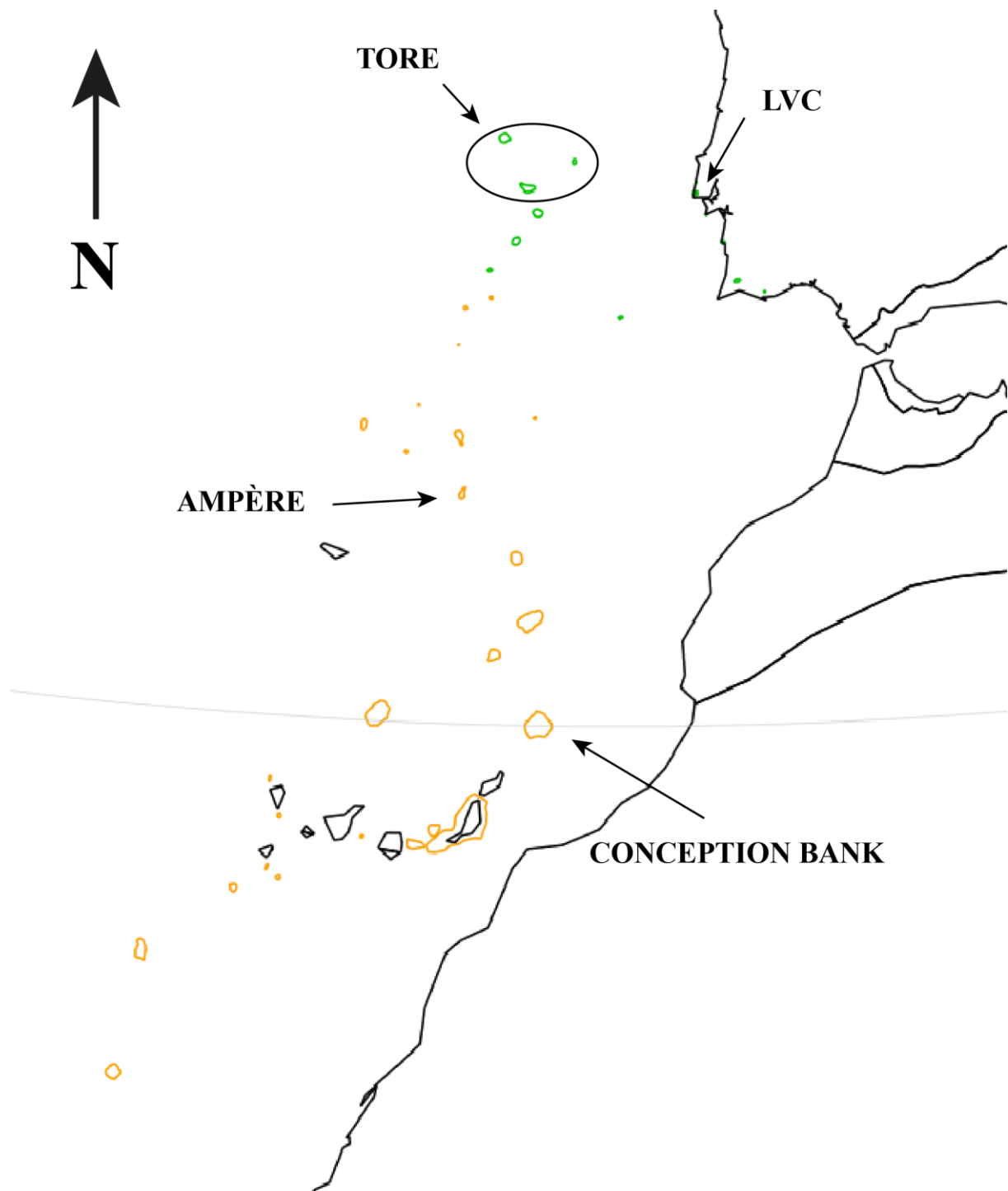


Figure 5.7 – Two groups of plumes, the Eurasian group in green, and the African group in orange.

6. DISCUSSION

MOTION PATHS AND THEIR CONNECTION TO THE HYPOTHESES

As previously mentioned, the main objective of this study was to establish a viable and logical link among the dispersed Late Cretaceous magmatic events within the WIM. To achieve this goal, various motion paths were generated, yielding insightful findings that establish a connection between the WIM and the CISP.

The first path tested was the one that led to the creation of this study, the possible correlated origin of the WIM magmatism, whether onshore or offshore. The motion path extracted for the LVC was analysed and a 75 Km radius of influence (buffer) was postulated, to investigate the area of influence of a possible static mantle plume and the trajectory of the Iberia microplate from the Late Cretaceous onwards (Fig. 6.4).

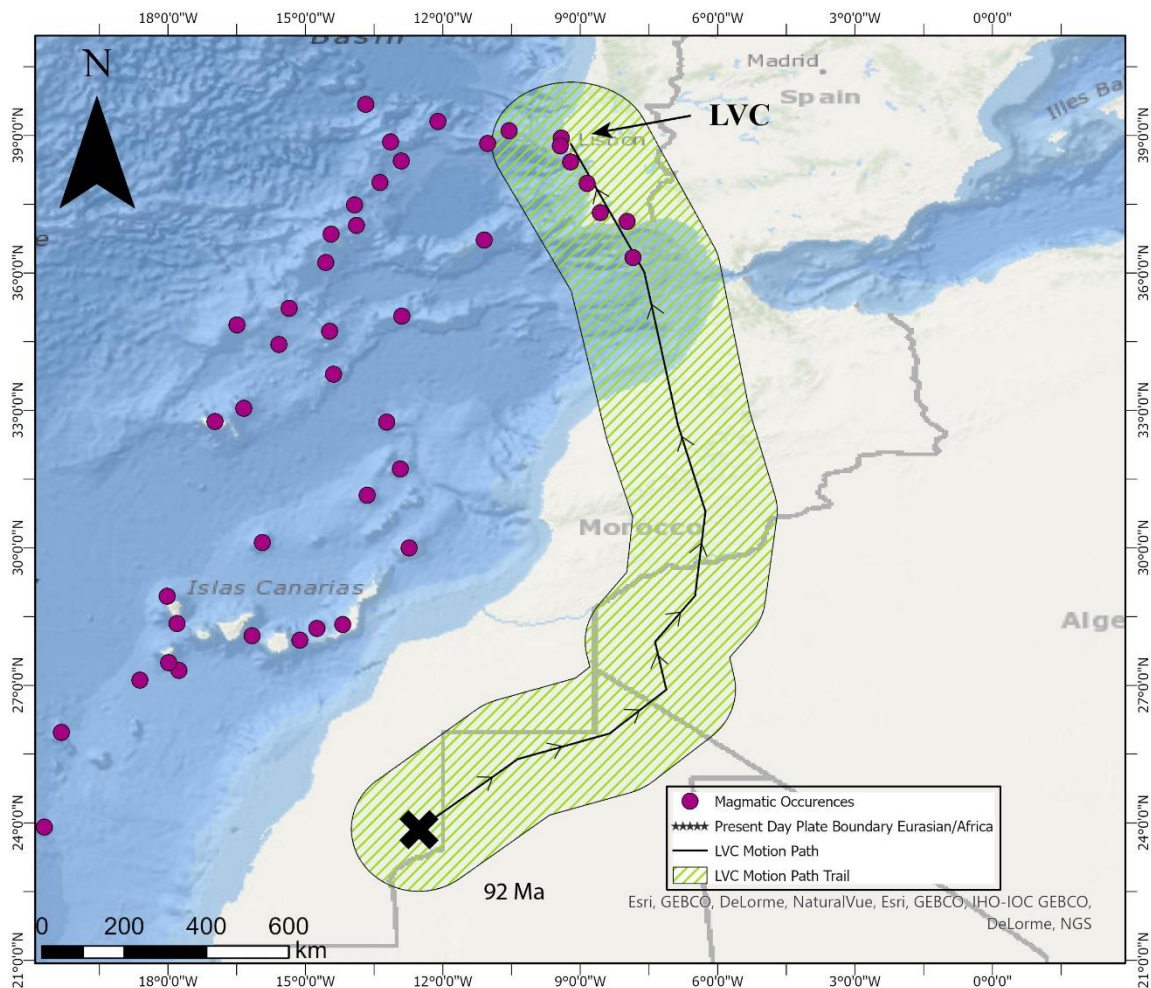


Figure 6.1 - Map with the area of influence (75 km) along the LVC motion path, the major effect was on the earlier stages that led to the intrusion of the WIM bodies.

The path analysis reveals that the onshore magmatic occurrences can be connected, evident through the motion path and its trail. Notably, all occurrences within the WIM region lie between this path, suggesting the possibility of a single source generating these magmatic occurrences.

However, the geochronology of magmatic features indicates distinct ages of formation. The Sintra massif includes granites of 78 Ma to gabbros of 82 Ma that cannot be fully explained by a single hot spot trail, with the postulate mantle upwelling source yielding magma at discrete timings. The Sines (77-71 Ma) and Monchique (75-70 Ma) massifs, despite having a relatively narrow age range still exhibit the challenge highlighted earlier. Given the ongoing movement of tectonic plates., it becomes apparent that a single hotspot would face significant difficulties in generating multiple polyphasic intrusions, especially with intervals of nearly 5 Ma. But this problem can be fixed if instead of a single hot spot, it is thought of as a stagnant mantelic structure (Super Plume) that generates episodic magmatism (Plumelets). This episodic magmatism can accompany the non-linear movement of the tectonic plates since there is no direct connection between the MTZ and the lithosphere, allowing it to generate a consistent alkaline geochemical signature observable on several intrusions.

Furthermore, the study also encompassed the analysis of the Monchique path, which yielded interesting results. This motion path revealed a convincing linkage between the WIM and the CISP at both ends. This noteworthy connection to the CISP, which was not evident in the LVC path, emerged as a significant revelation from the Monchique path analysis (Fig. 6.2).

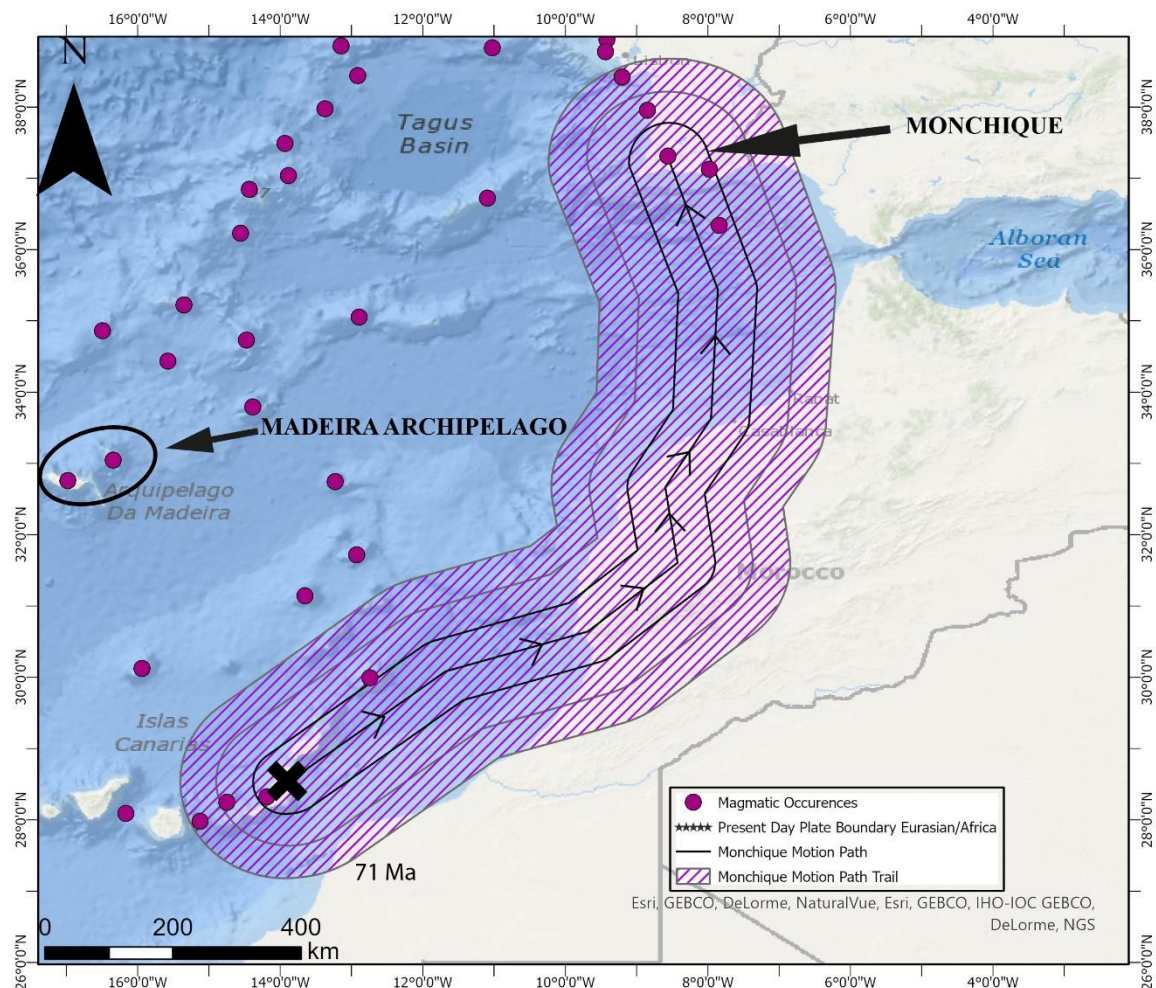


Figure 6.2 – Map with the area of effect caused by the Monchique motion path, here it can be seen two clusters of occurrences. One on the Iberian Plate, the WIM occurrences, and the other in the CISP, where the volcanism can be significantly younger.

Indeed, the paths of the LVC and Monchique magmatic occurrences appear to terminate in different locations, making it challenging to establish equivalence between them. Additionally, proving such a connection is difficult, especially considering that the model and files used have inherent errors due to their global scope rather than being specific to the regional context of the study. Moreover, the magmatic bodies themselves are not uniformly positioned in space, and the tectonic plates exhibit non-linear motions, which influence the observable outcomes.

With the progress of the study, it was needed to add other areas that could correlate to the WIM, the Tore-Madeira Rise was one of them. The Tore motion path was performed to test the hypothesis proposed by Ribeiro et al. (1979). It is observable that this motion path (Fig. 6.3) does not go through the WIM, in fact does not approach the ESI or the FV, the closest occurrences of the WIM. Instead goes South, does not connect to the Madeira Archipelago, and finishes at the CISP. This path has the same description as the previous path, as the sudden direction changes accordingly to the crossing of the AGFZ. The hypothesis proposed by Ribeiro et al. (1979) appears to be unsupported by the findings of this study. The analysis of tectonic plate motions suggests that there is no spatial proximity between the occurrences in the WIM and the proposed hypothesis. Instead, the results indicate a potential correlation between the northern intrusions of the TMR and the occurrences in the CISP. This divergence in spatial relationships challenges the validity of the Ribeiro et al. (1979) hypothesis in explaining the observed magmatic occurrences.

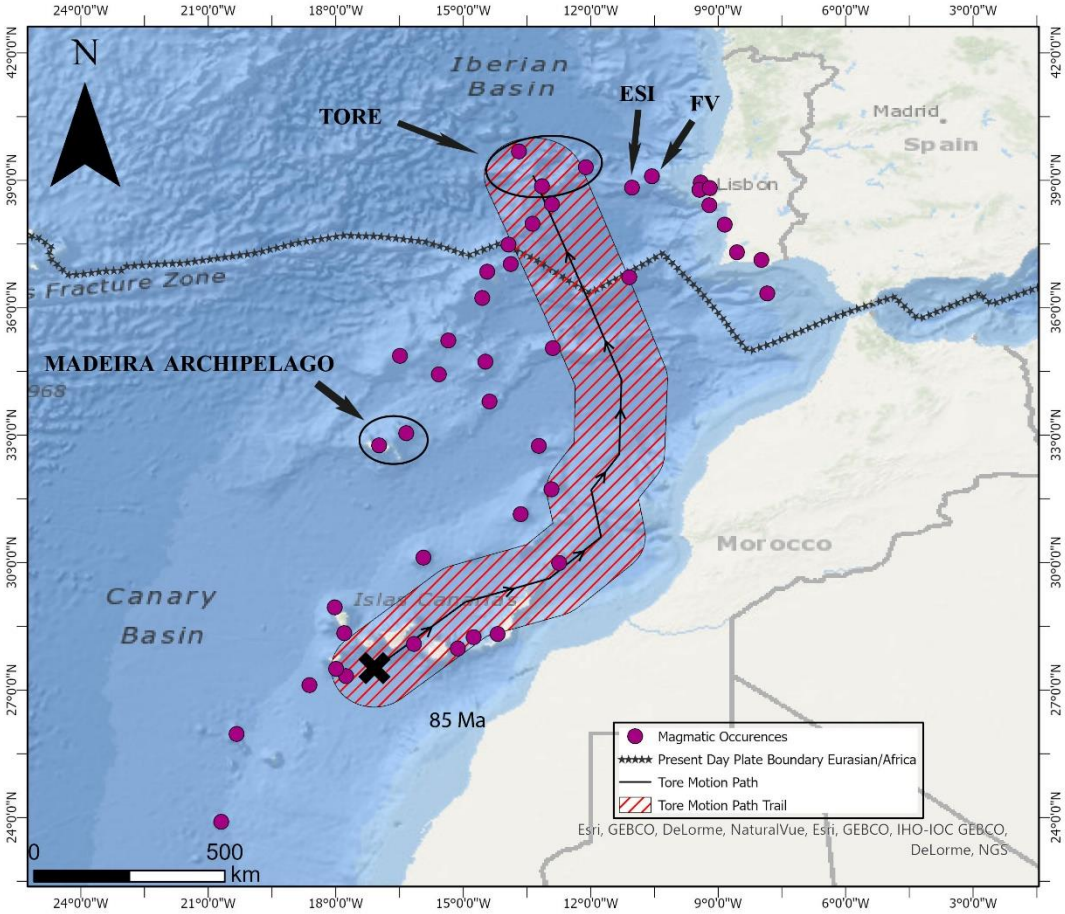


Figure 6.3 - Map with the postulated area of effect caused by the Tore motion path, displaying no connection whether to the WIM or the Madeira Archipelago.

Merle et al. (2018), proposed a hot-spot track linking the Monchique intrusion and various seamounts, including the Madeira Archipelago (Fig. 6.5). To assess this hypothesis, the Monchique path was examined (Fig. 6.2), yet it did not establish a connection with the Madeira Archipelago. Instead, the outcomes indicate a potential correlation along the Ampère motion path (Fig. 6.4) for the latter.

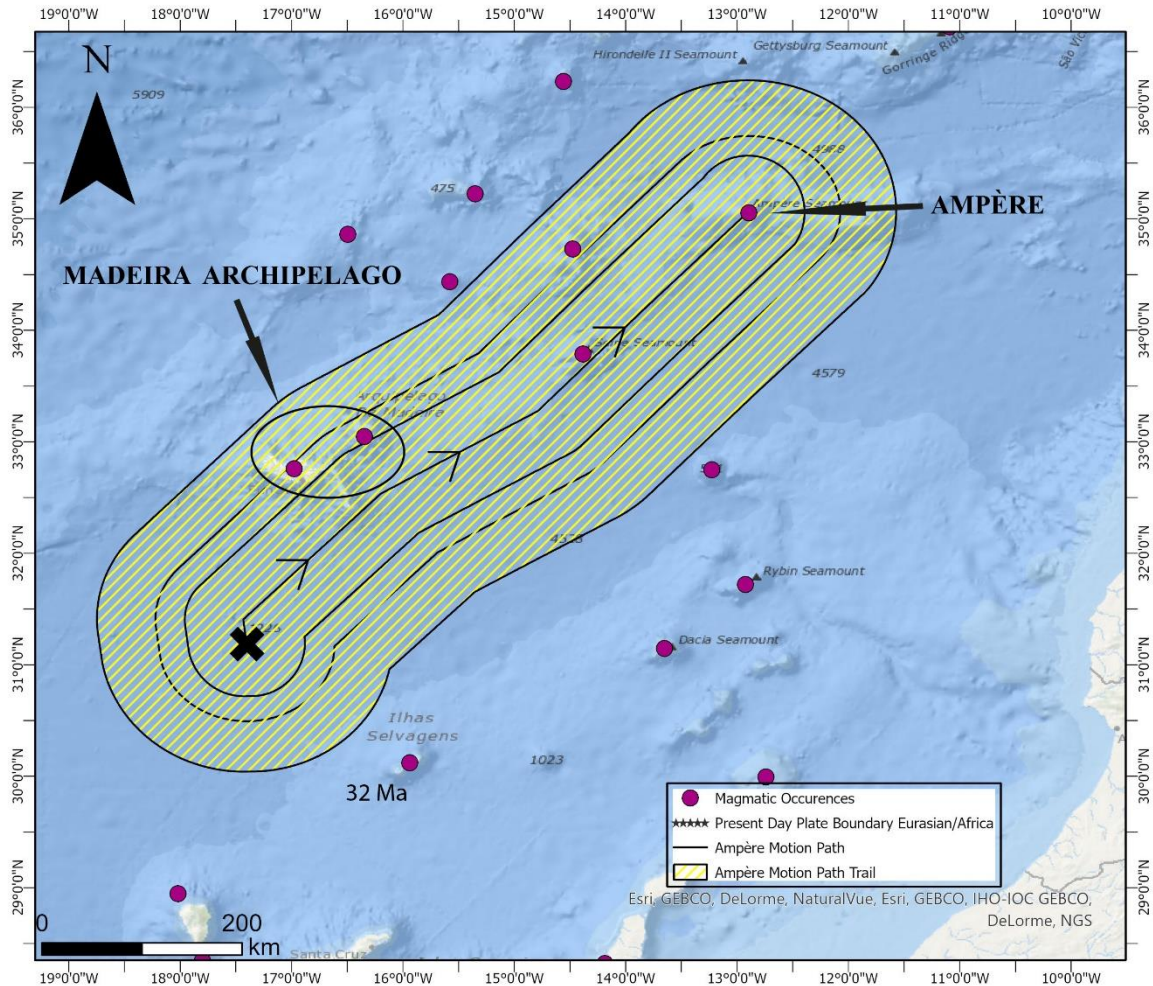


Figure 6.4 - Map with the area of effect caused by the Ampère motion path, here it can be seen a continuous trail that led to the formation of several occurrences. All of them are correlated as proven by (Geldmacher et al., 2005).

In Fig. 6.5, it is tested a plume track, a plume track which is the spatial and chronological traces left by mantle plumes as they ascend from the Earth's deep interior to the surface. These tracks are characterized by volcanic activity, including the formation of volcanic islands, seamounts, and continental flood basalts. Plume tracks are instrumental in understanding the movement and evolution of mantle plumes over time, providing valuable insights into the dynamic processes shaping the Earth's surface (Morgan, 1971). Unlike the paths, which suggest motion, the tracks represent multiple magmatic occurrences and lack a sense of movement. Therefore, the arrows in the tracks indicate an age progression of these events.

Among the tested hypotheses, the single linear hot spot could be conclusively disproven, encompassing both its static and mobile variants. The displayed patterns on the maps for all scenarios do not align with the concept of a single linear hot spot. However, even the idea of several linear hot spots was refuted by seismic studies conducted by Civiero et al. (2021).

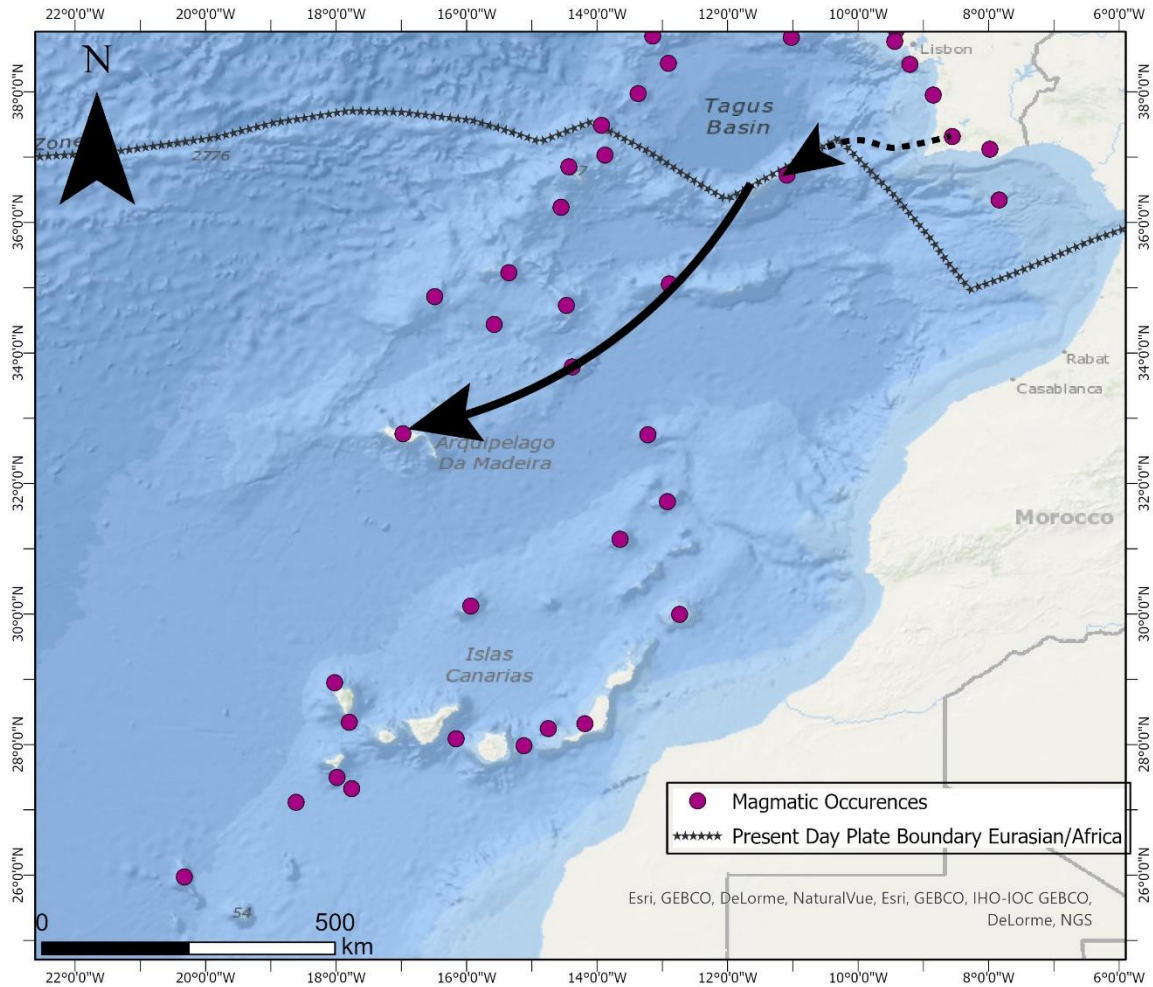


Figure 6.5 - Map of the plume tracks proposed in Geldmacher et al. (2005) and Merle et al. (2018), modified from Geldmacher et al. (2005) and Merle et al. (2018). The complete proposed track consists of both the full arrow and the dashed arrow. However, due to the significant age difference between the occurrence indicated by the dashed arrow and the occurrences depicted by the full arrow, a connection seems unlikely. So, it is proposed in this work that only the full arrow should be considered as previously discussed and displayed from the Monchique and Ampère motion paths (Fig. 6.2 and 6.4)

This finding supports the idea that a common deep magmatic source, probably on the MTZ, might be responsible for the formation of multiple and diachronous magma plumelets responsible for the onshore occurrences within the WIM area. So, the superplume hypothesis is also reinforced by these results because it would explain the diverse geochemical signatures found in the various study areas. But it would also justify the similar signatures in the occurrences that are related to the Madeira to Ampère occurrences.

The EDC hypothesis does not require a deep mantelic source, something that is observable, and it is present in the study area (Civiero et al., 2021), as previously mentioned, a prerequisite for these mechanisms is a substantial continental crust thickness, a condition unmet by both the WIM and the TMR, but notably evident in the CISP. This mechanism must be revoked as a possible magma origin, mainly caused by the lack of ideal convection conditions. But it also does not explain polyphasic intrusions observed on the WIM, since the magmatism occurs on a small scale and the mantle heterogeneity cannot explain the range of geochemical signatures.

MULTIPLE MANTLE PLUME PROVINCES

The other main result deriving from this study reveals the possibility of two large clusters of small intrusions that could lead to a plume being present, justified by the possibility of the Super Plume with plumelets. These groups can be connected whether timely or spatially or even both (Fig. 6.6). The main divisions occur based on the occurrence location, and time also portrays an essential role. The five eldest occurrences of the African plate magmatism, all appearing between 142 to 91 Ma in the CISP (Fig. 6.7). The second group is all the remaining occurrences apart from the Fuerteventura, this group includes all the Iberian plate magmatism (WIM and some TMR), and the remaining African plate magmatism, ranging from 103 Ma to the present (Fig. 6.8).

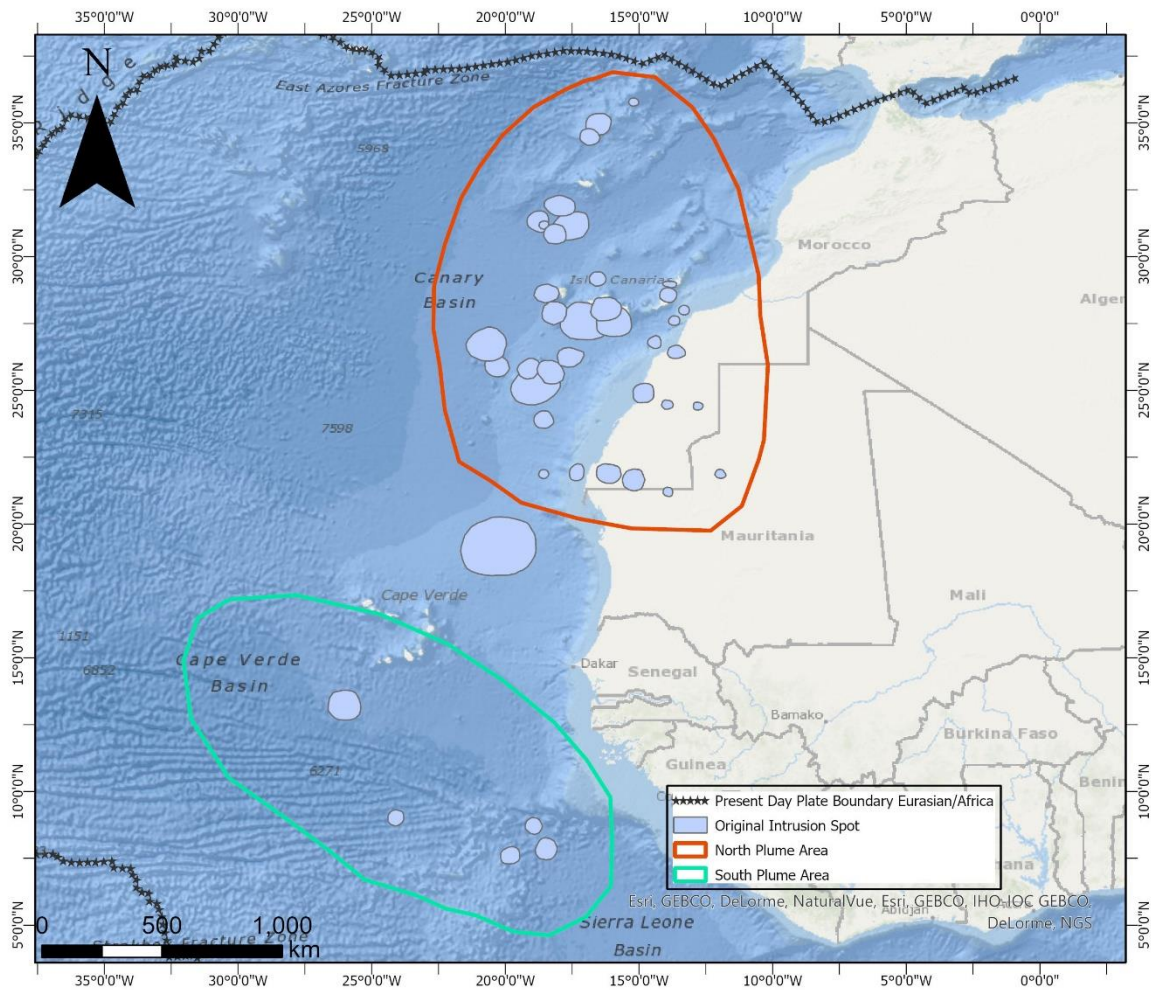


Figure 6.6 – Map with two plume areas. These regions encompass the surface projection of the underlying magmatic plume. The demarcation of these areas is derived from the multiple intrusion points identified, represented by the blue polygons.

Even though all the original locus of the Iberian occurrences are nowadays present at the African plate there could be a geochemical signature concordance between the Iberian bodies and the African occurrences (Geldmacher et al., 2005).

7. CONCLUDING REMARKS

The main objective of this study was to explore the potential correlation among the Sintra, Sines, Monchique massifs, and the Lisbon Volcanic Complex as the main evidence of the Atlantic Alkaline Province controlling magmatism on the West Iberian Margin. Three hypotheses were considered as possible explanations for this magmatism and its potential connections. The first hypothesis is the Hot Spot hypothesis, suggesting the influence of a stationary mantle heat source in generating magmatic activity. The second hypothesis is the Super Plume hypothesis, which proposes large-scale upwellings of hot material from the mantle as the driving force behind the magmatic events. The third hypothesis invokes the Edge Driven Convection process, which postulates that the movement of tectonic plates triggers the upward movement of hot material from the mantle, resulting in a magmatic activity. By modelling the paleogeographic constraints of mobile plates moving above a deep mantle source, the age of magmatism in West Iberia and northwest Africa, this study aimed to gain insights into the mechanisms and possible links between the magmatic occurrences in the mentioned massifs within the Western Iberian Margin.

The workflow went through making this model and its iterations to try to model the places of the original intrusion sites of the massifs under study. Using GPlates software, allowed us to discern the diverse positions of these massifs, and to track their positions through time to assess the different models of mantle upwelling responsible for the distinct magmatic features. As the work progressed, it became necessary to incorporate additional regions such as the Tore-Madeira Rise and the Canary Island Seamount Province.

Results consistently suggest that the Hot Spot hypothesis cannot be supported. The intrusion sites of the various magmatic bodies were observed to be scattered rather than proximal which, associated with the discrete average ages of magmatic emplacement, means that a simple hot spot mechanism could not explain the evidence. Instead, the results strongly support that a stagnant mantle source, a Super Plume, that emitted plumelets that reached the shallower crustal levels or the surface to generate volcanism, is the most probable explanation for the magmatic activity observed. Another observed outcome was the division into two distinct clusters of intrusion sites that are interconnected within each cluster. This observation shows a more complex magmatic system, characterised by multiple plumes or clusters, rather than a single, linear source. These findings contribute to a deeper understanding of the geodynamic processes driving magmatism in the Western Iberian Margin and shed light on the spatial organisation of magmatic events in the studied area.

8. BIBLIOGRAPHY

- Alves, T. M., Moita, C., Cunha, T., Ullnaess, M., Myklebust, R., Monteiro, J. H., & Manuppella, G. (2009). Diachronous evolution of late jurassic-cretaceous continental rifting in the northeast atlantic (west iberian margin). *Tectonics*, 28(4). <https://doi.org/10.1029/2008TC002337>
- Bernard-Griffiths, J., Gruau, G. R., Cornen, G., Azambre, B., & Macé, J. (1997). Continental Lithospheric Contribution to Alkaline Magmatism: Isotopic (Nd, Sr, Pb) and Geochemical (REE) Evidence from Serra de Monchique and Mount Ormonde Complexes. In *JOURNAL OF PETROLOGY* (Vol. 38).
- Blum, R. (1861). Foyait, ein neues Gestein aus Sud-Portugal. *Neues Jb Miner Geol Paläont*, 426–433.
- Boillot, G., & Coulon, C. (1998). *La Déchirure Continentale et L'ouverture Océanique: Géologie Des Marges Passives* (Editions scientifiques GB - Gordon and Breach, Ed.).
- Boillot, G., Féraud, G., Recq, M., & Girardeau, J. (1989). Undercrusting by serpentinite beneath rifted margins. *Nature*, 341(6242), 523–525. <https://doi.org/10.1038/341523a0>
- Boillot, G., Girardeau, J., & Kornprobst, J. (1988). Rifting of the Galicia margin: crustal thinning and emplacement of mantle rocks on the seafloor. *Proc. Scientific Results, ODP, Leg 103, Galicia Margin*. <https://doi.org/10.2973/odp.proc.sr.103.179.1988>
- Bradley, R. S. (2015). Dating Methods I. In *Paleoclimatology*. <https://doi.org/10.1016/b978-0-12-386913-5.00003-x>
- Bronner, A., Sauter, D., Manatschal, G., Péron-Pinvidic, G., & Munsch, M. (2011). Magmatic breakup as an explanation for magnetic anomalies at magma-poor rifted margins. *Nature Geoscience*, 4(8). <https://doi.org/10.1038/ngeo1201>
- Canilho, M. H. (1972). Estudo geológico-petrográfico do maciço eruptivo de Sines. *Bol. Mus. Lab. Miner. Geol. Fac. Ciên. Univ. Lisboa*, 12(2), 77–161.
- Canilho, M. H. (1989). Elementos de geoquímica das rochas do maciço ígneo de Sines. *Ciências Da Terra* 10, 10.
- Cao, X., Zahirovic, S., Li, S., Suo, Y., Wang, P., Liu, J., & Müller, R. D. (2022). A deforming plate tectonic model of the South China Block since the Jurassic. *Gondwana Research*, 102, 3–16. <https://doi.org/10.1016/j.gr.2020.11.010>
- Carracedo, J. C. (1999). Growth, structure, instability and collapse of Canarian volcanoes and comparisons with Hawaiian volcanoes. *Journal of Volcanology and Geothermal Research*, 94(1–4), 1–19. [https://doi.org/10.1016/S0377-0273\(99\)00095-5](https://doi.org/10.1016/S0377-0273(99)00095-5)
- Carracedo, J. C., Day, S., Guillou, H., Rodríguez Badiola, E., Canas, J. A., & Pérez Torrado, F. J. (1998). Hotspot volcanism close to a passive continental margin: the Canary Islands. *Geological Magazine*, 135(5), 591–604. <https://doi.org/10.1017/S0016756898001447>
- Cebriá, J. M., López-Ruiz, J., Doblas, M., Martins, L. T., & Munha, J. (2003). Geochemistry of the early Jurassic Messejana- Plasencia dyke (Portugal-Spain): Implications on the origin of the Central Atlantic magmatic province. *Journal of Petrology*, 44(3). <https://doi.org/10.1093/petrology/44.3.547>
- Civiero, C., Custódio, S., Neres, M., Schlaphorst, D., Mata, J., & Silveira, G. (2021). The Role of the Seismically Slow Central-East Atlantic Anomaly in the Genesis of the Canary and Madeira Volcanic Provinces. *Geophysical Research Letters*, 48(13). <https://doi.org/10.1029/2021GL092874>
- Cloetingh, S., Koptev, A., Lavecchia, A., Kovács, I. J., & Beekman, F. (2022). Fingerprinting secondary mantle plumes. *Earth and Planetary Science Letters*, 597. <https://doi.org/10.1016/j.epsl.2022.117819>

- Courtillot, V., Davaille, A., Besse, J., & Stock, J. (2003). Three distinct types of hotspots in the Earth's mantle. *Earth and Planetary Science Letters*, 205(3–4). [https://doi.org/10.1016/S0012-821X\(02\)01048-8](https://doi.org/10.1016/S0012-821X(02)01048-8)
- Dannberg, J., & Sobolev, S. V. (2015). Low-buoyancy thermochemical plumes resolve controversy of classical mantle plume concept. *Nature Communications*, 6. <https://doi.org/10.1038/ncomms7960>
- Desmurs, L., Manatschal, G., & Bernoulli, D. (2001). The Steinmann Trinity revisited: mantle exhumation and magmatism along an ocean-continent transition: the Platta nappe, eastern Switzerland. *Geological Society, London, Special Publications*, 187(1), 235–266. <https://doi.org/10.1144/GSL.SP.2001.187.01.12>
- Doré, T., & Lundin, E. (2015). Hyperextended continental margins—Knowns and unknowns. *Geology*, 43(1), 95–96. <https://doi.org/10.1130/focus012015.1>
- Elder, J. (1976). *The Bowels of the Earth*. Oxford University Press.
- Escada, C. (2019). *Post-rift magmatism on the central West Iberian Margin (Estremadura Spur): new evidences from potential field data*. Faculdade de Ciências da Universidade de Lisboa.
- Escada, C., Represas, P., Santos, F., Pereira, R., Mata, J., & Rosas, F. M. (2022). New evidence of Late Cretaceous magmatism on the offshore central West Iberian Margin (Estremadura Spur) from potential field data. *Tectonophysics*, 832. <https://doi.org/10.1016/j.tecto.2022.229354>
- Escada, C., Santos, F., Represas, P., Pereira, R., Mata, J., Rosas, F., & Silva, B. (2019). Post-Rift Magmatism on the Central West Iberian Margin: New Evidence from Magnetic and Gravimetric Data Inversion in the Estremadura Spur. *EGU General Assembly 2019*.
- Féraud, G., Girardeau, J., Beslier, M. O., & Boillot, G. (1988). Datation ³⁹Ar-⁴⁰Ar de la mise en place des péridotites bordant la marge de la Galice (Espagne). *Comptes Rendus de l'Académie Des Sciences. Série 2, Mécanique, Physique, Chimie, Sciences de l'univers, Sciences de La Terre*, 307(1), 49–55.
- Ferreira, M., & Macedo, C. (1979). Idade radiométrica K-Ar do filão das Gaeiras. *Proc. VII Semana de Geoq. Resumos de Comunic*, 1.
- Foulger, G. R., & Anderson, D. L. (2005). A cool model for the Iceland hotspot. *Journal of Volcanology and Geothermal Research*, 141(1–2), 1–22. <https://doi.org/10.1016/j.jvolgeores.2004.10.007>
- Franke, D. (2013). Rifting, lithosphere breakup and volcanism: Comparison of magma-poor and volcanic rifted margins. In *Marine and Petroleum Geology* (Vol. 43). <https://doi.org/10.1016/j.marpetgeo.2012.11.003>
- Gaina, C., Nasuti, A., Kimbell, G. S., & Blischke, A. (2017). Break-up and seafloor spreading domains in the NE Atlantic. *Geological Society, London, Special Publications*, 447, 393–417. <https://doi.org/https://doi.org/10.1144/SP447.12>
- Gaina, C., Watson, R., & Cirbus, J. (2015). Late Mesozoic- Cenozoic plate boundaries in the North Atlantic & Arctic: Quantitative reconstructions using Hellinger criterion in GPlates. *EGU General Assembly*, 17(2). www.gplates.org
- Gamboa, D., & Pereira, R. (2023). *Assessing permanent CO2 storage volume in a buried volcano offshore West Iberia*. <https://doi.org/10.5194/egusphere-egu23-5973>
- Geldmacher, J., Hoernle, K., Bogaard, P. V.D., Duggen, S., & Werner, R. (2005). New ⁴⁰Ar/³⁹Ar age and geochemical data from seamounts in the Canary and Madeira volcanic provinces: Support for the mantle plume hypothesis. *Earth and Planetary Science Letters*, 237(1–2). <https://doi.org/10.1016/j.epsl.2005.04.037>
- Geldmacher, J., Hoernle, K., Klügel, A., v.d. Bogaard, P., Wombacher, F., & Berning, B. (2006). Origin and geochemical evolution of the Madeira-Tore Rise (eastern North Atlantic). *Journal of Geophysical Research: Solid Earth*, 111(9). <https://doi.org/10.1029/2005JB003931>
- Geoffroy, L. (2005). Volcanic passive margins. In *Comptes Rendus - Geoscience* (Vol. 337, Issue 16, pp. 1395–1408). Elsevier Masson SAS. <https://doi.org/10.1016/j.crte.2005.10.006>

- González-Clavijo, E. J., & Valadares, V. (2003). *A estrutura do complexo de Monchique*.
- Grange, M., Schärer, U., Cornen, G., & Girardeau, J. (2008). First alkaline magmatism during Iberia-Newfoundland rifting. *Terra Nova*, 20(6). <https://doi.org/10.1111/j.1365-3121.2008.00847.x>
- Grange, M., Schärer, U., Merle, R., Girardeau, J., & Cornen, G. (2010). Plume-lithosphere interaction during migration of cretaceous alkaline magmatism in SW Portugal: Evidence from U-Pb Ages and Pb-Sr-Hf isotopes. *Journal of Petrology*, 51(5), 1143–1170. <https://doi.org/10.1093/petrology/egq018>
- Hunter, M., & Rosenbusch, H. (1890). Über Monchiquit, ein camptonitisches Ganggestein aus der Gefolgschaft der Eläolithsyenite. *Tschermaks Mineralogische Und Petrographische Mitteilungen*, 11, 445–466.
- Inverno, C. M. C., Manupella, G., Zbyszewski, G., Pais, J., & Ribeiro, M. L. (1993). *Notícia explicativa da folha 42-C, Santiago do Cacém, 1: 50.000*.
- Inverno, C., Manupella, G., & Zbyszewski, G. (1986). *Carta Geológica de Portugal na escala 1:50000 - Folha 42-C Santiago do Cacém*. Serviços Geológicos de Portugal.
- King, S. D. (2007). Hotspots and edge-driven convection. *Geology*, 35(3). <https://doi.org/10.1130/G23291A.1>
- King, S. D., & Anderson, D. L. (1995). An alternative mechanism of flood basalt formation. *Earth and Planetary Science Letters*, 136(3–4). [https://doi.org/10.1016/0012-821X\(95\)00205-Q](https://doi.org/10.1016/0012-821X(95)00205-Q)
- King, S. D., & Anderson, D. L. (1998). Edge-driven convection. *Earth and Planetary Science Letters*, 160(3–4). [https://doi.org/10.1016/S0012-821X\(98\)00089-2](https://doi.org/10.1016/S0012-821X(98)00089-2)
- King, S. D., & Ritsema, J. (2000). African hot spot volcanism: Small-scale convection in the upper mantle beneath cratons. *Science*, 290(5494). <https://doi.org/10.1126/science.290.5494.1137>
- Kneller, E. A., Johnson, C. A., Karner, G. D., Einhorn, J., & Queffelec, T. A. (2012). Inverse methods for modeling non-rigid plate kinematics: Application to mesozoic plate reconstructions of the Central Atlantic. *Computers & Geosciences*, 49, 217–230. <https://doi.org/10.1016/j.cageo.2012.06.019>
- Kono, M. (1980). Magnetic Properties of DSDP Leg 55 Basalts. In *Initial Reports of the Deep Sea Drilling Project*, 55. <https://doi.org/10.2973/dsdp.proc.55.134.1980>
- Koppers, A. A. P. (2011). Mantle plumes persevere. *Nature Geoscience*, 4(12). <https://doi.org/10.1038/ngeo1334>
- Kullberg, M. C., & Kullberg, J. C. (2000). Tectónica da região de Sintra. *Tectónica Das Regiões de Sintra e Arrábida, Mem. Geociências, Museu Nac. Hist. Nat. Univ. Lisboa*, 2.
- Kullberg, M. C., & Kullberg, J. C. (2020). Landforms and Geology of the Serra de Sintra and Its Surroundings. In *World Geomorphological Landscapes*. https://doi.org/10.1007/978-3-319-03641-0_19
- Lacombe, O., Romagny, A., Jolivet, L., Menant, A., Bessièrre, E., Maillard, A., Canva, A., Gorini, C., & Augier, R. (2020). Detailed tectonic reconstructions of the Western Mediterranean region for the last 35 Ma, insights on driving mechanisms. *BSGF - Earth Sciences Bulletin*, 191(37). <https://doi.org/10.1051/bsgf/2020040>
- Lawver, L. A., & Müller, R. D. (1994). Iceland hotspot track. *Geology*, 22(4), 311–314.
- Leal, N. (1991). *Caracterização geoquímica do Maciço Eruptivo de Sintra. Conjecturas de ordem petrogenética baseadas em dados geoquímicos*.
- Long, X., Geldmacher, J., Hoernle, K., Hauff, F., Wartho, J. A., & Garbe-Schönberg, C. D. (2020). Origin of isolated seamounts in the Canary Basin (East Atlantic): The role of plume material in the origin of seamounts not associated with hotspot tracks. *Terra Nova*, 32(5). <https://doi.org/10.1111/ter.12468>
- Macintyre, R. M., & Berger, G. W. (1982). A note on the geochronology of the Iberian Alkaline Province. *Lithos*, 15(2), 133–136. [https://doi.org/10.1016/0024-4937\(82\)90005-6](https://doi.org/10.1016/0024-4937(82)90005-6)

- Mahmoudi, A. (1991). *Quelques intrusions alcalines et basiques du crétacé supérieur au Portugal (région de Lisbonne)* [These de Doctorat]. Université Henry Poincaré - Nancy I.
- Manatschal, G., & Bernoulli, D. (1999). Architecture and tectonic evolution of nonvolcanic margins: Present-day Galicia and ancient Adria. *Tectonics*, 18(6), 1099–1119. <https://doi.org/10.1029/1999TC900041>
- Manuppella, G., Ferreira, A. B., Ribeiro, M. L., Pais, J., Rebêlo, L., Cabral, J., Moniz, C., Baptista, R., Henriques, P., Falé, P., Lourenço, C., Sampaio, J., Midões, C., & Zbyszewski, G. (2011). *Notícia Explicativa da Folha 34-B Loures*.
- Marques, F. O., Azerêdo, A. C., Cabral, M. C., & Santos, V. (1998). Preliminary study of a proposed new cartographic unit in the Lisbon region: the Fanhões conglomerates. *Proceedings V Congresso Nacional de Geologia, Volume 84*, A107–A110.
- Martins, L. (1991). *Actividade ígnea Mesozoica em Portugal (Contribuição Petrológica e Geoquímica)*. Universidade de Lisboa.
- Martins, L., Miranda, R., Alves, C., Mata, J., Madeira, J., Munhá, J., Terrinha, P., Youbi, N., & Bensalah, K. (2010). Mesozoic magmatism at the West Iberian Margins: timing and geochemistry. In R. Pena dos Reis & N. Pimentel (Eds.), *II Central & North Atlantic Conjugate Margins Conference* (pp. 172–175).
- Martins, L. T., Madeira, J., Youbi, N., Munhá, J., Mata, J., & Kerrich, R. (2008). Rift-related magmatism of the Central Atlantic magmatic province in Algarve, Southern Portugal. *Lithos*, 101(1–2), 102–124. <https://doi.org/10.1016/j.lithos.2007.07.010>
- Marzoli, A., Callegaro, S., Dal Corso, J., Davies, J. H. F. L., Chiaradia, M., Youbi, N., Bertrand, H., Reisberg, L., Merle, R., & Jourdan, F. (2018). *The Central Atlantic Magmatic Province (CAMP): A Review* (pp. 91–125). https://doi.org/10.1007/978-3-319-68009-5_4
- Marzoli, A., Renne, P. R., Piccirillo, E. M., Ernesto, M., Bellieni, G., & De Min, A. (1999). Extensive 200-million-year-old continental flood basalts of the Central Atlantic Magmatic Province. *Science*, 284(5414). <https://doi.org/10.1126/science.284.5414.616>
- Mata, J., Alves, C. F., Martins, L., Miranda, R., Madeira, J., Pimentel, N., Martins, S., Azevedo, M. R., Youbi, N., De Min, A., Almeida, I. M., Bensalah, M. K., & Terrinha, P. (2015). 40Ar/39Ar ages and petrogenesis of the West Iberian Margin onshore magmatism at the Jurassic-Cretaceous transition: Geodynamic implications and assessment of open-system processes involving saline materials. *Lithos*, 236–237, 156–172. <https://doi.org/10.1016/j.lithos.2015.09.001>
- Matton, G., & Jébrak, M. (2009). The Cretaceous Peri-Atlantic Alkaline Pulse (PAAP): Deep mantle plume origin or shallow lithospheric break-up? *Tectonophysics*, 469(1–4), 1–12. <https://doi.org/10.1016/j.tecto.2009.01.001>
- Mendes, F. J., & Bernard-Griffiths, J. (1973). Nota sobre a datagem de um dos episódios do complexo basáltico de Lisboa. *Garcia de Orta, Série de Geologia*, 1(2), 37–41.
- Menzies, M. A., Klemperer, S. L., Ebinger, C. J., & Baker, J. (2002). Characteristics of volcanic rifted margins. In *Volcanic Rifted Margins*. Geological Society of America. <https://doi.org/10.1130/0-8137-2362-0.1>
- Merle, R. (2006). *Age and origin of Tore-Madeira Rise: Beginning of Atlantic Ocean spreading or hotspot track. Petrology, Geochemistry, U–Pb Geochronology and Pb–Sr–Hf isotopes*. University of Nantes.
- Merle, R. E., Jourdan, F., Chiaradia, M., Olierook, H. K. H., & Manatschal, G. (2019). Origin of widespread Cretaceous alkaline magmatism in the Central Atlantic: A single melting anomaly? *Lithos*, 342–343, 480–498. <https://doi.org/10.1016/j.lithos.2019.06.002>
- Merle, R., Jourdan, F., & Girardeau, J. (2018). Geochronology of the Tore-Madeira Rise seamounts and surrounding areas: a review. In *Australian Journal of Earth Sciences* (Vol. 65, Issue 5, pp. 591–605). Taylor and Francis Ltd. <https://doi.org/10.1080/08120099.2018.1471005>

- Merle, R., Jourdan, F., Marzoli, A., Renne, P. R., Grange, M., & Girardeau, J. (2009). Evidence of multi-phase Cretaceous to Quaternary alkaline magmatism on Tore-Madeira Rise and neighbouring seamounts from $^{40}\text{Ar}/^{39}\text{Ar}$ ages. *Journal of the Geological Society*, *166*(5). <https://doi.org/10.1144/0016-76492008-060>
- Miguel Leal Miranda, R. (2010). *UNIVERSIDADE DE LISBOA FACULDADE DE CIÊNCIAS DEPARTAMENTO DE GEOLOGIA PETROGENESIS AND GEOCHRONOLOGY OF THE LATE CRETACEOUS ALKALINE MAGMATISM IN THE WEST IBERIAN MARGIN DOUTORAMENTO EM GEOLOGIA (GEODINÂMICA INTERNA)*.
- Miranda, R., Valadares, V., Terrinha, P., Mata, J., Azevedo, M. do R., Gaspar, M., Kullberg, J. C., & Ribeiro, C. (2009). Age constraints on the Late Cretaceous alkaline magmatism on the West Iberian Margin. *Cretaceous Research*, *30*(3), 575–586. <https://doi.org/10.1016/j.cretres.2008.11.002>
- Missenard, Y., & Cadoux, A. (2012). Can Moroccan Atlas lithospheric thinning and volcanism be induced by Edge-Driven Convection? *Terra Nova*, *24*(1), 27–33. <https://doi.org/10.1111/j.1365-3121.2011.01033.x>
- Moita, P., Berrezueta, E., Pedro, J., Miguel, C., Beltrame, M., Galacho, C., Barrulas, P., Mirão, J., Araújo, A., Lopes, L., & Carneiro, J. (2020). *Experiments on mineral carbonation of CO₂ in gabbro from the Sines massif—first results of project InCarbon Ensaios de carbonatação mineral de CO₂ no gabro do maciço de Sines—primeiros resultados do projeto InCarbon*. https://www.lneg.pt/wp-content/uploads/2020/05/Volume_107_CIG.pdf
- Morgan, W. J. (1971). Convection Plumes in the Lower Mantle. *Nature*, *230*(5288), 42–43. <https://doi.org/10.1038/230042a0>
- Morgan, W. J. (1972). Plate motions and deep mantle convection. *Memoir of the Geological Society of America*, *132*. <https://doi.org/10.1130/MEM132-p7>
- Müller, R. D., Cannon, J., Qin, X., Watson, R. J., Gurnis, M., Williams, S., Pfaffelmoser, T., Seton, M., Russell, S. H. J., & Zahirovic, S. (2018). GPlates: Building a Virtual Earth Through Deep Time. *Geochemistry, Geophysics, Geosystems*, *19*(7). <https://doi.org/10.1029/2018GC007584>
- Müller, R. D., Zahirovic, S., Williams, S. E., Cannon, J., Seton, M., Bower, D. J., Tetley, M. G., Heine, C., Le Breton, E., Liu, S., Russell, S. H. J., Yang, T., Leonard, J., & Gurnis, M. (2019). A Global Plate Model Including Lithospheric Deformation Along Major Rifts and Orogens Since the Triassic. *Tectonics*, *38*(6). <https://doi.org/10.1029/2018TC005462>
- Mutter, J. C., Buck, W. R., & Zehnder, C. M. (1988). Convective partial melting: 1. A model for the formation of thick basaltic sequences during the initiation of spreading. *Journal of Geophysical Research*, *93*(B2), 1031. <https://doi.org/10.1029/JB093iB02p01031>
- Negredo, A. M., van Hunen, J., Rodríguez-González, J., & Fulla, J. (2022). On the origin of the Canary Islands: Insights from mantle convection modelling. *Earth and Planetary Science Letters*, *584*. <https://doi.org/10.1016/j.epsl.2022.117506>
- Neres, M., Bouchez, J. L., Terrinha, P., Font, E., Moreira, M., Miranda, R., Launeau, P., & Carvalho, C. (2014). Magnetic fabric in a Cretaceous sill (Foz da Fonte, Portugal): Flow model and implications for regional magmatism. *Geophysical Journal International*, *199*(1). <https://doi.org/10.1093/gji/ggu250>
- Neres, M., Font, E., Miranda, J. M., Camps, P., Terrinha, P., & Mirão, J. (2012). Reconciling Cretaceous paleomagnetic and marine magnetic data for Iberia: New Iberian paleomagnetic poles. *Journal of Geophysical Research: Solid Earth*, *117*(6). <https://doi.org/10.1029/2011JB009067>
- Neres, M., & Ranero, C. R. (2023). An appraisal using magnetic data of the Continent to Ocean Transition Structure West of Iberia. *Geophysical Journal International*, *24*(3), 1819–1834. <https://doi.org/10.1093/gji/ggad163/7120036>

- Neres, M., Terrinha, P., Custódio, S., Silva, S. M., Luis, J., & Miranda, J. M. (2018). Geophysical evidence for a magmatic intrusion in the ocean-continent transition of the SW Iberia margin. *Tectonophysics*, 744, 118–133. <https://doi.org/10.1016/j.tecto.2018.06.014>
- Neres, M., Terrinha, P., Noiva, J., Brito, P., Rosa, M., Batista, L., & Ribeiro, C. (2023). New Late Cretaceous and CAMP magmatic sources off West Iberia, from high-resolution magnetic surveys on the continental shelf. *Tectonics*. <https://doi.org/10.1029/2022tc007637>
- Nirrengarten, M., Manatschal, G., Tugend, J., Kuszniir, N. J., & Sauter, D. (2017). Nature and origin of the J-magnetic anomaly offshore Iberia–Newfoundland: implications for plate reconstructions. *Terra Nova*, 29(1), 20–28. <https://doi.org/10.1111/ter.12240>
- Nirrengarten, M., Manatschal, G., Tugend, J., Kuszniir, N., & Sauter, D. (2018). Kinematic Evolution of the Southern North Atlantic: Implications for the Formation of Hyperextended Rift Systems. *Tectonics*, 37(1), 89–118. <https://doi.org/10.1002/2017TC004495>
- Pais, J., Moniz, C., Cabral, J., Cardoso, J. L., Legoinha, P., Machado, S., Morais, M. A., Lourenço, C., Ribeiro, M. L., Henriques, P., & Falé, P. (2006). *Notícia Explicativa da Folha 34-D Lisboa*.
- Palácios, T., Alves, C. A. M., Leal, N., & Muinhá, J. (1995). Mineralogia química do Maciço Eruptivo de Sintra. *Fac. Ciênc. Mus. Lab. Min. Geol Univ. Porto*, 775–779.
- Palácios, T. P. (1985). *Petrologia do complexo vulcânico de Lisboa* [Tese de Doutoramento]. Faculdade de Ciências da Universidade de Lisboa.
- Pedro, J., Araújo, A. A., Moita, P., Beltrame, M., Lopes, L., Chambel, A., Berrezueta, E., & Carneiro, J. (2020). Mineral Carbonation of CO₂ in Mafic Plutonic Rocks, I—Screening Criteria and Application to a Case Study in Southwest Portugal. *Applied Sciences*, 10(14), 4879. <https://doi.org/10.3390/app10144879>
- Pereira, R., & Alves, T. M. (2011). Margin segmentation prior to continental break-up: A seismic-stratigraphic record of multiphased rifting in the North Atlantic (Southwest Iberia). *Tectonophysics*, 505(1–4). <https://doi.org/10.1016/j.tecto.2011.03.011>
- Pereira, R., Mata, J., Ramalho, R. S., Rosas, F. M., & Silva, B. (2022). Nature, timing and magnitude of buried Late Cretaceous magmatism on the central West Iberian Margin. *Basin Research*, 34, 771–796. <https://doi.org/https://doi.org/10.1111/bre.12640>
- Pereira, R., Rosas, F., Mata, J., Represas, P., Escada, C., & Silva, B. (2021). Interplay of tectonics and magmatism during post-rift inversion on the central West Iberian Margin (Estremadura Spur). *Basin Research*, 33(2), 1497–1519. <https://doi.org/10.1111/bre.12524>
- Péron-Pinvidic, G., & Manatschal, G. (2009). The final rifting evolution at deep magma-poor passive margins from Iberia–Newfoundland: A new point of view. *International Journal of Earth Sciences*, 98(7), 1581–1597. <https://doi.org/10.1007/s00531-008-0337-9>
- Ramalho, M. M., Ribeiro, M. L., Serralheiro, A., & Moitinho de Almeida, F. (1999). *Carta Geológica de Portugal na escala 1:50000 - Folha 34-C Cascais*. Instituto Geológico e Mineiro.
- Reston, T. J. (2009). The structure, evolution and symmetry of the magma-poor rifted margins of the North and Central Atlantic: A synthesis. *Tectonophysics*, 468(1–4), 6–27. <https://doi.org/10.1016/j.tecto.2008.09.002>
- Reston, T., & Manatschal, G. (2011). *Rifted Margins: Building Blocks of Later Collision* (pp. 3–21). https://doi.org/10.1007/978-3-540-88558-0_1
- Ribeiro, A., Antunes, M. T., Ferreira, M. P., Rocha, R. B., Soares, A. F., Zbyszewski, G., Almeida, F. M. de, Carvalho, D. de, & Monteiro, J. H. (1979). Introduction à la géologie générale du Portugal. In *26e Congr.internat.Géol.*, 1980.
- Ribeiro, P., Silva, P. F., Moita, P., Kratinová, Z., Marques, F. O., & Henry, B. (2013). Palaeomagnetism in the Sines massif (SW Iberia) revisited: Evidences for late cretaceous hydrothermal alteration and associated partial remagnetization. *Geophysical Journal International*, 195(1), 176–191. <https://doi.org/10.1093/gji/ggt261>

- Rock, N. M. S. (1976). The Comparative Strontium Isotopic Composition of Alkaline Rocks: New Data from Southern Portugal and East Africa. In *Contrib. Mineral. Petrol* (Vol. 56).
- Rock, N. M. S. (1978). Petrology and petrogenesis of the monchique alkaline complex, southern portugal. *Journal of Petrology*, 19(2). <https://doi.org/10.1093/petrology/19.2.171>
- Rock, N. M. S. (1982). *The Late Cretaceous Alkaline Igneous Province in the Iberian Peninsula, and its tectonic significance.*
- Sahabi, M., Aslanian, D., & Olivet, J.-L. (2004). Un nouveau point de départ pour l'histoire de l'Atlantique central. *Comptes Rendus Geoscience*, 336(12), 1041–1052. <https://doi.org/10.1016/j.crte.2004.03.017>
- Sanchez, G., Merle, R., Hirschberger, F., Thion, I., & Girardeau, J. (2019). Post-spreading deformation and associated magmatism along the Iberia-Morocco Atlantic margins: Insight from submarine volcanoes of the Tore-Madeira Rise. *Marine Geology*, 407, 76–93. <https://doi.org/10.1016/j.margeo.2018.10.011>
- Sawyer, S., Dale, M., F., C., Reston, J., Timothy, S., M., J., & Hopper, R. (2007). COBBOOM: The Continental Breakup and Birth of Oceans Mission. *Scientific Drilling*, 5, Sept 2007. <https://doi.org/10.2204/iodp.sd.5.02.2007>
- Schermerhorn, L. J. G., Priem, H. N. A., Boelrijk, N. A. I. M., Hebeda, E. H., Verdurmen, E. A. Th., & Verschure, R. H. (1978). Age and Origin of the Messejana Dolerite Fault-Dike System (Portugal and Spain) in the Light of the Opening of the North Atlantic Ocean. *The Journal of Geology*, 86(3), 299–309. <https://doi.org/10.1086/649692>
- Schettino, A., & Turco, E. (2009). Breakup of Pangaea and plate kinematics of the central Atlantic and Atlas regions. *Geophysical Journal International*, 178(2), 1078–1097. <https://doi.org/10.1111/j.1365-246X.2009.04186.x>
- Schott, J.-J., Montigny, R., & Thuizat, R. (1981). Paleomagnetism and potassium-argon age of the Messejana Dike (Portugal and Spain)" angular limitation to the rotation of the Iberian Peninsula since the Middle Jurassic. In *Earth and Planetary Science Letters* (Vol. 53).
- Sibuet, J. C., Srivastava, S. P., & Spakman, W. (2004). Pyrenean orogeny and plate kinematics. *Journal of Geophysical Research: Solid Earth*, 109(8). <https://doi.org/10.1029/2003JB002514>
- Silva, E. A., Miranda, J. M., Luis, J. F., & Galdeano, A. (2000). Correlation between the Palaeozoic structures from West Iberian and Grand Banks margins using inversion of magnetic anomalies. *Tectonophysics*, 321(1). [https://doi.org/10.1016/S0040-1951\(00\)00080-9](https://doi.org/10.1016/S0040-1951(00)00080-9)
- Srivastava, S. P., Sibuet, J.-C., Cande, S., Roest, W. R., & Reid, I. D. (2000). Magnetic evidence for slow seafloor spreading during the formation of the Newfoundland and Iberian margins. *Earth and Planetary Science Letters*, 182(1), 61–76. [https://doi.org/10.1016/S0012-821X\(00\)00231-4](https://doi.org/10.1016/S0012-821X(00)00231-4)
- Storétvedt, K. M., Mogstad, H., Abranches, M. C., Mitchell, J. G., & Serralheiro, A. (1987). Palaeomagnetism and isotopic age data from Upper Cretaceous igneous rocks of W. Portugal; geological correlation and plate tectonic aspects. *Geophysical Journal of the Royal Astronomical Society*, 88(1), 241–263. <https://doi.org/10.1111/j.1365-246X.1987.tb01378.x>
- Szameitat, L. S. A., Manatschal, G., Nirrengarten, M., Ferreira, F. J. F., & Heilbron, M. (2020). Magnetic characterization of the zigzag shaped J-anomaly: Implications for kinematics and breakup processes at the Iberia–Newfoundland margins. *Terra Nova*, 32(5), 369–380. <https://doi.org/10.1111/ter.12466>
- Tarduno, J. A., Duncan, R. A., Scholl, D. W., Cottrell, R. D., Steinberger, B., Thordarson, T., Kerr, B. C., Neal, C. R., Frey, F. A., Torii, M., & Carvallo, C. (2003). The Emperor Seamounts: Southward motion of the Hawaiian hotspot plume in earth's mantle. *Science*, 301(5636). <https://doi.org/10.1126/science.1086442>

- Teixeira, C. (1962). La structure annulaire subvolcanique des massifs éruptives de Sintra, Sines et Monchique. In *Estudos Científicos. Homenagem ao Prof. Doutor J. Carrington da Costa*. (pp. 461–493). Junta de Investigações do Ultramar.
- Terrinha, P., Aranguren, A., Kullberg, M. C., Pueyo, E., Kullberg, J. C., Casas Sainz, A. M., & Rillo, C. (2003). *Complexo ígneo de Sintra – um modelo de instalação constrangido por novos dados de gravimetria e ASM*.
- Terrinha, P., Pueyo, E. L., Aranguren, A., Kullberg, J. C., Kullberg, M. C., Casas-Sainz, A., & Azevedo, M. do R. (2018). Gravimetric and magnetic fabric study of the Sintra Igneous complex: laccolith-plug emplacement in the Western Iberian passive margin. *International Journal of Earth Sciences*, *107*(5), 1807–1833. <https://doi.org/10.1007/s00531-017-1573-7>
- Tucholke, B. E., & Ludwig, W. J. (1982). Structure and Origin of the J Anomaly Ridge, Western North Atlantic Ocean. In *JOURNAL OF GEOPHYSICAL RESEARCH* (Vol. 87).
- Tucholke, B. E., Sawyer, D. S., & Sibuet, J. C. (2007). Breakup of the Newfoundland-Iberia rift. *Geological Society Special Publication*, *282*. <https://doi.org/10.1144/SP282.2>
- Tugend, J., Gillard, M., Manatschal, G., Nirrengarten, M., Epin, M.-E., Sauter, D., Autin, J., Kuszniir, N., & McDermott, K. (2020). Reappraisal of the Magma-rich versus Magma-poor Rifted Margin Archetypes. *Geological Society*, *476*, 23–47. <https://doi.org/10.1144/SP476.9>
- Van Den Bogaard, P. (2013). The origin of the Canary Island Seamount Province-New ages of old seamounts. *Scientific Reports*, *3*. <https://doi.org/10.1038/srep02107>
- Verati, C., Rapaille, C., Féraud, G., Marzoli, A., Bertrand, H., & Youbi, N. (2007). 40Ar/39Ar ages and duration of the Central Atlantic Magmatic Province volcanism in Morocco and Portugal and its relation to the Triassic-Jurassic boundary. *Palaeogeography, Palaeoclimatology, Palaeoecology*, *244*(1–4). <https://doi.org/10.1016/j.palaeo.2006.06.033>
- Voo, R. van der. (1993). *Paleomagnetism of the Atlantic, Tethys and Iapetus Oceans*. Cambridge University Press. <https://doi.org/10.1017/CBO9780511524936>
- White, R. S., McKenzie, D., & O’Nions, R. K. (1992). Oceanic crustal thickness from seismic measurements and rare earth element inversions. *Journal of Geophysical Research*, *97*(B13), 19683. <https://doi.org/10.1029/92JB01749>
- Whitmarsh, R. B., Manatschal, G., & Minshull, T. A. (2001). Evolution of magma-poor continental margins from rifting to seafloor spreading. *Nature*, *413*(6852), 150–154. <https://doi.org/10.1038/35093085>
- Whitmarsh, R. B., Minshull, T. A., Russell, S. M., Dean, S. M., Loudon, K. E., & Chian, D. (2001). The role of syn-rift magmatism in the rift-to-drift evolution of the West Iberia continental margin: geophysical observations. *Geological Society, London, Special Publications*, *187*(1), 107–124. <https://doi.org/10.1144/GSL.SP.2001.187.01.06>
- Young, A., Flament, N., Maloney, K., Williams, S., Matthews, K., Zahirovic, S., & Müller, R. D. (2019). Global kinematics of tectonic plates and subduction zones since the late Paleozoic Era. *Geoscience Frontiers*, *10*(3), 989–1013. <https://doi.org/10.1016/j.gsf.2018.05.011>